Reassessment of the phylogenetic position of the spiny-scale pricklefish *Hispidoberyx ambagiosus* (Beryciformes: Hispidoberycidae)

（キンメダイ目魚類 *Hispidoberyx ambagiosus* の系統的位置の再検証）

北海道大学大学院水産科学院
海洋生物資源科学専攻
Graduate School of Fisheries Sciences
Division of Marine Bioresource and Environmental Science

木村克也
Katsuya Kimura

2020 年

Contents

Disclaimer. This work is not issued for purposes of zoological nomenclature.

I. Introduction

The spiny-scale pricklefish *Hispidoberyx ambagiosus* Kotlyar, 1981 (Fig. 1) is a sole member of the family Hispidoberycidae which belongs to the series Berycida, order Beryciformes, suborder Stephanoberycoidei and superfamily Stephanoberycoidea (Nelson et al., 2016). This species has been known only from a few specimens collected from the tropical waters of the Indo-West Pacific Ocean at depths of 560–1360 m (Paxton et al., 2001; Kotlyar, 2004a). The species is characterized by spinulose scales, a long and stout spine on the opercle, the vomer and palatine with teeth, the dorsal fin with four or five spines and 10 soft rays, the anal fin with two or three spines and nine soft rays, the pelvic fin with one spine and seven soft rays, 32–34 lateral line scales, and 34–35 vertebrae (Kotlyar, 1981, 2004a).

In the original description of *Hispidoberyx ambagiosus* by Kotlyar (1981), the new family Hispidoberycidae was established to include the sole species and provisionally placed in the beryciform suborder Berycoidei defined by Greenwood et al. (1966), based on several characters shared with berycoids. Subsequently, Yang et al. (1988), who reported the second record of the species, pointed out that characters which led Kotlyar (1981) to place the family in Berycoidei are primitive in Beryciformes and of little value to determine its phylogenetic position. Kotlyar (1991a) described the osteology of the species based on a single additional specimen and suggested a placement of the family in the suborder Stephanoberycoidei, which also includes Stephanoberycidae, Gibberichthyidae and Melamphaidae. He also proposed establishment of a separate superfamily Hispidoberycoidea in the suborder and assumed its closer relationship with Stephanoberycoidea (including Stephanoberycidae and Gibberichthyidae) than Melamphaoidea (including Melamphaidae) in the suborder. Moore (1993) conducted a phylogenetic analysis including *H. ambagiosus* for the first time in his phylogenetic study of the order Trachichthyiformes (sensu Moore, 1993) based on osteology and external morphology, and inferred a sister relationship of Hispidoberycidae and Stephanoberycidae. However, because only one synapomorphy supported the clade including

these two families (9–11 procurrent caudal-fin spines in both dorsal and ventral lobes), such a placement of the family is not strongly supported.

In 2004–2005, eleven specimens of *Hispidoberyx ambagiosus* were newly collected from off Sumatra and Java, the eastern Indian Ocean during the Japan-Indonesia Deep Sea Fishery Resource Joint Exploration Project (for detail of the project, see Overseas Fishery Cooperation Foundation, Japan & Agency for Marine and Fisheries Research, Ministry of Marine Affairs and Fisheries, Indonesia, 2006). However, morphological study treating *H. ambagiosus* has never been carried out after Moore's (1993) study, and no molecular phylogenetic study including the species has been conducted because of the difficulty to obtain fresh samples. Therefore, the phylogenetic position of the species is not well understood at present.

The purposes of this study are: 1) to describe osteology, myology and other morphology of *Hispidoberyx ambagiosus* in detail; 2) to reconstruct the phylogenetic relationships of the species and related taxa; and 3) to reassess the phylogenetic position of the species based on the phylogenetic relationships.

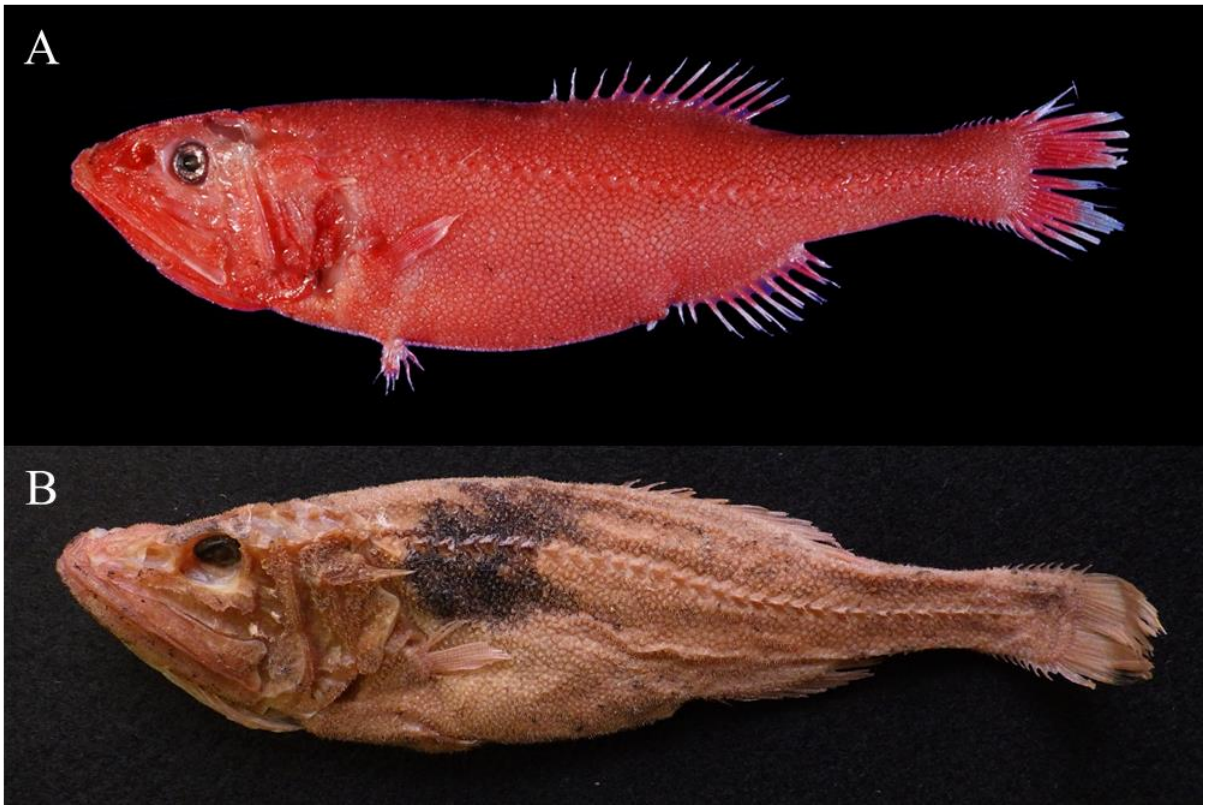

Figure 1. *Hispidoberyx ambagiosus*. A, HUMZ 193967, 173.9 mm SL, collected from off Sumatra, eastern Indian Ocean, 834–890 m depth, fresh. B, ZMMU P-15416, holotype, 171.0 mm SL, collected from off Sumatra, eastern Indian Ocean, 800–875 m depth, preserved.

II. Materials and methods

Examinations of osteology, myology and some other internal morphology were made on specimens stained with Alizarin Red-S and Alcian Blue. Stereomicroscopes with a camera lucida were used for dissection and making sketches. Terminology follows Rojo (1991) for general osteology, Stiassny (1986) for bony condyles and ligaments of the upper jaw, Stiassny & Moore (1992) for bony structures of the pelvic bone and related elements, Fujita (1990) for cartilaginous elements of caudal skeleton, Patterson & Johnson (1995) for intermuscular bones, Winterbottom (1974) for myology and Webb (1989) for the lateral line system. Initial classification including each species examined in this study higher than family level followed Nelson et al. (2016). Standard length is abbreviated as SL. Abbreviations of "D", "E" and "X" indicate specimens used for dissection, external observation and examination of partial osteology on X-ray photographs, respectively. Institutional abbreviations follow Fricke & Eschmeyer (2019) with an addition of Aomori Prefectural Museum, Aomori, Japan (AOPM).

Materials examined

Berycida

Beryciformes

Barbourisiidae: *Barbourisia rufa* Parr, 1945, HUMZ 129364, 207.6 mm SL (E), HUMZ 130423, 295.2 mm SL (D), HUMZ 143626, 153.6 mm SL (E).

Berycidae: *Beryx decadactylus* Cuvier, 1829, HUMZ 47735, 219.6 mm SL (D); *Centroberyx lineatus* (Cuvier, 1829), HUMZ 52363, 125.0 mm SL (D).

Cetomimidae: *Cetostoma regani* Zugmayer, 1914, BMNH 1996.2.14.40–43 (2 of 4 specimens), 89.2–129.0 mm SL (D).

Gibberichthyidae: *Gibberichthys pumilus* Parr, 1933, NSMT-P 44413, 72.4 mm SL (D).

Hispidoberycidae: *Hispidoberyx ambagiosus* Kotlyar, 1981, HUMZ 190932, 175.2 mm SL (E, X), HUMZ 193670, 178.8 mm SL (D), HUMZ 193671, 191.2 mm SL (E, X, partially

dissected to observe Tominaga's organ and gonad), HUMZ 193967, 173.9 mm SL (E, X), HUMZ 194315, 130.1 mm SL (E, X, partially dissected to observe Tominaga's organ and gonad), HUMZ 194634, 180.7 mm SL (D), ZMMU P-15416, 171.0 mm SL (E) (holotype).

Melamphaidae: *Melamphaes typhlops* (Lowe, 1843), USNM 248477, 70.8 mm SL (D); *Poromitra unicornis* (Gilbert, 1905), HUMZ 130322, 119.8 mm SL (D), HUMZ 144012, 84.0 mm SL (D); *Scopelogadus mizolepis* (Günther, 1878), HUMZ 130318, 83.3 mm SL (D).

Rondeletiidae: *Rondeletia loricata* Abe & Hotta, 1963, HUMZ 130180, 76.8 mm SL (D), HUMZ 192725, 74.9 mm SL (D).

Stephanoberycidae: *Acanthochaenus luetkenii* Gill, 1884, USNM 307916, 89.1 mm SL (D); *Stephanoberyx monae* Gill, 1883, HUMZ 230037 (formerly USNM 208284), 88.8 mm SL (D), USNM 304376, 101.9 mm SL (E).

Trachichthyiformes

Anomalopidae: *Anomalops katoptron* (Bleeker, 1856), HUMZ 40200, unmeasured (D), KPM-NI 010182, 87.1 mm SL (D).

Anoplogastridae: *Anoplogaster cornuta* (Valenciennes, 1833), HUMZ 130183, 113.0 mm SL (D), HUMZ 197375, 132.9 mm SL (D).

Diretmidae: *Diretmus argenteus* Johnson, 1864, HUMZ 40225, 78.7 mm SL (D).

Monocentridae: *Monocentris japonica* (Houttuyn, 1782), HUMZ 33613, 136.0 mm SL (D), HUMZ 40406, 108.9 mm SL (D).

Trachichthyidae: *Hoplostethus mediterraneus* Cuvier, 1829, HUMZ 52125, 144.2 mm SL (D), NSMT-P 43389, 140.7 mm SL (D); *Paratrachichthys trailli* (Hutton, 1875), HUMZ 66835, 154.2 mm SL (D), HUMZ 91426, 130.2 mm SL (D); *Trachichthys australis* Shaw, 1799, AMS I.15912-007, 96.7 mm SL (D), HUMZ 40221, 111.0 mm SL (D).

Holocentriformes

Holocentridae: *Holocentrus adscensionis* (Osbeck, 1765), USNM 79882, 148.4 mm SL (D); *Neoniphon sammara* (Forsskål, 1775), HUMZ 40434, 151.8 mm SL (D), HUMZ

165317, ca. 99.0 mm SL (D); *Ostichthys japonicus* (Cuvier, 1829), HUMZ 122195, 91.1 mm SL (D).

Percomorpha

Ophidiiformes

Ophidiidae: *Hoplobrotula armata* (Temminck & Schlegel, 1846), HUMZ 109335, 154.4 mm SL (D), HUMZ 201333, 202.4 mm SL (D).

Carangiformes

Carangidae: *Trachurus japonicus* (Temminck & Schlegel, 1844), HUMZ 186697, 144.6 mm SL (D), HUMZ 187384, 85.2 mm SL (D).

Perciformes

Lateolabracidae: *Lateolabrax japonicus* (Cuvier, 1828), HUMZ 185288, 119.7 mm SL (D).

Latidae: *Lates mariae* Steindachner, 1909, HUMZ 125958, 112.3 mm SL (D).

Paracanthopterygii

Polymixiiformes

Polymixiiformes: *Polymixia japonica* Günther, 1877, HUMZ 47731, 154.8 mm SL (D).

Lamprimorpha

Lampriformes

Veliferidae: *Velifer hypselopterus* Bleeker, 1879, HUMZ 36467, 181.0 mm SL (D).

Comparative materials

Myctophiformes

Neoscopelidae: *Neoscopelus microchir* Matsubara, 1943, HUMZ 80156, 101.4 mm SL (D).

Aulopiformes

Aulopidae: *Hime japonica* (Günther, 1877), HUMZ 114349, 131.1 mm SL (D), HUMZ 200012, 160.7 mm SL (D).

Synodontidae: *Trachinocephalus trachinus* (Temminck & Schlegel, 1846), HUMZ 103511,

172.0 mm SL (D), HUMZ 109109, 175.0 mm SL (D), HUMZ uncatalogued, 81.9 mm SL (D).

III. Systematic methodology

Phylogenetic relationships of *Hispidoberyx ambagiosus* and its related taxa were inferred by the cladistic methodology (Henning, 1966). Outgroup comparison was applied to determine character polarity (Watrous & Wheeler, 1981; Wiley, 1981). Because *H. ambagiosus* has spiny rays on the dorsal, anal and pelvic fins, seven soft rays on the pelvic fin, and 19 principal caudal fin rays, it is highly possible that this species is included in the series Berycida (sensu Nelson et al., 2016). However, the monophyly of Berycida is uncertain as suggested by many morphological (e.g., Stiassny & Moore, 1992; Moore, 1993; Johnson & Patterson, 1993) and molecular studies (e.g., Miya et al., 2003; Betancur-R et al., 2017; Hughes et al., 2018) showing the non-monophyly of Berycida. Therefore, in addition to 22 species from 14 families of Berycida, representatives of related taxa of Berycida (i.e., four species from three orders of Percomorpha, one species from Lampriformes and one species from Polymixiiformes) (e.g., Stiassny & Moore, 1992; Miya et al., 2003; Davesne et al., 2016; Betancur-R et al., 2017) were also included in ingroups of the phylogenetic analysis. One species from Myctophiformes, which is considered as a sister groups of Acanthomorpha including all ingroups, and two species from Aulopiformes, which is considered as a sister groups of Ctenosquamata including Acanthomorpha and Myctophiformes (e.g., Johnson, 1992; Near et al., 2013; Betancur-R et al., 2017), were employed as outgroups of the analysis.

The character matrix was made by using Mesquite ver. 3.51 (Maddison & Maddison, 2018) and analyzed by using PAUP*4.0a (build 166) (Swofford, 2002) with following options: heuristic search algorithms; random addition sequence with 100 replicates; TBR branch swapping; and multistate taxa interpreted as polymorphisms. Most character evolutions were assumed as “ordered” (Wagner parsimony: Farris, 1970), while some character evolutions were assumed as “unordered” due to difficulties of inferring the order (Fitch parsimony: Fitch, 1971). Character optimizations were performed by using PAUP*4.0a (build 166) including both ACCTRAN and DELTRAN (Swofford & Maddison, 1987). Evolutions of characters not

used for the analysis were estimated in the cladogram by using MacClade version 4.0 (Maddison & Maddison, 2000) including both ACCTRAN and DELTRAN. Evolutionary transition of inhabiting depths was estimated in the cladogram following the zoogeographical methodology shown by Sawada (1982). Autapomorphies observed only in terminal taxa and synapomorphies observed in all ingroups were not used for the analysis because they had no influence on the determination of relationships. Although several disagreements of characters were observed between the present and previous studies, they were fundamentally regarded as intraspecific variations, except for where reasons for exclusion of previously reported conditions were especially noted.

In many stephanoberycoids and melamphaids, various bony elements of the hole body are composed of quite thin laminate bones and mostly cartilaginous bones. Because such weak ossifications of bony elements are generally observed in various deep-sea fishes, e.g., Alepocephaloidea (Greenwood & Rosen, 1971), Ateleopodidae (Sasaki et al., 2006), and Liparidae (Kido, 1988), it is considered that weak ossification occurring in each bone is strongly associated with each other and possibly related to adaptation to the deep-sea environment. In this study, therefore, character variations apparently subject to the degree of the ossification (e.g., extent of cartilages in neurocranium, cartilaginous or ossified in the basihyal, and distal pterygiophores of the dorsal and anal fin) were not used for the analysis to avoid weighting to the particular nature, weak ossification, by adoptions of them for the analysis.

IV. Anatomical description

4-1. Osteology

4-1-1. Circumorbital bones (Figs. 2–4)

Description

The circumorbital bones consist of six infraorbitals. An antorbital is absent. Each of the infraorbitals has a wide and shallow groove for the infraorbital canal, which is posterodorsally continuous with the supraorbital and otic canals on the frontal and pterotic, respectively. The lateral aspects of the infraorbitals are covered with many small spines in large parts of the upper (first to third elements) or anterior (fourth to sixth) margins and small parts of the lower (first and second), lower and posterior (third), or posterior (fourth to sixth) margins. All elements lack a subocular shelf.

The first infraorbital (= lachrymal) is the anteriormost and largest element of the infraorbitals. This bone has a glenoid cavity dorsomedially which articulates with a condyle of the lateral ethmoid. The anterior portion of the bone has a bony bridge over the infraorbital canal. This bone has three pores for the buccal nerves innervating canal neuromasts of the infraorbital canal.

The second infraorbital is rectangular and situated posterior to the first infraorbital. This bone has two pores for the buccal nerves innervating canal neuromasts.

The third infraorbital, a medium size angular bone, is attached to the second infraorbital anteriorly and the fourth infraorbital dorsally. This bone has two pores for the buccal nerves innervating canal neuromasts.

The fourth and fifth infraorbitals are small rectangular elements, located between the third and sixth infraorbitals, and have one pore for the buccal nerve innervating a canal neuromast, respectively.

The sixth infraorbital (= dermosphenotic), a small oval bone, is situated on the posterodorsal portion of the infraorbitals and attached to the sphenotic dorsomedially, the

frontal anterodorsally and the pterotic posterodorsally. This bone has one pore for the buccal nerve innervating a canal neuromast.

Character recognition

TS 1. Subocular shelf (0: absent; 1: present)

Ingroups. A subocular shelf is absent in *Hispidoberyx ambagiosus*, stephanoberycids, *Gibberichthys pumilus*, *Rondeletia loricata*, *Barbourisia rufa*, *Cetostoma regani*, melamphaids, *Velifer hypselopterus* and *Hoplobrotula armata* (character 1-0), whereas it is present in other ingroups (character 1-1).

Outgroups. All outgroups lack a subocular shelf.

Remarks. Moore (1993) recognized the following three conditions of the subocular shelf among taxa of Berycida: (1) continuous on two or more infraorbitals or very wide-based on the third infraorbital; (2) replaced by an expanded orbital margin on the third infraorbital; and (3) restricted to the third infraorbital and narrow-based, tapered and often hooked anteriorly. The first condition was considered to be primitive, while the second condition was considered as an autapomorphic character of Anoplogastridae, and the third condition was recognized to be derived in Trachichthyidae and Monocentridae by Moore (1993). In my examination, however, the difference between the first and third conditions is unclear because the width of the base of the subocular shelf serially varies from narrow to wide conditions, and it was unable to recognize them as different characters (Fig. 3). Therefore, the condition of the subocular shelf is not used for the analysis.

TS 2. First and third infraorbitals (0: separated by second infraorbital; 1: attached)

Ingroups. The first and third infraorbitals are attached to each other in berycids and *Hoplobrotula armata* (Fig. 2C) (character 2-1), while they are separated by the second infraorbital in other ingroups (character 2-0).

Outgroups. The first and third infraorbitals are separated by the second infraorbital in all

outgroups.

TS 3. Third and fourth infraorbitals (0: autogenous; 1: fused)

Ingroups. The third and fourth infraorbitals are fused in stephanoberycids (Fig. 2B) (character 3-1), but autogenous in other ingroups (character 3-0).

Outgroups. The third and fourth infraorbitals are autogenous in all outgroups.

Remarks. In most species of Berycida examined, the second and third infraorbitals have two pores for the buccal nerves innervating canal neuromasts, and the fourth infraorbital possesses one pore. In stephanoberycids having five infraorbitals, therefore, the large "third" element with three pores is assumed to be caused by the fusion of the third and fourth infraorbitals.

TS 4. Antorbital (0: present; 1: absent)

Ingroups. The antorbital is present and situated anterior to the lateral ethmoid in holocentrids and *Polymixia japonica* (character 4-0), while it is absent in other ingroups (character 4-1).

Outgroups. All outgroups have the antorbital.

Other variations

Bony bridges supporting infraorbital canal. Among ingroups, differently developed bony bridges supporting the infraorbital canal are observed on the infraorbitals. For example, *Stephanoberyx monae* has no bridges on all elements (Fig. 2B), while *Paratrachichthys trailli* has incomplete bridges on the third to fifth (Fig. 4D) (the bridge on the fifth element is complete in the other specimen, HUMZ 66835, 154.2 mm SL). *Hoplostethus mediterraneus* has complete narrow bridges on the first and third to fifth elements (Fig. 4C), and *Neoniphon sammara* has complete wide bridges on the first infraorbital (Fig. 4B). Moreover, *Anomalops katoptron* has wide bridges which cover the canal almost completely and form tube-like structures on each bone (Fig. 4A). Accordingly, the degree of the development of bony

bridges varies serially among ingroups, and it cannot be separated into any distinct characters. Therefore, the conditions of bony bridges on the infraorbitals are not used for the analysis, as well as those on other cephalic sensory canals (supraorbital, otic, postotic, supratemporal, preopercular and mandibular canals, and temporal portion of main trunk canal) having the serial variations.

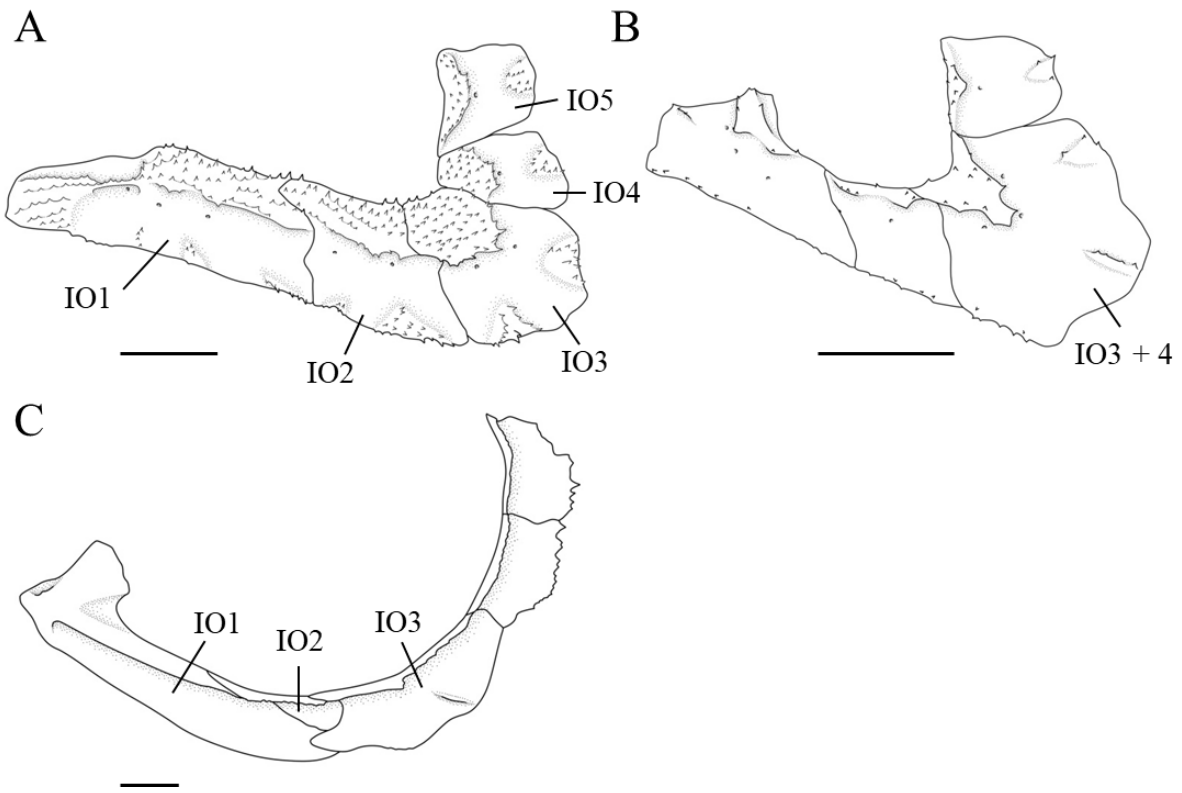

Figure 2. Lateral aspects of circumorbital bones in (A) *Hispidoberyx ambagiosus*, (B) *Stephanoberyx monae* and (C) *Beryx decadactylus*. IO1–5, first to fifth infraorbitals. Sixth infraorbital is depicted with neurocranium. Scales indicate 5 mm.

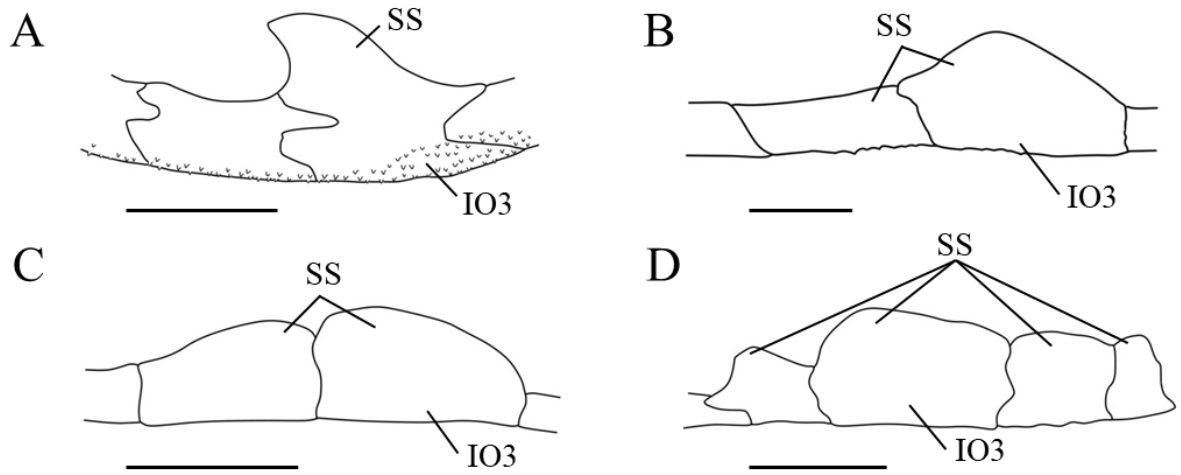

Figure 3. Dorsal aspects of circumorbital bones in (A) *Trachichthys australis*, (B) *Beryx decadactylus*, (C) *Diretmus argenteus* and (D) *Neoniphon sammara*. IO3, third infraorbital; SS, subocular shelf. Scales indicate 5 mm.

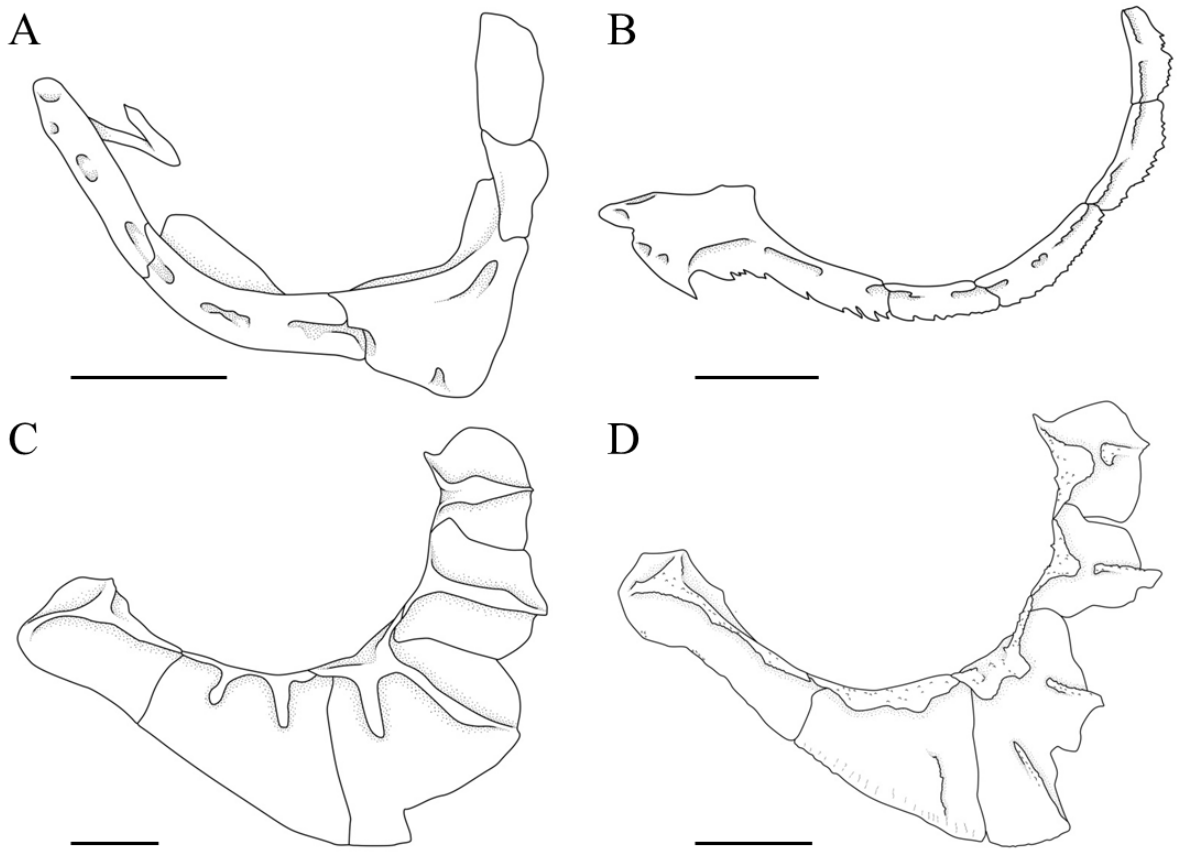

Figure 4. Lateral aspects of circumorbital bones in (A) *Anomalops katoptron*, (B) *Neoniphon sammara* (C) *Hoplostethus mediterraneus* and (D) *Paratrachichthys trailli*. Scales indicate 5 mm.

4-1-2. Neurocranium (Figs. 5, 6)

Description

The neurocranium is composed of the nasal, vomer, ethmoid, lateral ethmoid, frontal, pterosphenoid, basisphenoid, parasphenoid, sphenotic, pterotic, epiotic, prootic, intercalar, supraoccipital, exoccipital and basioccipital. Of these bones, the vomer, ethmoid, basisphenoid, parasphenoid, supraoccipital and basioccipital are unpaired elements, while the others are paired. An orbitosphenoid and autogenous parietal are absent.

The nasal is a reticular bone and situated on the anteriormost portion of the dorsal aspect of the neurocranium. This bone is attached to the nasal on the opposite side medially, the ethmoid posteromedially and the frontal posteriorly. The dorsal aspect of this bone has a wide groove for the supraorbital canal, which is continuous with that of the frontal. The anterior portion of the groove has one bony bridge (the canal under the bridge is closed in the left side of the other specimen, HUMZ 193670, 178.8 mm SL). The lateral, anterior and medial portions of the dorsal aspect of the bone are covered with small spines.

The vomer, a rhomboid bone, is located on the anteriormost portion of the ventral aspect of the neurocranium. This bone is attached to the parasphenoid posteriorly. The anterolateral portion of the bone is connected with the palatine and endopterygoid via the posterior palato-vomerine ligament. Granular teeth form a small tooth patch on the anteroventral surface of the bone.

The ethmoid is a large rectangular bone, situated on the anterodorsal portion of the neurocranium. This bone is attached to the nasal and frontal posterodorsally, and the lateral ethmoid ventrolaterally. An anterolateral process is weakly developed on the dorsal portion of the bone, which is connected with the maxilla via the ethmo-maxillary ligament.

The lateral ethmoid, located on the anterolateral portion of the neurocranium, is attached to the frontal dorsally and the ethmoid ventromedially. This bone ventrolaterally has a condyle articulating with the glenoid cavity of the first infraorbital.

The frontal is a large bone situated the central portion of the dorsal aspect of the neurocranium. This bone is attached to the nasal anteriorly, the lateral ethmoid and lateral ethmoid anteroventrally, the frontal on the opposite side medially, the supraoccipital posteromedially, the epiotic posteriorly, the pterotic, sphenotic and sixth infraorbital posterolaterally, and the pterosphenoid posteroventrally. The dorsal surface of the bone has bony ridges (with H-shaped pattern sensu Kotlyar, 1991a or Y-shaped pattern sensu Moore, 1993) covered with small spines and wide grooves for the supraorbital canal. The grooves of the bone are continuous with that of the nasal anteriorly, the pterotic and sixth infraorbital posterolaterally, and the frontal on the opposite side medially. The commissure of the groove on each side is largely expanded (= median mucus cavity sensu Johnson & Patterson, 1993) and continuous with the groove on the extrascapula for the supratemporal canal.

The pterosphenoid is situated on the posterodorsal portion of the orbit and attached to the frontal dorsally, the sphenotic and prootic posteriorly, and the basisphenoid posteroventrally.

The basisphenoid, a small rod-like bone, is located on the posteroventral portion of the orbit. This bone is attached to the pterosphenoid and prootic posterodorsally, and the parasphenoid anteroventrally.

The parasphenoid is a long bone situated the central portion of the ventral aspect of the neurocranium. This bone is attached to the vomer anteriorly, the prootic posterodorsally and the basioccipital posteriorly. The central portion of this bone has a small ascending process with a foramen for the internal carotid artery situated posterior to its base.

The sphenotic, located on the posterior portion of the orbit, is attached to the pterosphenoid anteromedially, the frontal dorsomedially, the sixth infraorbital dorsally, the pterotic posteriorly and the prootic ventrally. An oblong socket is present between the sphenotic, prootic and pterotic, and articulates with the dorsal condyle of the hyomandibula.

The pterotic, situated on the posterolateral portion of the neurocranium, is attached to the sphenotic anteriorly, the sixth infraorbital anterodorsally, the frontal anteromedially, the

epiotic posteromedially, the intercalar posteriorly and the prootic anteroventrally. The dorsal surface of this bone has a wide groove for the otic canal, which is continuous with that of the extrascapula posteriorly and the preopercle posteroventrally.

The epiotic is situated on the posterodorsal portion of the neurocranium and attached to the frontal anteriorly, the supraoccipital medially, the exoccipital posteroventrally and the pterotic laterally. This bone dorsally has a facet articulating with the dorsal limb of the posttemporal.

The prootic, located on the posterior portion of the orbit, is attached to the basisphenoid and pterosphenoid anteriorly, the sphenotic and pterotic dorsally, and the parasphenoid anteroventrally. The anteroventral portion of the bone suspends the first pharyngobranchial. The anterodorsal portion of the bone has the trigemino-facial chamber.

The intercalar, a small bone situated on the posterior portion of the neurocranium, is attached to the pterotic anterolaterally and the exoccipital posteromedially. This bone is posterodorsally connected with the ventral limb of the posttemporal via a short ligament.

The supraoccipital, located on the posterodorsal portion of the neurocranium, is attached to the frontal anterolaterally, the epiotic posterolaterally and the exoccipital posteroventrally. The dorsal midline of the bone has a thin and slightly low bony crest. The spina occipitalis (sensu Stiassny, 1986) is weakly developed on the posteroventral portion of the bone; its tip not reaching the foramen magnum.

The exoccipital is situated on the posterior portion of the neurocranium and attached to the supraoccipital and epiotic anterodorsally, the intercalar anterolaterally, the basioccipital ventrally, and the exoccipital on the opposite side medially. The posterior portion of this bone has a condyle articulating with the first abdominal vertebra. The condyles of the exoccipitals on both sides are detached to each other.

The basioccipital, located on the posteroventral portion of the neurocranium, is attached to the parasphenoid anteriorly and the exoccipital dorsally, and articulates with the first abdominal vertebra posteriorly.

Character recognition

TS 5. Vomerine teeth (0: present; 1: absent)

Ingroups. Vomerine teeth are absent in stephanoberycids, *Gibberichthys pumilus*, *Rondeletia loricata*, melamphaids, *Anomalops katoptron*, *Monocentris japonica*, *Anoplogaster cornuta*, *Diretmus argenteus* and *Velifer hypselopterus* (character 5-1), whereas it is present in other ingroups (character 5-0).

Outgroups. *Neoscopelus microchir* and *Hime japonica* have vomerine teeth. *Trachinocephalus trachinus* was coded as "?" due to absence of the vomer.

TS 6. Size of ethmoid (0: large; 1: small)

Ingroups. The ethmoid is small and confined to the dorsomedial portion of the lateral ethmoid in trachichthyids, *Anomalops katoptron*, *Monocentris japonica*, *Anoplogaster cornuta*, *Diretmus argenteus* and *Velifer hypselopterus* (character 6-1), whereas it is large and extends well beyond the lateral ethmoid (character 6-0).

Outgroups. The ethmoid is large and extends anterior to the lateral ethmoid in all outgroups.

TS 7. Anterolateral process of ethmoid (0: absent or weakly developed; 1: well developed)

Ingroups. A well developed anterolateral process is present in melamphaids and berycids (Fig. 6E, F) (character 7-1), while it is absent or weakly developed in other ingroups (character 7-0).

Outgroups. The process is absent or weakly developed in all outgroups.

TS 8. Y-shaped pattern of frontal ridges (0: absent; 1: present)

Ingroups. A Y-shaped pattern of the frontal ridges is present in *Hispidoberyx ambagiosus*, stephanoberycids and *Gibberichthys pumilus* (character 8-1), while it is absent in other ingroups (character 8-0).

Outgroups. All outgroups lack such a pattern of the frontal ridges.

TS 9. Orbitosphenoid (0: absent; 1: present)

Ingroups. The orbitosphenoid is present and located anterior to the pterosphenoid in trachichthyids, *Anomalops katoptron*, *Monocentris japonica*, *Anoplogaster cornuta*, *Diretmus argenteus*, berycids, holocentrids, *Polymixia japonica* and *Velifer hypselopterus* (character 9-1), whereas it is absent in other ingroups (character 9-0).

Outgroups. All outgroups lack an orbitosphenoid.

TS 10. Basisphenoid (0: present; 1: absent)

Ingroups. The basisphenoid is absent in *Barbourisia rufa*, *Cetostoma regani*, melamphaids, *Diretmus argenteus* and *Hoplobrotula armata* (character 10-1), while it is present in other ingroups (character 10-0).

Outgroups. *Trachinocephalus trachinus* and *Hime japonica* have the basisphenoid, whereas *Neoscopelus microchir* lacks it.

TS 11. Exoccipital condyles on both sides (0: attached; 1: detached)

Ingroups. The exoccipital condyles on both sides are detached in *Hispidoberyx ambagiosus*, stephanoberycids, *Gibberichthys pumilus*, *Rondeletia loricata*, *Barbourisia rufa* and *Cetostoma regani* (character 11-1), but attached medially in other ingroups (character 11-0).

Outgroups. The exoccipital condyles are attached in all outgroups.

Other variations

Contact of nasals on both sides. Various conditions of the contact of the nasals on both sides are observed among ingroups. For instance, the nasals are attached at the entire medial margin in *Stephanoberyx monae* (Fig. 6A), while they are attached at the posterior half of the medial margin in *Hispidoberyx ambagiosus* (Fig. 5), and detached to each other in holocentrids (Fig. 6D). The extent of the contact of the nasals, however, serially varies among ingroups, and distinct characters cannot be clearly defined. Therefore, the conditions of the contact of the nasals are not used for the analysis.

Patterns of frontal ridges. Moore (1993) recognized a modified X pattern of the frontal ridges as one of synapomorphies of Trachichthyoidei defined by him. In addition, Johnson & Patterson (1993) noted that a transformation series could be inferred among the modified X pattern and other patterns in berycids and holocentrids. Although the similarity of the pattern of the frontal ridges among trachichthyoids was also confirmed in this study, it is difficult to define and separate the condition in trachichthyoids from berycid and holocentrid conditions due to complexity and variation among those conditions. In this study, therefore, the conditions of patterns of the frontal ridges are not used for the analysis, except for a Y-shaped pattern in *Hispidoberyx ambagiosus*, stephanoberycids and *Gibberichthys pumilus* (TS 8), which can be clearly defined.

Parietal. This study found that an autogenous parietal was absent in *Hispidoberyx ambagiosus*, while Kotlyar (1991a) described that *H. ambagiosus* has an autogenous parietal posterior to the frontal and that the parietal possesses a spiny crest along the posterior margin. However, the latter feature, a crest on the posterior margin of the parietal, is absent in other members of Berycida observed in this study. On the other hand, the anteromedial portion of the extrascapula in *H. ambagiosus* posteromedially has a spiny crest and occupies the region where the parietal is located, according to Kotlyar (1991a). Moreover, the extrascapula illustrated by him appears to be shorter anteromedially than the bone examined in this study (Fig. 19). Consequently, it is assumed that Kotlyar (1991a) mistakenly recognized the anteromedial portion of the extrascapula as the parietal. On the other hand, this study found that the posterior margin of the frontal in *H. ambagiosus* is slightly convex. Because the parietal is usually located on this region in other taxa, this condition suggests that the parietal may be fused with the frontal anteriorly. However, to confirm this inference, ontogenetic examination is needed.

In addition, this study also recognized that an autogenous parietal was absent in *Acanthochaenus luetkenii* and *Gibberichthys pumilus*, as Kotlyar (1991b) examined in the

former species and other species of *Gibberichthys* [contra Johnson & Patterson (1993), who recognized the bone in *Gibberichthys*, according to a character matrix of Ctenosquamata (see their table 3)]. Although the posterior margin of the frontal lacks a convexity, and then it is implied that the parietal may be lost in these two taxa, ontogenetic examination is needed to confirm this assumption.

Accordingly, because the reason of the absence of the autogenous parietal in *H. ambagiosus*, *A. luetkenii* and *G. pumilus* cannot be determined, these conditions of the parietal are not used for the analysis due to uncertainty of the homology.

Spina occipitalis. The spina occipitalis is a ventral expansion of the supraoccipital that separates the exoccipitals on both sides and reaches the foramen magnum, and has been considered as a synapomorphy of Acanthomorpha excluding lampridiforms (Johnson & Patterson, 1993; Davesne et al., 2016). However, the degree of development of the spina occipitalis serially varies among ingroups, and it is unable to separate it into any distinct characters. Accordingly, the condition of the spina occipitalis is not used for the analysis.

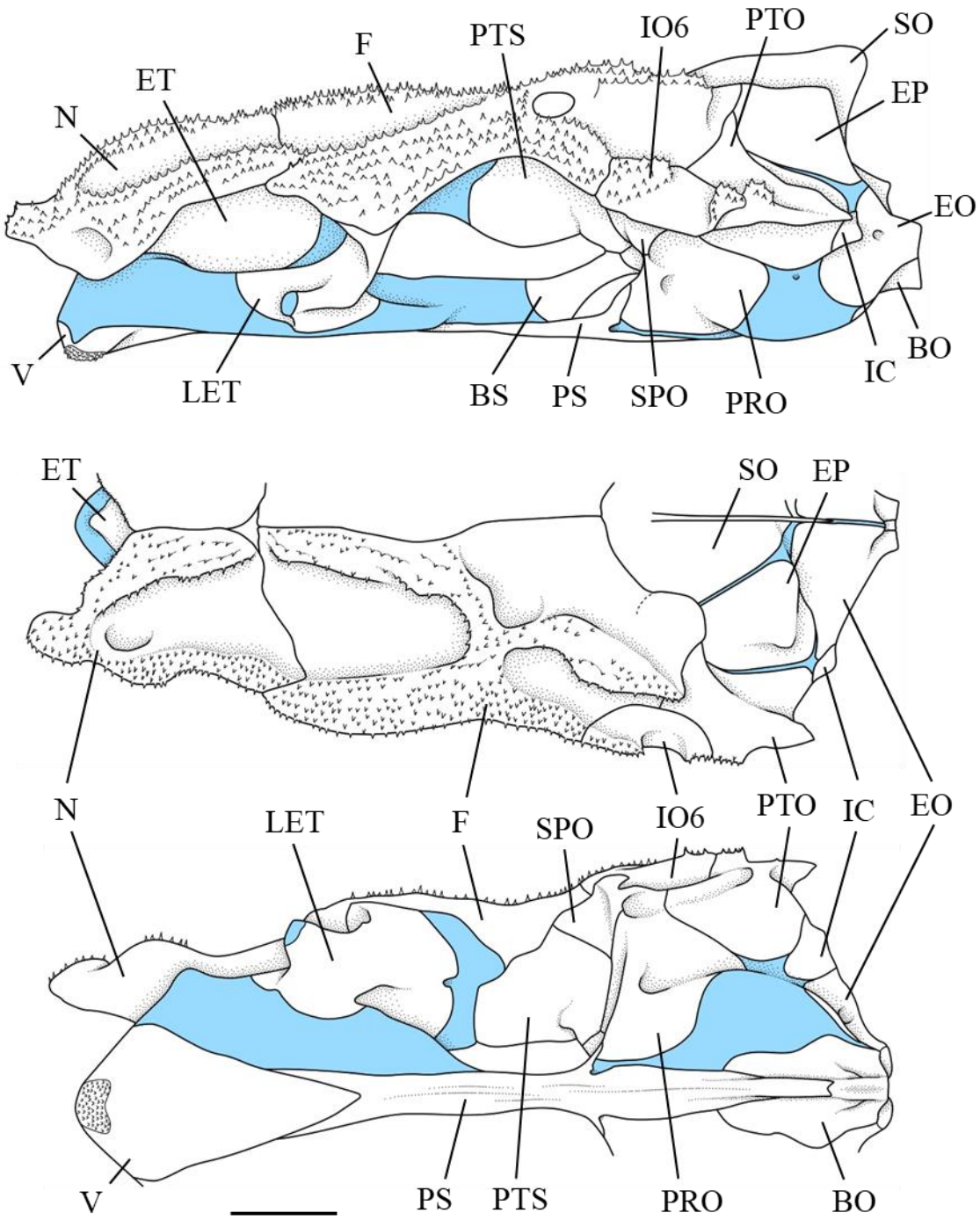

Figure 5. Lateral (upper), dorsal (middle) and ventral (lower) aspects of neurocranium in *Hispidoberyx ambagiosus*. BO, basioccipital; BS, basisphenoid; ET, ethmoid; EO, exoccipital; EP, epiotic; F, frontal; IC, intercalar; IO6, sixth infraorbital; LET, lateral ethmoid; N, nasal; PRO, prootic; PS, parasphenoid; PTO, pterotic; PTS, pterosphenoid; SO, supraoccipital; SPO, sphenotic; V, vomer. Scale indicates 5 mm.

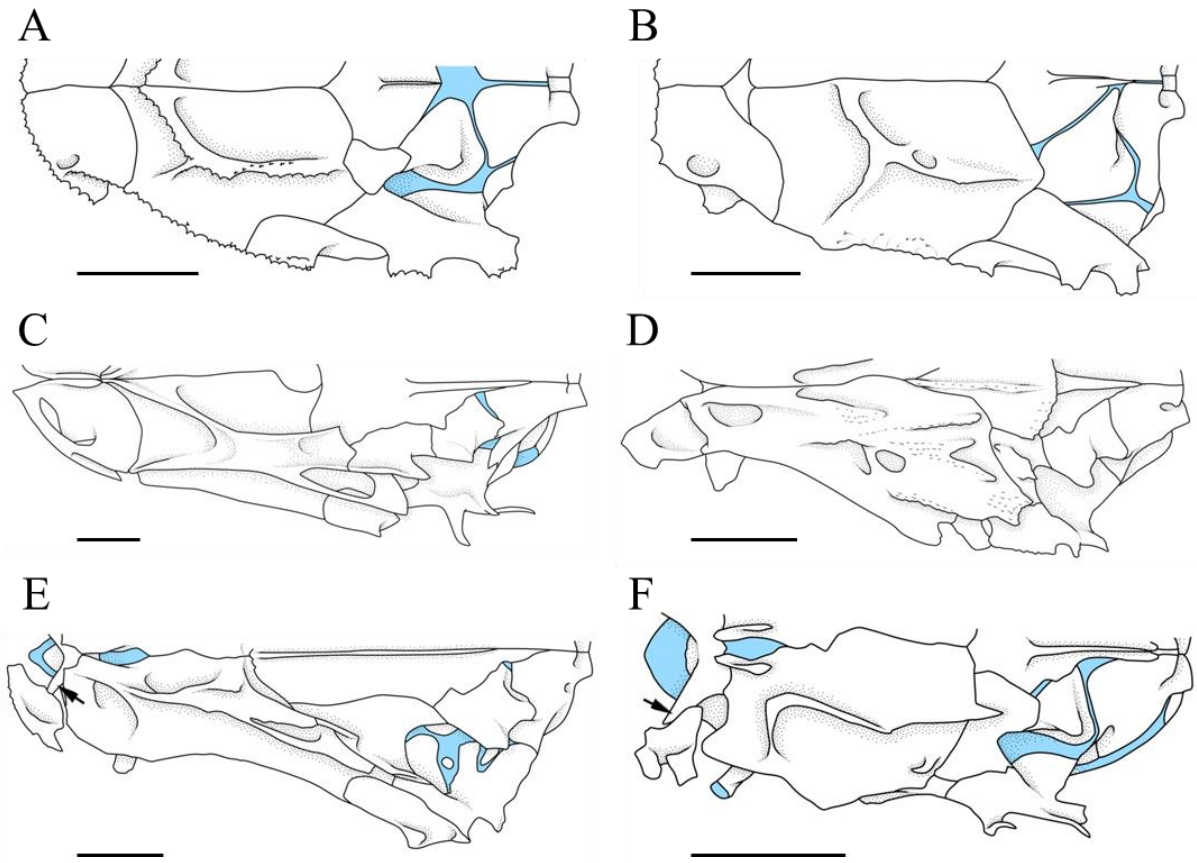

Figure 6. Dorsal aspects of neurocranium in (A) *Stephanoberyx monae*, (B) *Gibberichthys pumilus*, (C) *Hoplostethus mediterraneus*, (D) *Ostichthys japonicus*, (E) *Centroberyx lineatus* and (F) *Melamphaes typhlops*. Arrows indicate anterolateral process of ethmoid. F is shown as mirror image. Scales indicate 5 mm.

4-1-3. Jaws (Figs. 7–10)

Description

The jaws comprise the premaxilla, maxilla and supramaxilla in the upper jaw, and the dentary, anguloarticular, retroarticular and coronomeckelian in the lower jaw. The lateral aspects of the premaxilla, maxilla, supramaxilla, dentary and anguloarticular are covered with small spines and spinulose ridges.

The premaxilla, a long L-shaped bone, has the ascending, articular and alveolar processes. The ascending process is short and almost in same height with the articular process. The dorsomedial portion of the ascending process is attached to the rostral cartilage. The ascending process is connected to the palatine via the palato-premaxillary ligament. The articular process is situated just posterior to the ascending process, with a distinct incision between both processes. Granular teeth form a narrow tooth band on the ventral margin of the alveolar process. The postmaxillary process is absent or slightly developed on the anterior portion of the alveolar process.

The maxilla is a long rod-like bone, comprising an anterior head and a posterior shaft. The head of the maxilla has the lateral process, and premaxillary and cranial condyles. The lateral process is dorsomedially connected with the ethmoid via the ethmo-maxillary ligament and dorsally attached to the anterior process of the palatine. The premaxillary condyle anterolaterally articulates with the articular process of the premaxilla via a meniscus. The cranial condyle medially articulates with the vomer via a meniscus. This bone lacks a median palato-maxillary ligament.

The supramaxilla is a small wedge-shaped bone, located on the posterior portion of the upper jaw. This bone is ventromedially attached to the shaft of the maxilla.

The dentary, a V-shaped bone, is situated on the anterior portion of the lower jaw. The dorsal margin of the bone has a narrow tooth band of granular teeth. The ventral portion of this bone has a wide and shallow groove for the mandibular canal, which is posteriorly

continuous with that of the anguloarticular. The anterior part of the groove has a bony bridge. The Meckelian cartilage, a long rod-like element, is attached to the central portion of the medial surface of this bone and the anguloarticular.

The anguloarticular is a rectangular bone, situated on the posterior portion of the lower jaw. The anterior portion of the bone is inserted to a posterior notch of the dentary. This bone is posteroventrally attached to the retroarticular and posteriorly has a glenoid cavity articulating with the quadrate. The ventral portion of the bone has a wide and shallow groove for the mandibular canal, which is continuous with that of the dentary anteriorly and the preopercle posteriorly.

The retroarticular, a small oblong bone, is situated on the posteroventral corner of the lower jaw. This bone is attached to the anguloarticular anteriorly and connected with the interopercle via a ligament posterodorsally.

The coronomeckelian is a tiny bone, located on the lateral surface of the posterior end of the Meckelian cartilage.

Character recognition

TS 12. Number of supramaxillae (0: zero; 1: one; 2: two) (ordered as 0-1-2)

Ingroups. *Scopelogadus mizolepis* and *Velifer hypselopterus* have no supramaxilla (Fig. 10C) (character 12-0), while berycids, holocentrids and *Polymixia japonica* have two elements (Fig. 10A, B) (character 12-2), and other ingroups have a single elements (character 12-1).

Outgroups. *Neoscopelus microchir* has one supramaxilla, whereas *Hime japonica* and *Trachinocephalus microchir* have two and no element, respectively.

TS 13. Median palato-maxillary ligament (0: present; 1: absent)

Ingroups. The median palato-maxillary ligament connecting the anterior portion of the maxillary shaft and the anteroventral margin of the palatine is present in *Gibberichthys*

pumilus, *Rondeletia loricata*, *Cetostoma regani* and *Polymixia japonica* (Fig. 9) (character 13-0), while the ligament is absent in other ingroups (character 13-1).

Outgroups. All outgroups have the ligament.

Other variations

Incision between ascending and articular processes of premaxilla. Different conditions of the incision between the ascending and articular processes of the premaxilla are observed among ingroups. For instance, the holocentrids have a distinct incision (Fig. 10A), whereas the ascending and articular processes are coalesced into a single process without an incision in *Cetostoma regani* (Fig. 10D). However, the degree of the development of the incision serially varies among ingroups, and it is unable to separate it into any distinct characters. Accordingly, the conditions of the incision between the ascending and articular processes are not used for the analysis.

Postmaxillary process of premaxilla. The postmaxillary process of the premaxilla variously develops among ingroups. For example, holocentrids have a well developed postmaxillary process (Fig. 10A), while *Beryx decadactylus* has a weakly developed process (Fig. 10B) and *Cetostoma regani* completely lacks it (Fig. 10D). The degree of the development of the process, however, serially varies among ingroups, and clearly defined characters cannot be distinguished. Consequently, the conditions of the postmaxillary process are not used for the analysis.

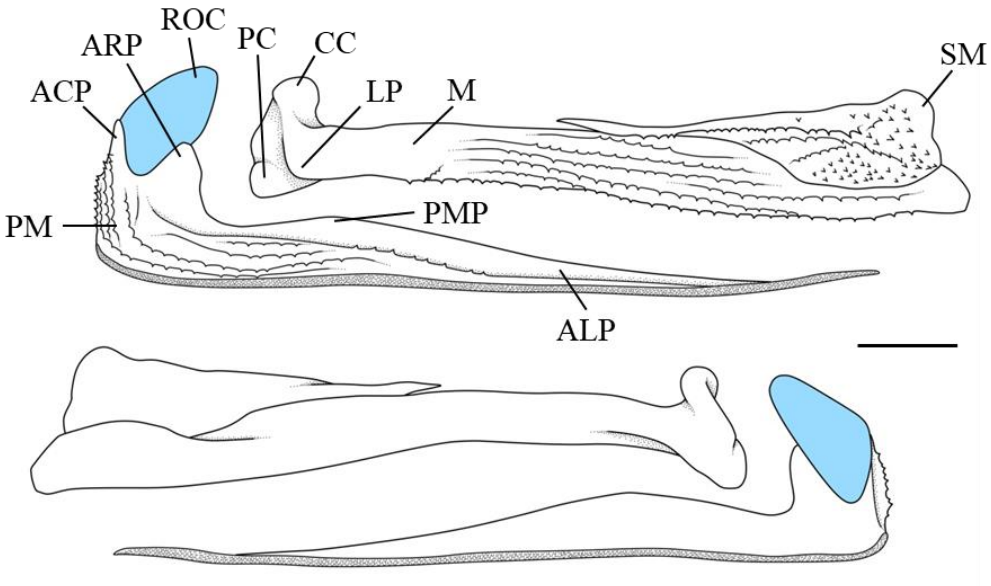

Figure 7. Lateral (upper) and medial (lower) aspects of upper jaw in *Hispidoberyx ambagiosus*. ACP, ascending process; ALP, alveolar process; ARP, articular process; CC, cranial condyle; LP, lateral process; M, maxilla; PC, premaxillary condyle; PM, premaxilla; PMP, post maxillary process; ROC, rostral cartilage; SM, supramaxilla. Scale indicates 5 mm.

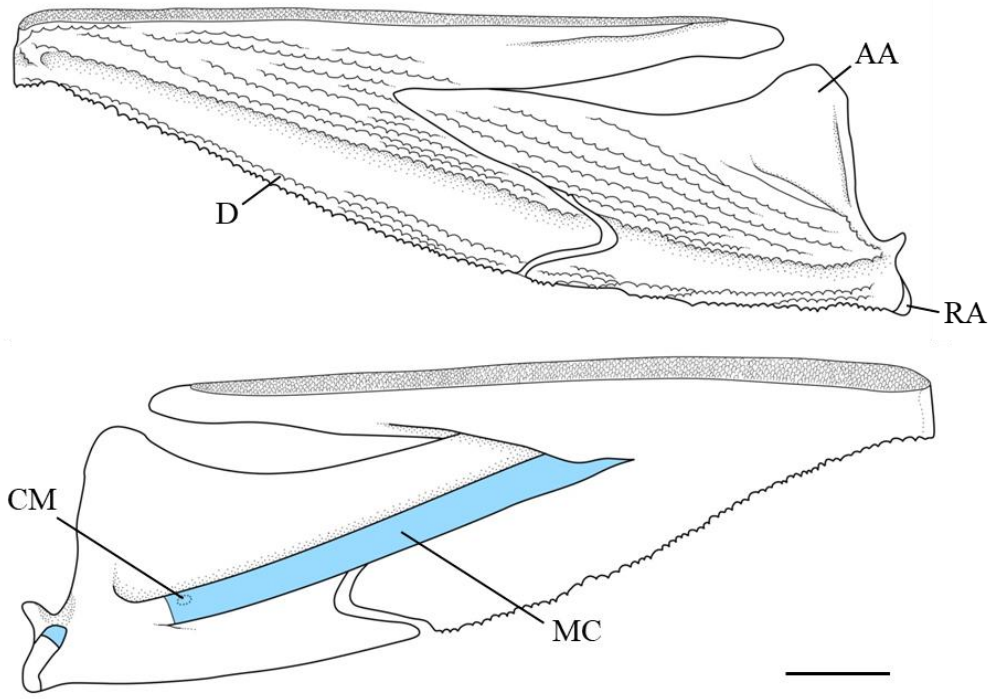

Figure 8. Lateral (upper) and medial (lower) aspects of lower jaw in *Hispidoberyx ambagiosus*. AA, anguloarticular; CM, coronomeckelian; D, dentary; MC, Meckelian cartilage; RA, retroarticular. Scale indicates 5 mm.

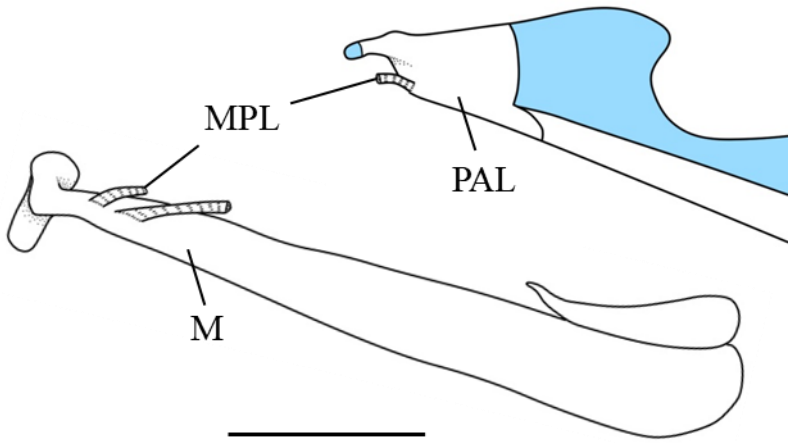

Figure 9. Lateral aspects of upper jaw and anterior part of suspensorium in *Rondeletia loricata*. M, maxilla; MPL, median palato-maxillary ligament; PAL, palatine. Scale indicates 5 mm.

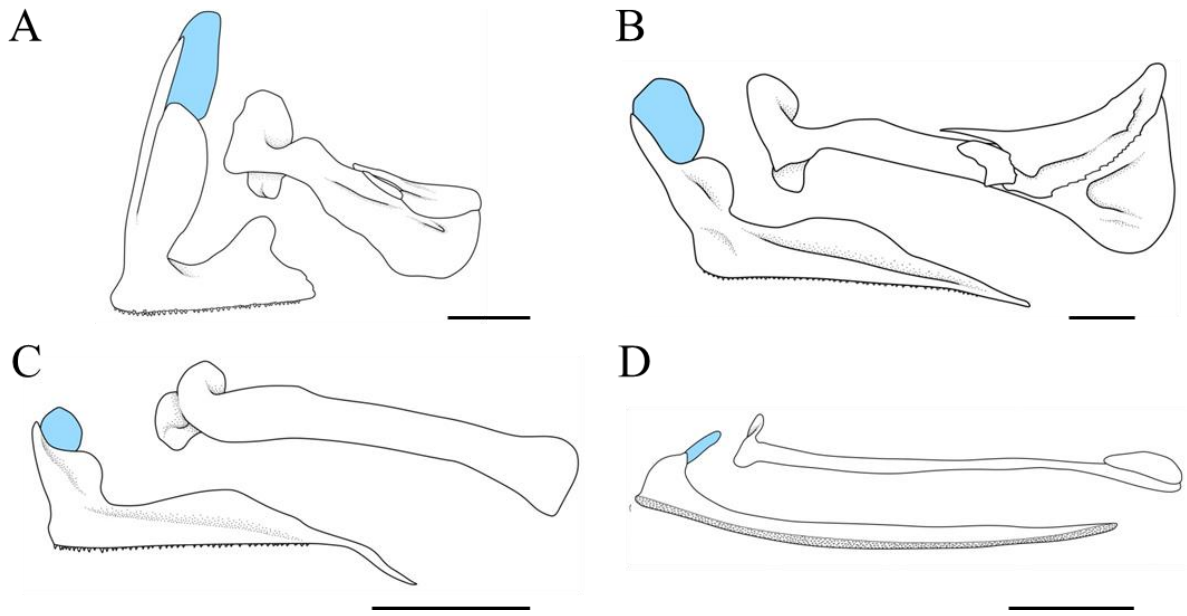

Figure 10. Lateral aspect of upper jaw in (A) *Neoniphon sammara*, (B) *Beryx decadactylus* (C) *Scopelogadus mizolepis* and (D) *Cetostoma regani*. Scales indicate 5 mm.

4-1-4. Suspensorium and opercular bones (Figs. 11–13)

Description

The suspensorium is composed of the palatine, endopterygoid, ectopterygoid, metapterygoid, quadrate, symplectic and hyomandibula. The opercular bones comprise the preopercle, opercle, interopercle and subopercle. The lateral aspects of the opercular bones are covered with many small spines and spinulose ridges.

The palatine is a stick-like bone, located on the anteriormost portion of the suspensorium. This bone anteriorly has a process with cartilaginous tip which articulates with the maxillary head. The dorsal portion of the anterior process is connected with the ascending process of the premaxilla via the palato-premaxillary ligament which is partially confluent with the ethmo-maxillary ligament (Fig. 12). The posterodorsal portion of the medial aspect of the bone is connected with the vomer via the posterior palato-vomerine ligament. This bone is attached to the ectopterygoid posteroventrally and the endopterygoid posteromedially. In the lateral aspect, this bone is posteriorly separated from the endopterygoid by a cartilaginous band. A narrow tooth band formed by granular teeth is present on the ventral margin of the bone.

The endopterygoid, a thin oval bone, is situated on the anterodorsal portion of the suspensorium. In the medial aspect, this bone is attached to the palatine anteriorly, the ectopterygoid ventrally and the metapterygoid posteriorly. In the lateral aspect, this bone is separated from those bones by a cartilaginous band. The anterior margin of the medial aspect of the bone is connected with the vomer via the posterior palato-vomerine ligament. This bone lacks teeth.

The ectopterygoid, a rod-like bone, is located on the anteroventral portion of the suspensorium. This bone is attached to the palatine anteriorly and the quadrate posteroventrally, and separated from the metapterygoid via a cartilaginous band posterodorsally. This bone is dorsally attached to the endopterygoid and separated from it by a cartilaginous band in the medial and lateral aspects, respectively. This bone lacks teeth.

The metapterygoid is an angular bone, situated on the central portion of the suspensorium. This bone is separated from the ectopterygoid anteroventrally and the quadrate ventrally by a cartilaginous band, and attached to the hyomandibula posterodorsally. This bone is anteriorly attached to the endopterygoid and separated from it by a cartilaginous band in the medial and lateral aspects, respectively.

The quadrate is a triangular bone, located on the posteroventral portion of the suspensorium. This bone is attached to the ectopterygoid anterodorsally and the preopercle posteroventrally, and separated from the metapterygoid by a cartilaginous band dorsally. The medial aspect of the bone has a socket into which the symplectic is inserted. The ventral condyle of the bone articulates with a glenoid cavity of the anguloarticular.

The symplectic, a small stick-like bone, is situated on the posteroventral portion of the suspensorium. The anteroventral tip of this bone is capped with a tiny cartilage and inserted into the socket of the quadrate. The dorsal tip of the bone is separated from the hyomandibula by a cartilage, which articulates with the interhyal.

The hyomandibula is a large T-shaped bone, situated on the posterodorsal portion of the suspensorium. This bone is attached to the metapterygoid anteroventrally and the preopercle posteriorly, and separated from the symplectic by a cartilage ventrally. This bone dorsally has a single oblong cartilaginous condyle articulating with the socket formed by the sphenotic, pterotic and prootic. The posterodorsal portion of the bone has a cartilaginous condyle which articulates with a glenoid cavity of the opercle.

The preopercle, a large L-shaped bone, is located on the anterior portion of the opercular bones. This bone is attached to the hyomandibula anterodorsally, the quadrate anteroventrally and the subopercle ventromedially. The lateral aspect of this bone has a wide and shallow groove for the preopercular canal which is continuous with those of the anguloarticular anteroventrally and the pterotic dorsally. The posterior margin of the bone lacks a prominent spine.

The opercle is a triangular bone, situated on the posterodorsal portion of the opercular bones. The anterodorsal portion of the bone has a glenoid cavity articulating with the posterior condyle of the hyomandibula. This bone posteroventrally attached to the subopercle. The posterodorsal margin of the bone has a prominent spine with ridges.

The interopercle is an oblong bone, situated on the anteroventral portion of the opercular bones. This bone is attached to the preopercle laterally and the subopercle posterodorsally. The anteroventral portion of this bone is connected with the retroarticular via a ligament. The central portion of the medial aspect of the bone is connected with the epihyal and interhyal via a ligament.

The subopercle, a rectangular bone, is located on the posteroventral portion of the opercular bones. This bone is attached to the interopercle anteroventrally and the opercle anterodorsally.

Character recognition

TS 14. Palatine teeth (0: present; 1: absent)

Ingroups. Palatine teeth are absent in stephanoberycids, *Gibberichthys pumilus*, *Rondeletia loricata*, *Barbourisia rufa*, melamphaids, *Diretmus argenteus* and *Velifer hypselopterus* (character 14-1), whereas those are present in other ingroups (character 14-0).

Outgroups. All outgroups have palatine teeth.

TS 15. Ectopterygoid teeth (0: present; 1: absent)

Ingroups. The ectopterygoid possesses teeth in *Barbourisia rufa*, *Cetostoma regani*, *Holocentrus adscensionis*, *Neoniphon sammara*, *Polymixia japonica* and *Lates mariae* (character 15-0), while this bone lacks teeth in other ingroups (character 15-1). Because *Anomalops katoptron* and *Monocentris japonica* have both conditions, “0” and “1” are coded for them.

Outgroups. *Neoscopelus microchir* and *Hime japonica* have ectopterygoid teeth, whereas *Trachinocephalus trachinus* lacks them.

Remarks. Zehren (1979) reported that *Anomalops katoptron* and *Monocentris japonica* lack ectopterygoid teeth. In this study, small tooth patch is present on the ectopterygoid in specimens of *A. katoptron* (KPM-NI 10182, 87.1 mm SL) and *M. japonica* (HUMZ 33613, 136.0 mm SL), while it is absent in other specimens of *A. katoptron* (HUMZ 40200, unmeasured) and *M. japonica* (HUMZ 40406, 108.9 mm SL).

TS 16. Endopterygoid teeth (0: present; 1: absent)

Ingroups. *Polymixia japonica* has endopterygoid teeth (character 16-0), but other ingroups lack them (character 16-1). Because *Anomalops katoptron* and *Monocentris japonica* have both conditions, "0" and "1" are coded for them.

Outgroups. Endopterygoid teeth are present in *Neoscopelus microchir* and *Hime japonica*, while those are absent in *Trachinocephalus trachinus*.

Remarks. Zehren (1979) reported that *Anomalops katoptron* and *Monocentris japonica* lack endopterygoid teeth. In this study, small tooth patch is present on the endopterygoid in specimens of *A. katoptron* (KPM-NI 10182, 87.1 mm SL) and *M. japonica* (HUMZ 33613, 136.0 mm SL), while it is absent in other specimens of *A. katoptron* (HUMZ 40200, unmeasured) and *M. japonica* (HUMZ 40406, 108.9 mm SL).

TS 17. Ethmo-maxillary and palato-premaxillary ligaments (0: separated; 1: partially confluent)

Ingroups. The ethmo-maxillary and palato-premaxillary ligaments are partially confluent in *Hispidoberyx ambagiosus*, stephanoberycids, *Gibberichthys pumilus*, *Rondeletia loricata*, *Barbourisia rufa*, *Diretmus argenteus* and *Hoplobrotula armata* (Fig. 12) (character 17-1), whereas those ligaments are separated in other ingroups (character 17-0). *Cetostoma regani* and *Velifer hypselopterus* are coded as "?" due to absence of those ligaments.

Outgroups. Those ligaments are separated in *Neoscopelus microchir* and *Hime japonica*. *Trachinocephalus trachinus* is coded as "?" due to absence of the palato-maxillary ligament.

TS 18. Number of dorsal condyles of hyomandibula (0: two; 1: one)

Ingroups. The hyomandibula has two dorsal condyles in holocentrids, *Polymixia japonica*, *Hoplobrotula armata*, *Lateolabrax japonicus*, *Lates mariae* and *Trachurus japonicus* (character 18-0), while this bone has a single condyle in other ingroups (character 18-1).

Outgroups. The number of dorsal condyles of the hyomandibula is two in all outgroups.

Other variations

Preopercular spine. The preopercular spines are variously developed among ingroups. For example, *Hoplostethus mediterraneus* and *Neoniphon sammara* have a single prominent spine (Fig. 13A, B), whereas *Anoplogaster cornuta* has one weak spine (Fig. 13C), and *Diretmus argenteus* completely lacks spines (Fig. 13D). The degree of the development of the spine, however, serially varies among ingroups, and it cannot be separated into any distinct characters. Therefore, the conditions of the preopercular spine are not used for the analysis.

Opercular spines. Differently developed opercular spines are observed among ingroups. For instance, *Hispidoberyx ambagiosus* has a single prominent spine (Fig. 11), while *Hoplostethus mediterraneus* and *Neoniphon sammara* have two moderately or weakly developed spines (Fig. 13A, B). Moreover, *Anoplogaster cornuta* has three weak spines (Fig. 13C), and *Diretmus argenteus* completely lacks spines (Fig. 13D). However, the homology of those spines in ingroups is unclear because the shape and position of each spine are various among ingroups. In addition, the degree of the development of each spine serially varies among ingroups, and clearly defined characters cannot be distinguished. Consequently, the conditions of the opercular spines are not used for the analysis.

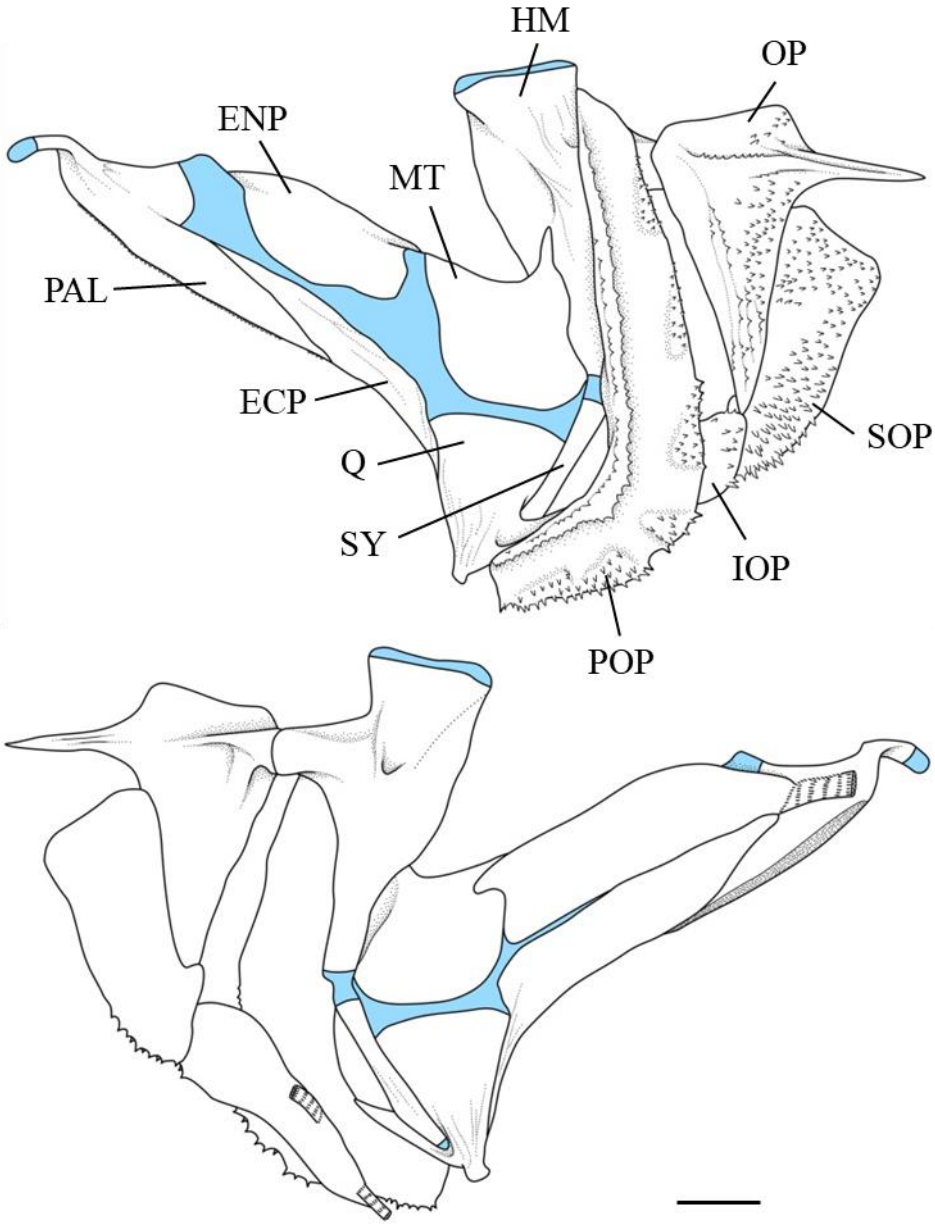

Figure 11. Lateral (upper) and medial (lower) aspects of suspensorium and opercular bones in *Hispidoberyx ambagiosus*. ECP, ectopterygoid; ENP, endopterygoid; HM, hyomandibular; IOP, interopercle; MT, metapterygoid; OP, opercle; PAL, palatine; POP, preopercle; Q, quadrate; SOP, subopercle; SY, symplectic. Scale indicates 5 mm.

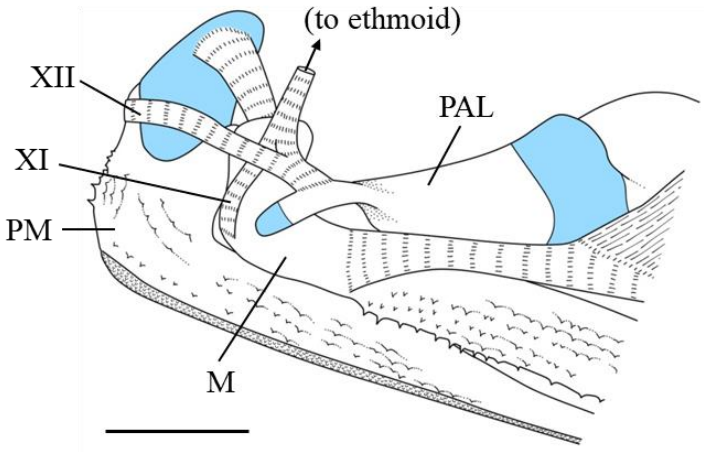

Figure 12. Lateral aspects of anterior portions of upper jaw and suspensorium in *Hispidoberyx ambagiosus*. M, maxilla; PAL, palatine; PM, premaxilla; XI, ethmo-maxillary ligament; XII, palato-premaxillary ligament. Scale indicates 5 mm.

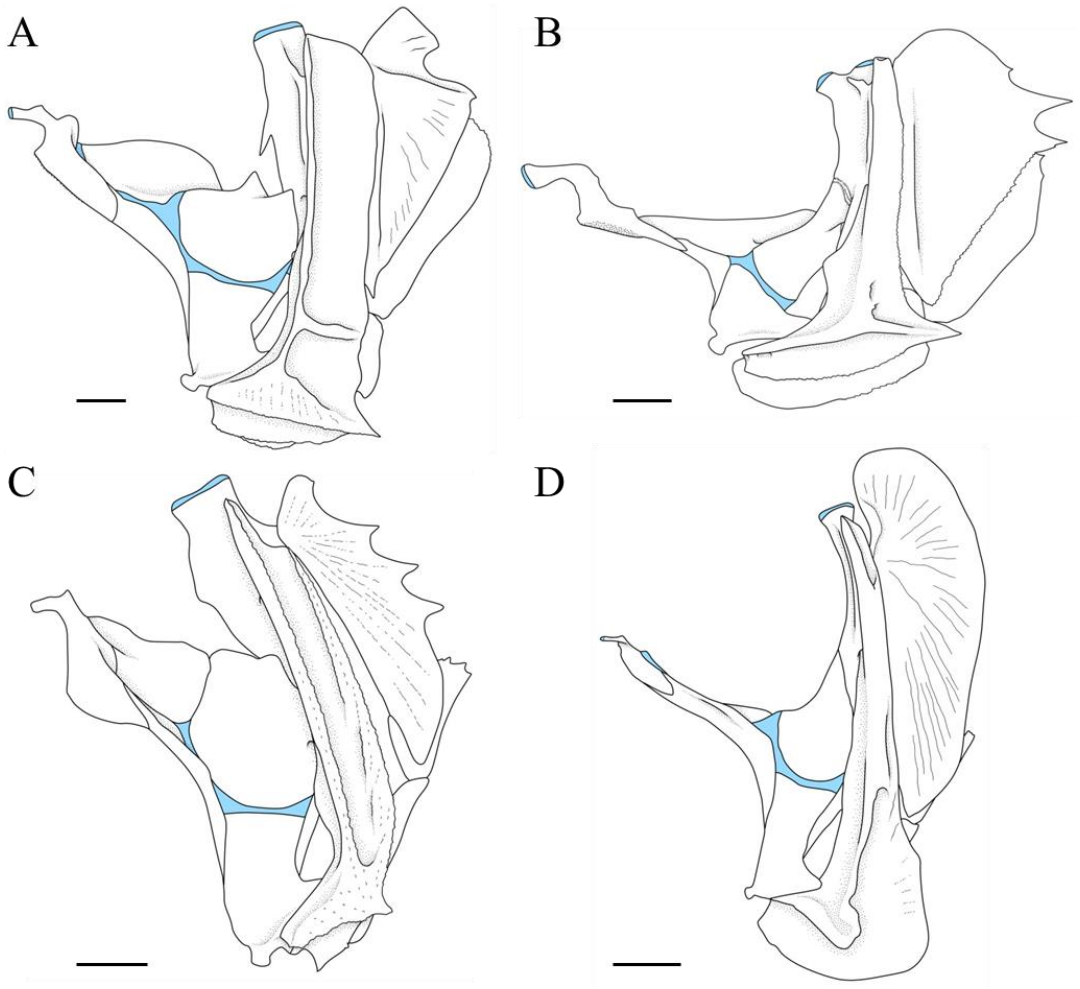

Figure 13. Lateral aspects of suspensorium and opercular bones in (A) *Hoplostethus mediterraneus*, (B) *Neoniphon sammara*, (C) *Anoplogaster cornuta* and (D) *Diretmus argenteus*. Scales indicate 5 mm.

4-1-5. Hyoid arch (Figs. 14–16)

Description

The hyoid arch consists of the basihyal, hypohyals, ceratohyal, epihyal, interhyal, urohyal and branchiostegal rays. The basihyal is described and discussed in the next section, Branchial arches.

The hypohyals, comprising the dorsal and ventral elements, are located on the anterior portion of the hyoid arch. The anteromedial portions of two elements articulate with the first basibranchial. The dorsal and ventral hypohyals are attached to each other directly or via a narrow cartilaginous band, and posteriorly connected with the ceratohyal via a connective tissue or cartilaginous bands. The anterior portion of the medial aspect of the dorsal element has a ligament connected with the first hypobranchial. The anterior portion of the medial aspect of the ventral element has two ligaments; the ventral one connected with the urohyal and the dorsal one with the first basibranchial. The hyoidean artery penetrates the anterior portion of the hyoid arch; the artery enters into the ventral hypohyal medially and passes through a cartilaginous band posterior to the hypohyals laterally.

The ceratohyal is a rectangular bone, located on the central part of the hyoid arch. This bone is anteriorly connected with the hypohyals via a connective tissue or cartilaginous bands. This bone is posteriorly separated from the epihyal by a narrow cartilaginous band. The central portion of the bone has a small beryciform foramen. The ventromedial and ventrolateral portions of the bone suspend four and one branchiostegal rays, respectively. This bone lacks a groove or tubular structure for the hyoidean artery.

The epihyal, a triangular bone, is situated on the posterior portion of the hyoid arch. This bone is anteriorly separated from the ceratohyal by a narrow cartilaginous band, and posterodorsally articulates with the interhyal via a ligament. The posterior portion of the lateral aspect of the bone is connected with the interopercle via a ligament. This bone ventrolaterally suspends three branchiostegal rays.

The interhyal, a small stick-like bone, is located on the posterodorsal portion of the hyoid arch. The dorsal and ventral tips of the bone are capped with small cartilages. The dorsal tip of the bone articulates with the cartilage between the symplectic and hyomandibula. The ventral tip of the bone articulates with the ceratohyal and is connected with the interopercle via ligaments.

The urohyal is a slender leaf-like bone, situated on the ventromedial portion of the hyoid arch. The anterior margin of the bone is connected with the ventral hypohyal via a ligament.

The branchiostegal rays, comprising eight long and flat bones, are situated on the ventral portion of the hyoid arch. The first to fourth, fifth, and sixth to eighth elements are suspended by the ventromedial portion of the ceratohyal, the ventrolateral portion of the ceratohyal, and the ventrolateral portion of the epihyal, respectively. The ventral margins of the posterior four to six elements bear serration.

Character recognition

TS 19. Ceratohyal and epihyal (0: separated by cartilage or shallowly sutured; 1: deeply sutured)

Ingroups. The ceratohyal and epihyal are deeply sutured with each other in the medial aspects in *Hoplobrotula armata*, *Lateolabrax japonicus*, *Lates mariae* and *Trachurus japonicus* (character 19-1), while those are separated by a cartilage or shallowly sutured in other ingroups (character 19-0).

Outgroups. Those bones are separated by a cartilage in all outgroups.

TS 20. Number of ligaments connecting ventral hypohyal and branchial arch (0: zero; 1: one; 2: two) (ordered as 0-1-2)

Ingroups. The number of ligaments connecting the ventral hypohyal with the first basibranchial and/or first hypobranchial is two in berycids (character 20-2), zero in *Rondeletia loricata*, *Holocentrus adscensionis*, *Polymixia japonica*, *Velifer hypselopterus* and

Trachurus japonicus (character 20-0), and one in other ingroups (character 20-1).

Outgroups. All outgroups lack the ligaments.

TS 21. Number of branchiostegal rays (0: nine or more; 1: eight; 2: seven; 3: six) (ordered as 0-1-2-3)

Ingroups. The number of the branchiostegal rays is nine in *Acanthochaenus luetkenii* and *Gibberichthys pumilus* (character 21-0), seven in *Diretmus argenteus*, *Polymixia japonica*, *Lateolabrax japonicus*, *Lates mariae* and *Trachurus japonicus* (character 21-2), six in *Velifer hypselopterus* (character 21-3), and eight in other ingroups (character 21-1).

Outgroups. The number of the branchiostegal rays is nine in *Neoscopelus microchir*, 13 in *Hime japonica* and 15 in *Trachinocephalus trachinus*.

Other variations

Beryciform foramen. Different conditions of the beryciform foramen on the ceratohyal are observed among ingroups. For instance, *Paratrachichthys trailli* has a large beryciform foramen (Fig. 15C), while *Hispidoberyx ambagiosus* has a small foramen (Fig. 14). In addition, *Holocentrus adscensionis* has a rudimentary slit-like foramen (Fig. 15A), whereas *Stephanoberyx monae* completely lacks a foramen (Fig. 15D). However, the absence or presence, and the degree of the development of the foramen serially varies among ingroups, and clearly defied characters cannot be distinguished. Accordingly, the conditions of the beryciform foramen are not used the analysis.

Structure for hyoidean artery on ceratohyal. Various structures for the hyoidean artery are developed on the ceratohyal among ingroups. For example, the anterior portion of the ceratohyal has a complete tubular structure for the artery in *Hoplostethus mediterraneus* (Fig. 15A), whereas it has an incomplete tubular structure in *Monocentris japonica* (Fig. 15B). Moreover, *Paratrachichthys trailli* has a groove for the artery on the ceratohyal (Fig. 15C), while *Stephanoberyx monae* has no supporting structures for the artery on the bone (Fig.

15D). The degree of the development of structures for the artery, however, serially varies among ingroups, and distinct characters cannot be defined. Therefore, the conditions of the structure for the hyoidean artery on the ceratohyal are not used for the analysis.

Configuration of urohyal. Although various configurations of the urohyal (e.g., an anterodorsal process, a concavity of the posterior margin, and lateral expansions on the ventral margin) are observed among ingroups, the degree of the development of each configuration serially varies among ingroups (Fig. 16). The configuration of the urohyal is not used for the analysis, because it is unable to be separated into any distinct characters.

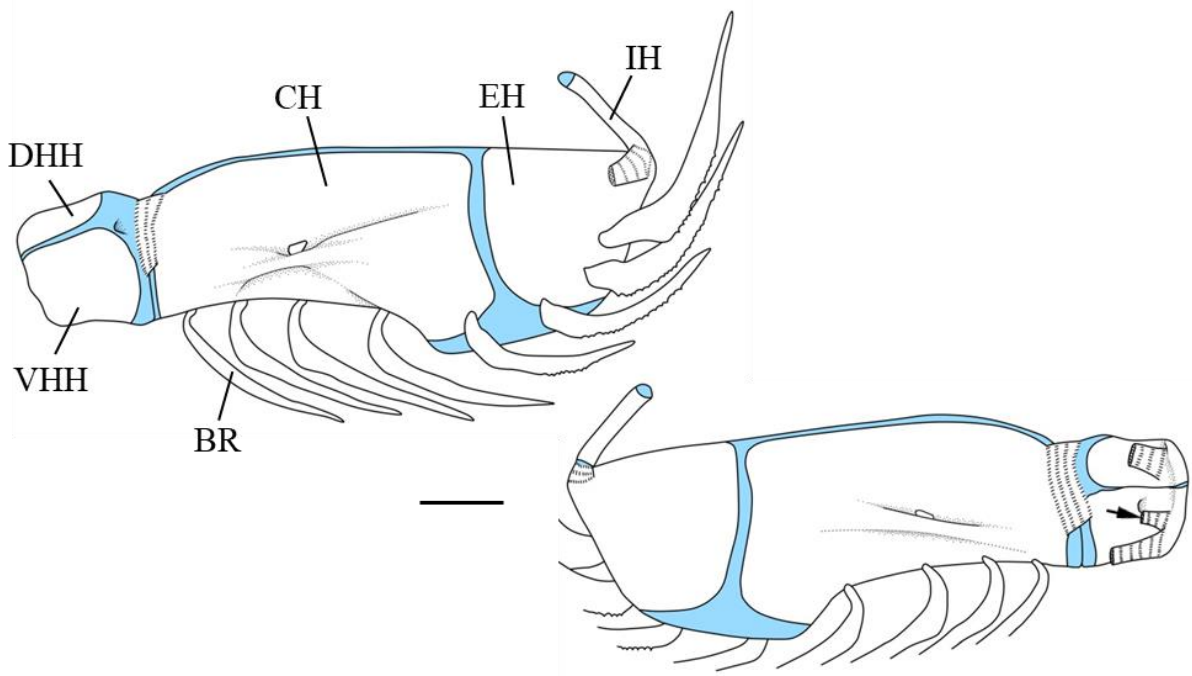

Figure 14. Lateral (upper) and medial (lower) aspects of hyoid arch in *Hispidoberyx ambagiosus*. BR, branchiostegal ray; CH, ceratohyal; DHH, dorsal hypohyal; EH, epihyal; IH, interhyal; VHH, ventral hypohyal. Arrow indicates ligament connecting ventral hypohyal with first basibranchial. Scale indicates 5 mm.

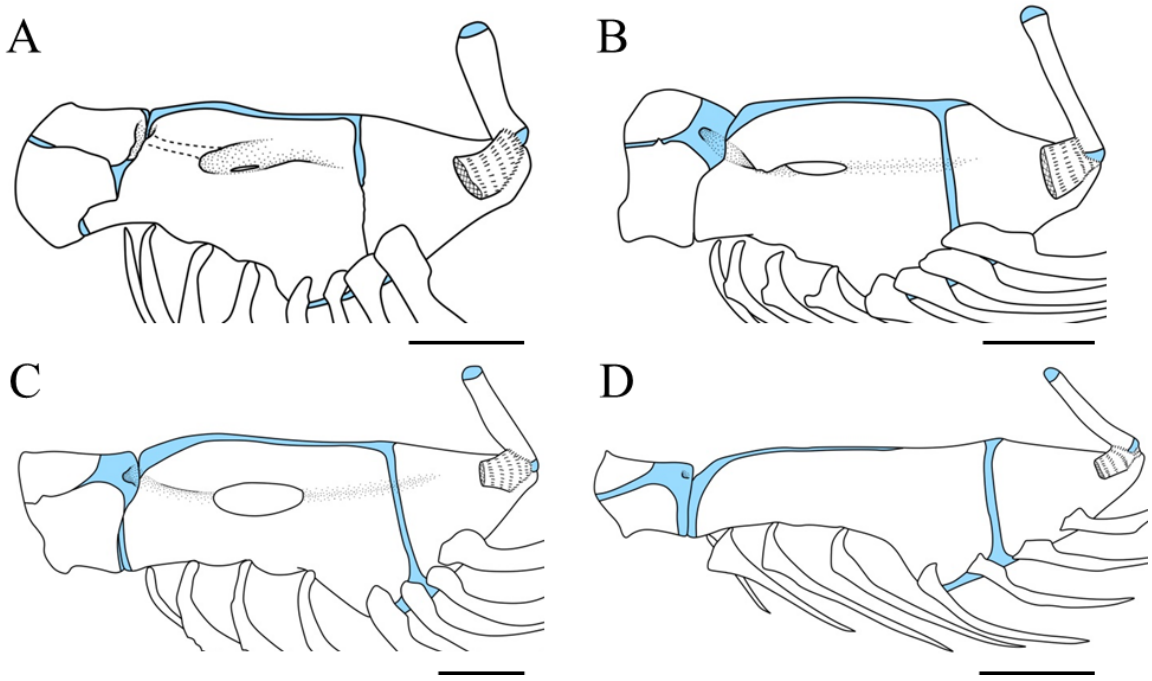

Figure 15. Lateral aspect of hyoid arch in (A) *Holocentrus adscensionis*, (B) *Monocentris japonica* (C) *Paratrachichthys trailli* and (D) *Stephanoberyx monae*. A is shown as mirror image. Scales indicate 5 mm.

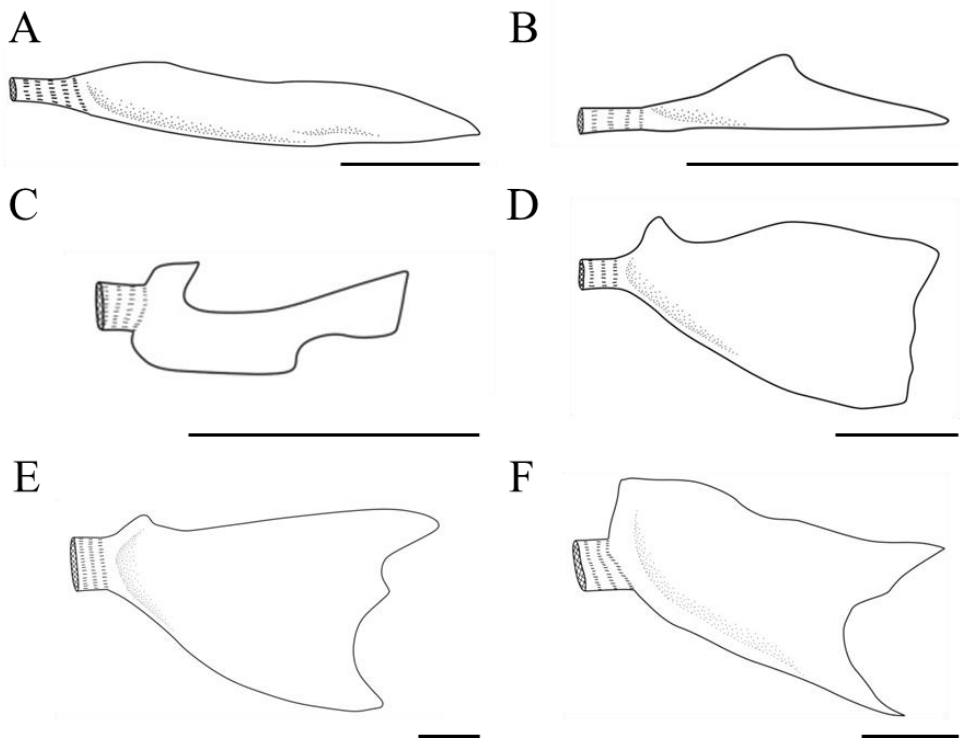

Figure16. Lateral aspect of urohyal in (A) *Hispidoberyx ambagiosus*, (B) *Stephanoberyx monae*, (C) *Melamphaes typhlops*, (D) *Neoniphon sammara*, (E) *Beryx decadactylus* and (F) *Hoplostethus mediterraneus*. C is shown as mirror image. Scales indicate 5 mm.

4-1-6. Branchial arches (Figs. 17, 18)

Description

The branchial arches consist of the basibranchials, hypobranchials and ceratobranchials in the lower part, and the epibranchials and pharyngobranchials in the upper part. The basihyal is also described and discussed in this section. Lower branchial tooth patches (sensu Moore, 1993) and an interarcual cartilage are absent.

The basihyal is a small cartilaginous element, situated on the anteriormost portion of the branchial arches. This bone is loosely connected with the first basibranchial posteriorly via connective tissue.

The basibranchials, comprising the first to third stick-like ossified elements and the fourth rounded cartilaginous element, are situated on the midline of the lower branchial part. The first basibranchial anterolaterally articulates with the hypohyals and is posteriorly attached to the second basibranchial via a cartilage. The anteroventral portion of the bone is margined with a cartilage. The posteroventral portion of the bone is connected with the ventral hypohyal via a ligament. The second basibranchial is attached to the first basibranchial anteriorly and the third basibranchial posteriorly via cartilages. The anterior portion of the second basibranchial and the posterior portion of the first basibranchial articulate with the first hypobranchial laterally. The third basibranchial is attached to the second basibranchial anteriorly via a cartilage. The posterior tip of the bone is capped with a small cartilage and posteriorly extends under the fourth basibranchial and third hypobranchial. The anterior portion of the third basibranchial and the posterior portion of the second basibranchial articulate with the second hypobranchial laterally. The fourth basibranchial articulates with the third hypobranchial anterolaterally and the fourth ceratobranchial posterolaterally, and connected with the fifth ceratobranchial via a ligament.

The hypobranchials, composed of three rod-like bones with cartilaginous posterior tips, are located on the medial portion of the lower branchial part. The first hypobranchial articulates

with the first and second basibranchials anteromedially and the first ceratobranchial posterolaterally. The anteromedial portion of the bone is connected with the dorsal hypohyal anteriorly and the second hypobranchial posteriorly via ligaments. The second hypobranchial articulates with the second and third basibranchials anteromedially and the second ceratobranchial posterolaterally. The anteromedial portion of the bone is connected with the first hypobranchial anteriorly and the third hypobranchial posteriorly via ligaments. The third hypobranchial articulates with the third hypohyal on the opposite side medially, the fourth basibranchial posteromedially and the third ceratobranchial posterolaterally. The anterolateral margin of the bone is connected with the second hypobranchial via a ligament.

The ceratobranchials, comprising five stick-like elements, are situated on the posterolateral portion of the lower branchial part. The anterior and posterior tips of the bones are capped with cartilages. The first to fourth element lack tooth patches and the fifth element dorsally has a tooth patch. The first to third ceratobranchials articulate with the first to third hypobranchials anteromedially and the first to third epibranchials posterodorsally, respectively. The fourth ceratobranchial articulates with the fourth basibranchial anteromedially and the fourth epibranchial posterodorsally. The fifth ceratobranchial is anteriorly connected with the fourth basibranchial via a ligament.

The epibranchials consist of four rod-like bones, located on the lateral portion of the upper branchial part. These bones lack tooth plates and have cartilages on their anterior and posterior tips. The first epibranchial articulates with the first pharyngobranchial anteromedially and the first ceratobranchial posteroventrally. This bone dorsomedially has a process with a cartilaginous cap on its tip, which articulates with the second pharyngobranchial. The second epibranchial articulates with the second and third pharyngobranchials anteromedially, and the second ceratobranchial posteroventrally. The third epibranchial articulates with the third pharyngobranchial anteromedially and the third ceratobranchial posteroventrally. This bone dorsomedially has a cartilage-capped process,

which articulates with a dorsolateral process of the fourth epibranchial. The fourth epibranchial articulates with the fourth pharyngobranchial anteromedially and the fourth ceratobranchial posteroventrally. This bone has dorsolateral and dorsomedial processes tipped with small cartilages, the former being attached to a dorsomedial process of the third epibranchial.

The pharyngobranchials, comprising four elements, located on the medial portion of the upper branchial part. The first pharyngobranchial is a small stick-like bone and has small cartilages on its upper and lower tips. This bone is dorsally suspended by the prootic and ventrally articulates with the first epibranchial. The second pharyngobranchial is a rod-like bone with cartilages on the anterior and posterior tips; the latter articulating with the second epibranchial. This bone dorsally has a cartilage-capped process which articulates with a dorsomedial process of the first epibranchial. This bone lacks a tooth plate. The third pharyngobranchial, a long plate-like bone, has cartilages on the anterior tip and posterior margin. This bone posteriorly articulates with the third epibranchial and fourth pharyngobranchial. The lateral portion of the dorsal aspect of the bone has a small process tipped with a cartilage, which articulates with the second epibranchial. The posterolateral portion of the ventral aspect of the bone has a tooth plate. The fourth pharyngobranchial, a small cartilaginous element, articulates with the third pharyngobranchial anteriorly and the fourth epibranchial posterolaterally. The ventral aspect of the bone has an autogenous tooth plate.

Character recognition

TS 22. Basihyal (0: present; 1: absent)

Ingroups. The basihyal is absent in *Acanthochaenus luetkenii*, *Cetostoma regani*, trachichthyids, *Anomalops katoptron*, *Monocentris japonica*, *Anoplogaster cornuta* and *Diretmus argenteus* (character 22-1), whereas it is present in other ingroups (character 22-0).

Outgroups. All outgroups have the basihyal.

Remarks. Kotlyar (1991a, 1995, 1996a) reported that the basihyal is absent in *Hispidoberyx ambagiosus*, *Rondeletia loricata* and *Barbourisia rufa*. Zehren (1979) also reported the absence of the bone in *Gibberichthys pumilus*. In those previous studies, however, the methods of the anatomical examination included staining of bones by alizarin, but staining of cartilages was not performed. Because the basihyals found in these species in present study are small cartilaginous elements, it can be assumed that previous studies merely failed to find these small elements. In Kotlyar's (1991a, 1995, 1996a) and Zehren's (1979) studies, actually, some small cartilaginous elements in other parts are not illustrated in their figures (e.g., caudal fin cartilages). Accordingly, the absence of the basihyal in species mentioned above reported by previous studies was not adapted for coding in this transformation series.

TS 23. Fourth basibranchial and fifth ceratobranchial (0: directly attached; 1: connected via ligament)

Ingroups. The fourth basibranchial and fifth ceratobranchial are directly attached to each other in *Gibberichthys pumilus*, *Rondeletia loricata* and *Anoplogaster cornuta* (Fig. 17B) (character 23-0), while those are connected via a ligament in other ingroups (character 23-1). As *Hispidoberyx ambagiosus* and *Cetostoma regani* have both conditions, "0" and "1" are coded for them.

Outgroups. Those bones are directly attached in *Trachinocephalus trachinus* and *Hime japonica*, and connected via a ligament in *Neoscopelus microchir*.

Remarks. Kotlyar (1991a) described that the fourth basibranchial and fifth ceratobranchial were directly attached to each other in *H. ambagiosus*, while these bones are connected via a ligament in two specimens examined in this study.

In *C. regani*, these bones are connected via a ligament in one specimen examined in this study (one of BMNH 1996.2.14.40–43, 129.0 mm SL), whereas they are directly attached to each other in the other specimen in BMNH 1996.2.14.40–43 (89.2 mm SL).

TS 24. Tooth plate on fifth ceratobranchial (0: present; 1: absent)

Ingroups. A tooth plate on the fifth ceratobranchial is absent in stephanoberycids, *Rondeletia loricata* and *Cetostoma regani* (Fig. 17B) (character 24-1), while it is present in other ingroups (character 24-0).

Outgroups. All outgroups have a tooth plate on the bone.

TS 25. Tooth plate on third epibranchial (0: present; 1: absent)

Ingroups. A tooth plate on the third epibranchial is absent in *Hispidoberyx ambagiosus*, *Acanthochaenus luetkenii*, *Rondeletia loricata*, *Cetostoma regani*, *Anoplogaster cornuta*, *Diretmus argenteus*, *Velifer hypselopterus* and *Trachurus japonicus* (character 25-1), whereas it is present in other ingroups (character 25-0).

Outgroups. *Neoscopelus microchir* and *Hime japonica* have a tooth plate on the bone, and *Trachinocephalus trachinus* lacks it.

TS 26. Anterior tip of fourth epibranchial (0: almost in same width or broader than third epibranchial; 1: distinctly thinner than third epibranchial)

Ingroups. The anterior tip of the fourth epibranchial is distinctly thinner than that of the third epibranchial in stephanoberycids (Fig. 18B) (character 26-1), whereas it is almost in same width or broader than the anterior tip of the third epibranchial in other ingroups (character 26-0).

Outgroups. The anterior tip of the fourth epibranchial is almost in same width or broader than the anterior tip of the third epibranchial in all outgroups.

TS 27. Tooth plate on second pharyngobranchial (0: present; 1: absent)

Ingroups. A tooth plate on the second pharyngobranchial is absent in *Hispidoberyx ambagiosus*, stephanoberycids, *Gibberichthys pumilus*, *Rondeletia loricata*, *Cetostoma regani* and *Diretmus argenteus* (character 27-1), whereas it is present in other ingroups (character 27-0).

Outgroups. All outgroups have a tooth plate on the bone.

TS 28. Fourth pharyngobranchial (0: present; 1: absent)

Ingroups. The fourth pharyngobranchial is absent in *Acanthochaenus luetkenii*, melamphaids, trachichthyids, *Anomalops katoptron*, *Monocentris japonica*, *Anoplogaster cornuta*, *Diretmus argenteus*, berycids and holocentrids (character 28-1), while it is present in other ingroups (character 28-0).

Outgroups. All outgroups have the bone.

Remarks. Kotlyar (1991a, 1995, 1996a) reported that the fourth pharyngobranchial is absent in *Hispidoberyx ambagiosus*, *Rondeletia loricata* and *Barbourisia rufa*. Because the fourth pharyngobranchials found in these species in present study are small cartilaginous elements, it can be assumed that Kotlyar merely failed to find these small elements (see Remarks of TS 22). Accordingly, the absence of the bone in species mentioned above reported by Kotlyar (1991a, 1995, 1996a) was not adapted for coding in this transformation series.

TS 29. Fourth pharyngobranchial tooth plate (0: autogenous; 1: fused with third pharyngobranchial tooth plate; 2: absent) (unordered)

Ingroups. The fourth pharyngobranchial tooth plate is fused with the third pharyngobranchial tooth plate in trachichthyids, *Anomalops katoptron* and *Monocentris japonica* (Fig. 18C) (character 29-1), whereas it is absent in stephanoberycids (Fig. 18B) (character 29-2), and autogenous in other ingroups (character 29-0).

Outgroups. The fourth pharyngobranchial tooth plate is autogenous in *Neoscopelus microchir* and *Hime japonica*, while it is absent in *Trachinocephalus trachinus*.

Remarks. In trachichthyids, *A. katoptron* and *M. japonica*, a tooth plate on the third pharyngobranchial is largely expanded beyond the posterior margin of the bone and occupies the area where an autogenous fourth pharyngobranchial tooth plate is situated in most other ingroups. Such a condition is assumed to be resulted from fusion of the third and fourth pharyngobranchial tooth plates as noted by Moore (1993).

TS 30. Interarcual cartilage (0: absent; 1: present)

Ingroups. The interarcual cartilage, connecting the first epibranchial with the second pharyngobranchial, is present in *Anomalops katoptron*, *Hoplobrotula armata*, *Lateolabrax japonicus*, *Lates mariae* and *Trachurus japonicus* (character 30-1), while it is absent in other ingroups (character 30-0).

Outgroups. All outgroups lack an interarcual cartilage.

Other variations

Lower branchial tooth patches. Moore (1993) considered that complete loss of lower branchial tooth patches which are not rudimentary gill rakers and associated with lower branchial bones, particularly the basibranchials and hypobranchials, is one of synapomorphies of Stephanoberycoidei. In addition, a tooth patch fused with the fourth ceratobranchial was observed only in berycids in this study. Among taxa possessing lower branchial tooth patches, however, those size, number and position are quite various, and then the homology of those tooth patches is unclear. Moreover, it is ambiguous in some taxa (e.g., *Neoniphon sammara* and *Ostichthys japonicus*) whether those tooth patches are homologous with rudimentary gill rakers or not. Therefore, the conditions of lower branchial tooth patches are not used for the analysis.

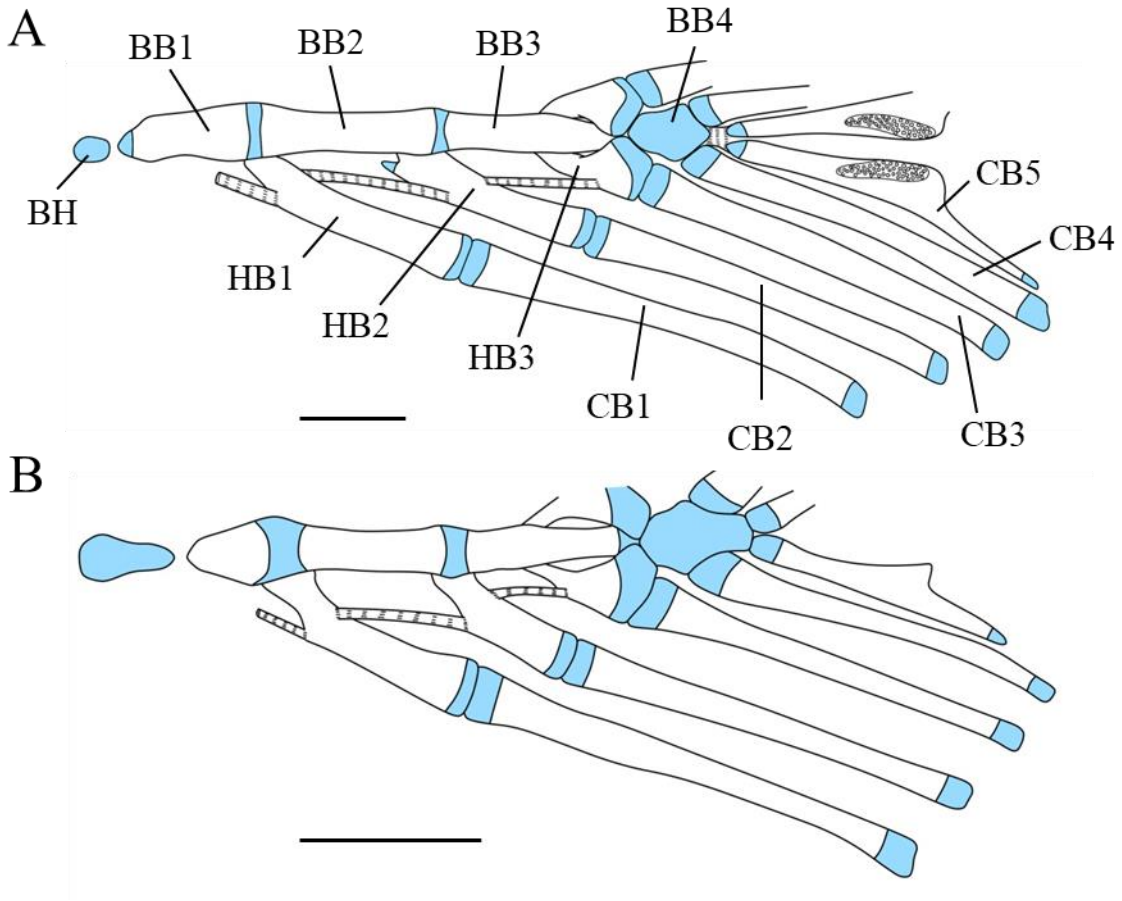

Figure 17. Dorsal aspects of lower branchial arches in (A) *Hispidoberyx ambagiosus* and (B) *Rondeletia loricata*. BB1–4, first to fourth basibranchials; BH, basihyal; CB1–5, first to fifth ceratobranchials; HB1–3, first to third hypobranchials. Scales indicate 5 mm.

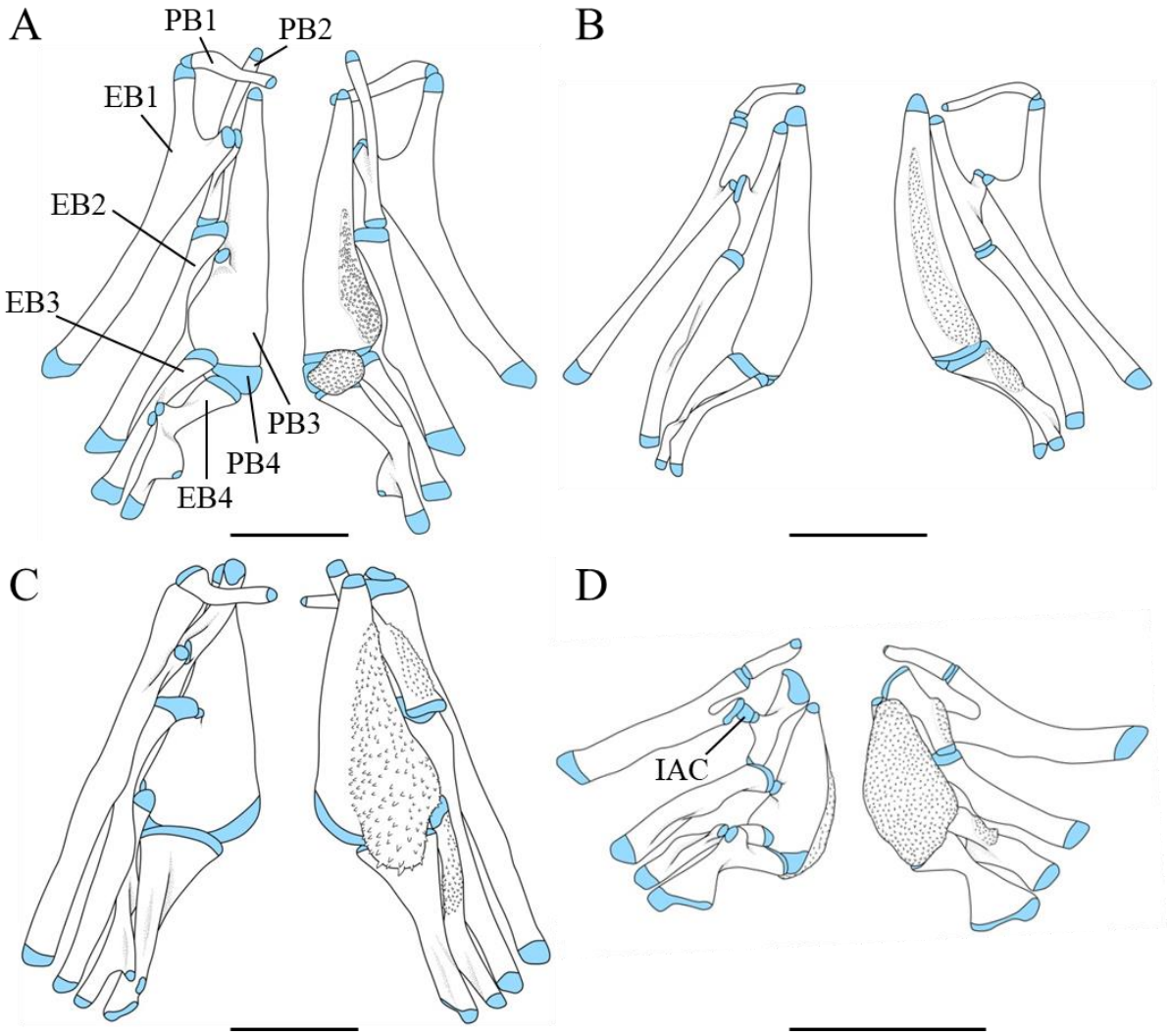

Figure 18. Dorsal (left) and ventral (right) aspects of upper branchial arches in (A) *Hispidoberyx ambagiosus*, (B) *Stephanoberyx monae*, (C) *Hoplostethus mediterraneus* and (D) *Anomalops katoptron*. EB1–4, first to fourth epibranchials; IAC, interarcual cartilage; PB1–4, first to fourth pharyngobranchials. Scales indicate 5 mm.

4-1-7. Pectoral girdle (Figs. 19–21)

Description

The pectoral girdle consists of the extrascapula, posttemporal, supracleithrum, cleithrum, postcleithra, scapula, coracoid and actinosts.

The extrascapula (= supratemporal) is a rectangular bone, located on the anterodorsal portion of the pectoral girdle. This bone is attached to the frontal and supraoccipital dorsomedially, and posttemporal posteroventrally. The dorsal surface of the bone, partially covered with small spines, has a wide and shallow groove for the supratemporal canal, which is continuous with that of the frontal (median mucus cavity) anterodorsally, the pterotic anteroventrally and the posttemporal posteroventrally.

The posttemporal, a V-shaped bone, is situated on the dorsal portion of the pectoral girdle. The dorsal limb of the bone is attached to the epiotic and the lower limb is connected with the intercalar via a short ligament. This bone posteroventrally articulates with the supracleithrum. The dorsolateral surface of the bone, partially covered with small spines, has a wide and shallow groove (thus tubular structure is absent) for the temporal portion of the main trunk canal, which lacks branches and is continuous with that of the extrascapula anteriorly and the trunk canal posteriorly.

The supracleithrum, a slender leaf-like bone, is located on the dorsal portion of the pectoral girdle. This bone articulates with the posttemporal dorsally and attached to the cleithrum ventromedially. This bone lacks a tubular structure for the temporal portion of the main trunk canal. The central portion of the medial aspect of the bone is connected with the first abdominal centrum via the Baudelot's ligament.

The cleithrum is a long lunate element, situated on the central to ventral portions of the pectoral girdle. This bone is attached to the supracleithrum dorsolaterally, the upper postcleithrum posteromedially, the scapula and coracoid on the posterior margin of the central portion, and the cleithrum on the opposite side medially at the anteroventral portion. The

lateral surface of the posterior corner of the bone is partially covered with small spines.

The postcleithra, comprising two elements, are located on the posteroventral portion of the pectoral girdle. The ellipse dorsal postcleithrum is attached to the cleithrum laterally and the stick-like ventral postcleithrum medially.

The scapula is an angular bone, located on the ventral portion of the pectoral girdle. This bone is attached to the coracoid ventrally via a narrow cartilage, and the cleithrum anteriorly via a narrow cartilage in the medial aspect and directly in the lateral aspect. This bone is posteriorly attached to the first to third actinosts. The posterodorsal portion of the bone has a facet, which supports the uppermost pectoral-fin ray. The anterior portion of the bone has a single foramen.

The coracoid, a long and curved bone, is situated on the ventral portion of the pectoral girdle. This bone is attached to the scapula dorsally via a narrow cartilage, and the cleithrum anteriorly via a narrow cartilage in the medial aspect and directly in the lateral aspect. The posterior margin of the bone is attached to the fourth actinost. The posteroventral portion of the bone has a short process. The tip of a long anteroventral process of the bone is capped with a small cartilage and attached to the cleithrum.

The actinosts are composed of four elements, located on the posteroventral portion of the pectoral girdle. The first to third and fourth actinosts are anteriorly attached to the scapula and coracoid, respectively. The posterior margins of these bones bear cartilaginous pads and support pectoral-fin rays.

Character recognition

TS 31. Posterolateral branch of temporal portion of main trunk canal on posttemporal (0: absent; 1: present)

Ingroups. A posterolateral branch of the temporal portion of the main trunk canal on the posttemporal is present and opened laterally in trachichthyids (Fig. 21B) (character 31-1), and

absent in other ingroups (character 31-0).

Outgroups. All outgroups lack the posterolateral branch of the temporal portion of the main trunk canal.

TS 32. Temporal portion of main trunk canal on supracleithrum (0: present; 1: absent)

Ingroups. The temporal portion of the main trunk canal on the supracleithrum is absent in *Hispidoberyx ambagiosus*, stephanoberycids, *Gibberichthys pumilus*, *Rondeletia loricata*, *Barbourisia rufa*, *Cetostoma regani*, melamphaids, *Diretmus argenteus* and *Hoplobrotula armata* (character 32-1), while it is present on the supracleithrum in other ingroups (character 32-0).

Outgroups. This canal is present on the supracleithrum in all outgroups.

TS 33. Number of foramina on scapula (0: one; 1: two)

Ingroups. The scapula has two foramina in melamphaids, *Hoplostethus mediterraneus* and *Paratrachichthys trailli* (Fig. 20) (character 33-1), and one foramen in other ingroups (character 33-0).

Outgroups. All outgroups have a single foramen on the scapula.

TS 34. Posterior process of coracoid (0: present; 1: absent)

Ingroups. The posterior process of the coracoid is absent in melamphaids (Fig. 20) (character 34-1), while it is present in other ingroups (character 34-0).

Outgroups. *Neoscopelus microchir* and *Hime japonica* have the posterior process on the coracoid, whereas *Trachinocephalus trachinus* lacks it.

TS 35. Fourth actinost (0: without notch; 1: with notch posteriorly)

Ingroups. The fourth actinost is posteriorly notched in melamphaids (Fig. 20) (character 35-1), while it lacks a notch in other ingroups (character 35-0).

Outgroups. All outgroups have the fourth actinost without a posterior notch.

TS 36. Number of postcleithra (0: three or two; 1: one; 2: zero) (ordered as 0-1-2)

Ingroups. Trachichthyids, *Anomalops katoptron*, *Monocentris japonica*, *Anoplogaster*

cornuta and *Diretmus argenteus* have one postcleithrum (character 36-1), while *Cetostoma regani* has no element (character 36-2) and other ingroups have two elements (character 36-0).

Outgroups. *Neoscopelus microchir* and *Trachinocephalus trachinus* have two elements, while *Hime japonica* has three elements.

Remarks. Paxton (1974) and Kotlyar (1996a) reported that the number of postcleithra is one in *Rondeletia loricata*. On the other hand, the present study found well ossified ventral postcleithrum and weakly ossified dorsal postcleithrum in two specimens of the species. Because the dorsal postcleithrum of the species is quite thin and very difficult to be found in this study, it is highly possible that Paxton (1974) and Kotlyar (1996a) failed to find this element. Therefore, the condition on the postcleithra in *Rondeletia loricata* reported by Paxton (1974) and Kotlyar (1996a) was not adapted for coding in this transformation series.

Other variations

Enlarged extrascapula covering parietal. Johnson & Patterson (1993) and Wiley & Johnson (2010) considered the enlarged extrascapula covering the parietal as a synapomorphy of Stephanoberyciformes defined by them. However, the size of extrascapula serially varies among ingroups, and clearly defined characters cannot be distinguished. In addition, the autogenous parietal is absent in *Hispidoberyx ambagiosus*, *Acanthochaenus luetkenii* and *Gibberichthys pumilus* (see Other variation in the former section of Neurocranium), and thus the relation of these bones cannot be evaluated in them. Therefore, this character is not used for the analysis

Posterodorsal branch of temporal portion of main trunk canal. Holocentrids have a branch of the temporal portion of the main trunk canal on the posttemporal. This branch is directed posterodorsally and opened dorsally (Fig. 21C) and considered to be not homologous with a branch on the bone in trachichthyids which is directed posterolaterally and opened laterally

(Fig. 21B). A bony structure separating the branch from the main canal in holocentrids has a possibility to be derived from a bony bridge over the dorsal opening of the tubular structure on the posttemporal, although ontogenetic examination is required to confirm it. However, even if this assumption is adequate, because bony bridges on the cephalic sensory canals are not used for the analysis in this study (see Other variation in the former section of Circumorbital bones), the conditions of the canals are also not used for the analysis.

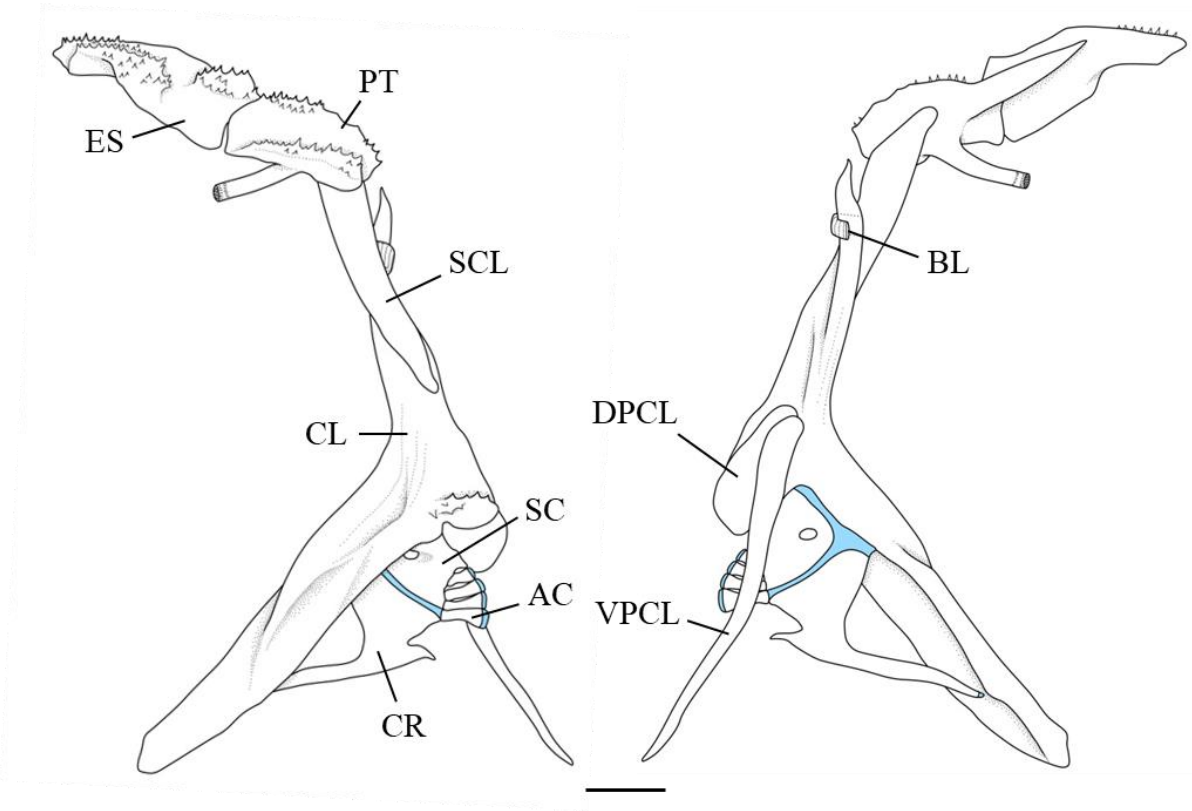

Figure 19. Lateral (left) and medial (right) aspects of pectoral girdle in *Hispidoberyx ambagiosus*. AC, actinost; BL, Baudelot's ligament; CL, cleithrum; CR, coracoid; DPCL, dorsal postcleithrum; ES, extrascapular; PT, posttemporal; SC, scapula; SCL, supracleithrum; VPCL, ventral postcleithrum. Scale indicates 5 mm.

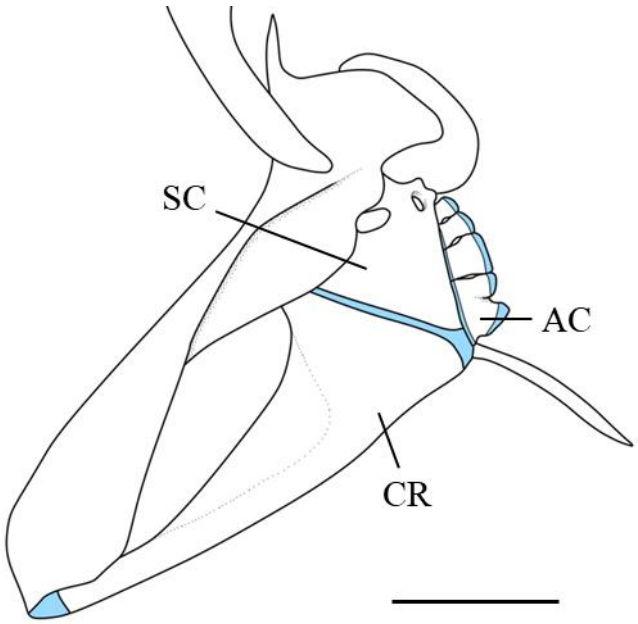

Figure 20. Lateral aspect of central to lower portions of pectoral girdle in *Poromitra unicornis*. AC, actinost; CR, coracoid; SC, scapula. Scale indicates 5 mm.

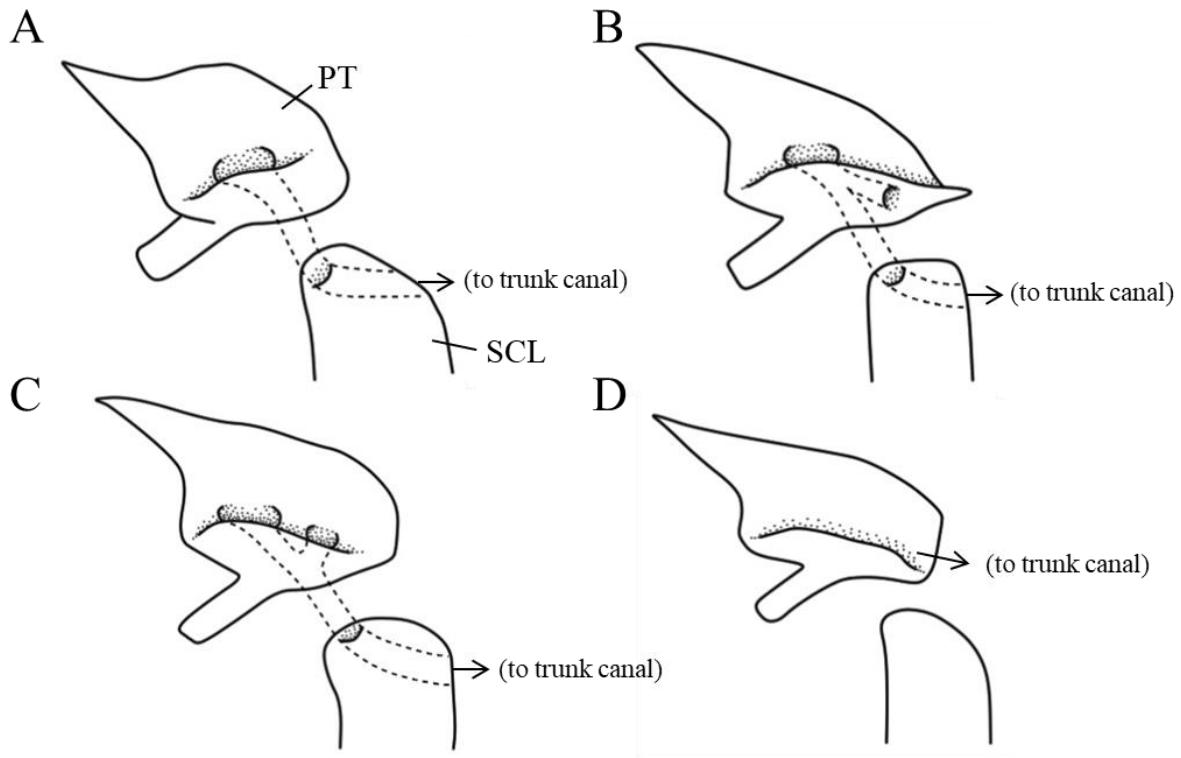

Figure 21. Diagrammatic illustration of posttemporal and supracleithrum in (A) *Monocentris japonica*, (B) *Paratrachichthys trailli*, (C) *Ostichthys japonicus* and (D) *Hispidoberyx ambagiosus*. PT, posttemporal; SCL, supracleithrum. Dashed lines indicate courses of tubular structures on posttemporal and supracleithrum. Scales indicate 5 mm.

4-1-8. Pelvic girdle (Figs. 22, 23)

Description

The pelvic girdle consists of the pelvic bone. The lateral and medial pelvic radials are absent.

The pelvic bone is a slender triangular bone. The anterior and posterior portions of the bone are loosely attached to those on the opposite side medially, while the middle portion of the bone is widely separated from that on the opposite side. A ligament connecting this bone and the ventral postcleithrum is absent. The anterior tip of the central part has a small cartilaginous cap and nearly reaches to the ventral portion of the cleithrum. The internal wing is medially developed, while external dorsal and ventral wings are indistinct. The posterolateral portion of the bone has the lateral process. The posterior process is present on the posterior portion of the bone. An anterior process is absent. The posterior portion of the bone supports the pelvic fin formed by one spine and seven soft rays. An interpelvic ligament (sensu Stiassny & Moore, 1992) is absent.

Character recognition

TS 37. Anterior process of pelvic bone (0: absent; 1: present)

Ingroups. The anterior process of the pelvic bone is present in melamphaids, *Hoplostethus mediterraneus*, *Paratrachichthys trailli*, *Anomalops katoptron*, *Diretmus argenteus*, berycids, holocentrids, *Lateolabrax japonicus*, *Lates mariae* and *Trachurus japonicus* (character 37-1), while it is absent in other ingroups (character 37-0). As *Hispidoberyx ambagiosus* has both conditions, “0” and “1” are coded for the species. Due to the absence of the pelvic girdle, “?” is coded for *Cetostoma regani*.

Outgroups. All outgroups lack an anterior process of the pelvic bone.

Remarks. Kotlyar (1991a) described that the pelvic bone in *H. ambagiosus* has the anterior process, whereas this bone lacks the process in two specimens examined in this study.

TS 38. Internal wing of pelvic bone (0: not expanded; 1: anterodorsally expanded)

Ingroups. The internal wing is anterodorsally expanded in berycids and holocentrids (Fig. 23A) (character 38-1), whereas it is not expanded in other ingroups (character 38-0). Because of the absence of the pelvic girdle, "?" is coded for *Cetostoma regani*.

Outgroups. The internal wing is not expanded in all outgroups.

TS 39. Pelvic-fin spine (0: absent; 1: present)

Ingroups. A pelvic spine is absent in stephanoberycids, *Rondeletia loricata*, *Barbourisia rufa*, *Anomalops katoptron*, *Anoplogaster cornuta*, *Polymixia japonica* and *Velifer hypselopterus* (character 39-0), while it is present in other ingroups (character 39-1). Due to the absence of the pelvic girdle, "?" is coded for *Cetostoma regani*.

Outgroups. All outgroups lack a pelvic-fin spine.

TS 40. Lateral pelvic radials (0: present; 1: absent)

Ingroups. Lateral pelvic radials are absent in *Hispidoberyx ambagiosus*, *Stephanoberyx monae*, *Gibberichthys pumilus*, *Rondeletia loricata*, *Monocentris japonica*, *Anoplogaster cornuta*, *Lateolabrax japonicus*, *Lates mariae* and *Trachurus japonicus* (character 40-1), whereas they are present in other ingroups (character 40-0). Because of the absence of the pelvic girdle, "?" is coded for *Cetostoma regani*.

Outgroups. All outgroups have lateral pelvic radials.

Other variations

Medial contact of pelvic bones. Stiassny & Moore (1992) recognized the following three conditions of the medial contact of the pelvic bones on both sides among Acanthomorpha: (1) loosely apposed; (2) posteromedially overlapping; and (3) posteromedially sutured. In this study, however, intermediate conditions between them were observed among ingroups, and it was unable to recognize these serial conditions as clearly different characters. Therefore, the conditions of the medial contact of the pelvic bones are not used for the analysis.

Shape of base of pelvic-fin spine. Johnson & Patterson (1993) recognized a complex configuration of the base of the pelvic-fin spine as a synapomorphy of Euacanthopterygii [Beryciformes (sensu Johnson & Patterson, 1993) + Percomorpha], in which the base of the pelvic-fin spine is asymmetrical and has medial processes grasping a bony shelf or ring at the posterolateral corner of the pelvic girdle. They also recognized a symmetrical configuration of the base of the pelvic fin in stephanoberyciforms as a different condition from the former. In my examination, however, the configurations of the base of the pelvic-fin spine serially vary among ingroups, and it is unable to separate them into discrete characters. Accordingly, the conditions of the shape of the base of the pelvic-fin spine are not used for the analysis.

Interpelvic ligament. According to Stiassny & Moore (1992), acanthomorphs primitively have the intrapelvic ligament which interconnects the bases of pelvic-fin rays and the pelvic bone on the same side. On the other hand, they found that the interpelvic ligament which interconnects the bases of pelvic-fin rays in both sides is present in holocentrids and 'higher percomorphs'. However, Johnson & Patterson (1993) pointed out that the interpelvic versus intrapelvic ligament differentiation may not be so clear cut as implied by Stiassny & Moore (1992). Among ingroups examined in this study, the difference of the two ligaments is also not clear and it is difficult to separate them into discrete characters. Therefore, the conditions on the interpelvic ligament are not used for the analysis.

Ligament between pelvic bone and ventral postcleithrum. Stiassny & Moore (1992) recognized the presence of a ligament between the pelvic bone and ventral postcleithrum is a synapomorphy of Acanthomorpha. Subsequently, Johnson & Patterson (1993) found that the ligament in some acanthomorph taxa is absent or obscure and that the presence of the ligament may not be an acanthomorph synapomorphy. Nevertheless, they found the specific ligament shared by Beryciformes and Percomorpha, and recognized it as a synapomorphy of Euacanthopterygii including them. In my examination, however, the degree of the distinctness of the ligament serially varies among ingroups, and it is difficult to recognize any discrete

characters. Consequently, the conditions of the ligament between the pelvic bone and ventral postcleithrum are not used for the analysis.

Association of pelvic girdle with pectoral girdle. Stiassny & Moore (1992) recognized the following two conditions on the association of the pelvic girdle with the pectoral girdle among Acanthomorpha: (1) no association and (2) pelvic girdle directly or ligamentously attached to cleithrum or coracoid. Subsequently, Davesne et al. (2016) recoded this transformation series and recognized the following four conditions: (1) no contact, with pelvic girdle posterior to pelvic girdle; (2) contact at level of cleithrum; (3) contact at level of coracoid; and (4) pelvic girdle anterior to pectoral girdle. In this study, however, the position of the pelvic girdle and its association with the pectoral girdle serially vary among ingroups, and it is unable to separate those conditions into clearly defined characters. Therefore, the conditions of the association of the pelvic girdle with the pectoral girdle are not used for the analysis.

Medial pelvic radial. According to Johnson (1992), fusion of the medial pelvic radial to the ventral half of the innermost ray is one of synapomorphies of Eurypterygii, in which the base of the ventral half of the innermost ray is modified so as to have a lateral process. He also found that *Stephanoberyx monae* and *Rondeletia loricata* exclusively have an autogenous medial radial. This study confirmed such a condition in those genera, and also found the autogenous medial radial in *Acanthochaenus luetkenii* and *Monocentris japonicus*. On the other hand, although *Hispidoberyx ambagiosus*, *Gibberichthys pumilus* and *Barbourisia rufa* lack the autogenous medial radial, the base of the ventral half of the innermost ray is not modified in these species. Although such conditions suggest that the medial radial might be lost in the early ontogenetic stage and it might be not fused with the innermost ray, ontogenetic examination is needed to confirm this assumption. Accordingly, because the reason of the absence of the autogenous medial radial in *H. ambagiosus*, *G. pumilus* and *B. rufa* cannot be specified, the conditions of the medial radial are not used for the analysis.

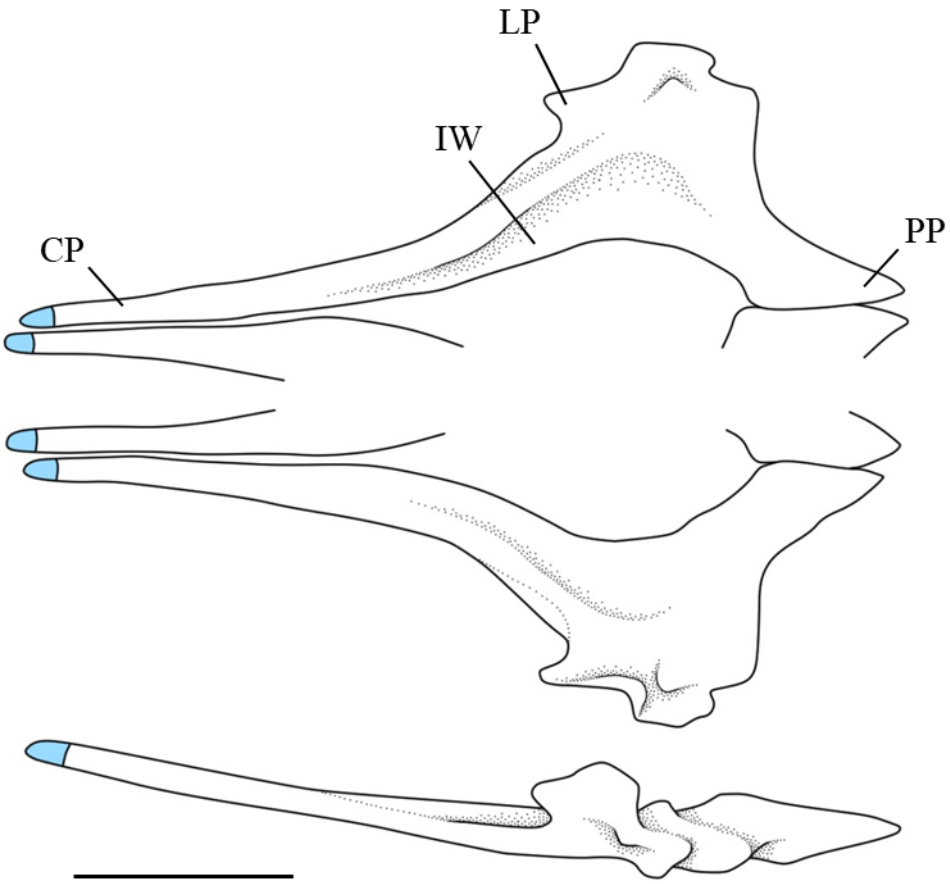

Figure 22. Ventral (upper), dorsal (middle) and lateral (lower) aspects of pelvic girdle in *Hispidoberyx ambagiosus*. CP, central part; IW, internal wing; LP, lateral process; PP, posterior process. Scale indicates 5 mm.

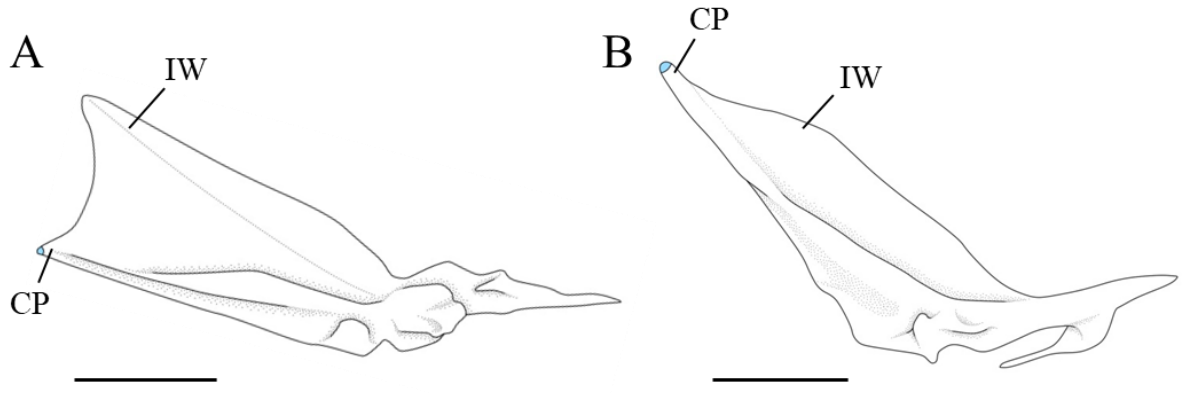

Figure 23. Lateral aspects of pelvic girdle in (A) *Neoniphon sammara* and (B) *Hoplostethus mediterraneus*. CP, central part; IW, internal wing. Scales indicate 5 mm.

4-1-9. Axial skeleton and median-fin supports (Fig. 24)

Description

The axial skeleton is composed of the vertebrae, pleural ribs and epineurals. The median-fin supports comprise the supraneurals, proximal, medial and distal pterygiophores, and stays. The epipleurals are absent.

The vertebrae are composed of the abdominal and caudal vertebrae. These bones dorsally have the neural arch and neural spine; all neural spines being fused with the centrum. The numbers of the abdominal and caudal vertebrae are 14–15 and 19, respectively (based on two specimens dissected), and the number of total vertebrae is 33–35 (based on six specimens examined).The first abdominal vertebra anteriorly possesses three facets for articulation with the exoccipital and basioccipital, and is ventrolaterally connected with the supracleithrum via the Baudelot's ligament. The seventh and posterior abdominal vertebrae ventrolaterally have the parapophysis, while the first to sixth abdominal vertebrae lack it. Abdominal hemal arches are absent on all abdominal vertebrae. The caudal vertebrae ventrally have the hemal arch and hemal spine.

The pleural ribs are slender rod-like bones, situated on the anterior portion of the body. The anterior elements are proximally attached to the centrum of the abdominal vertebrae, and the posterior elements are proximally attached to the parapophysis.

The epineurals are composed of two thin rod-like bones and located on the anterior portion of the body. The first and second elements are anteromedially attached to the centrum of the first and second abdominal vertebrae, respectively.

The supraneurals, comprising four slender bones, are situated between the neurocranium and dorsal-fin origin. The first element is located anterior to the first neural spine. The second to fourth elements are inserted between the second and third, fourth and fifth, and fifth and sixth neural spines, respectively, in HUMZ 194634, 180.7 mm SL, and the first and second, third and fourth, and fifth and sixth, respectively, in HUMZ 193670, 178.8 mm SL).

The proximal pterygiophores are slender bones, situated on the dorsal and anal-fin bases. The first proximal pterygiophore of the dorsal fin is inserted between the eighth and ninth neural spines. The first proximal pterygiophore of the dorsal and anal fins supports one and two spines, respectively. These fin spines lack chain-link articulations (sensu Johnson & Patterson, 1993) with the proximal and distal pterygiophores.

The medial pterygiophores are small elements, situated between the proximal and distal pterygiophores. Autogenous medial pterygiophores are absent in anterior three pterygiophores of the dorsal and anal fins.

The distal pterygiophores are small elements supporting dorsal and anal-fin rays. These bones are anteriorly attached to the medial or proximal pterygiophores.

The stay is a small element, situated on the posteroventral portion of the last pterygiophore in the dorsal fin, and the posterodorsal portion of the last pterygiophore in the anal fin.

Character recognition

TS 41. Neural spine of first abdominal vertebra (0: autogenous; 1: fused with centrum)

Ingroups. The neural spine of the first abdominal vertebra is autogenous in berycids, holocentrids, *Polymixia japonica*, *Hoplobrotula armata*, *Lateolabrax japonicus*, *Lates mariae* and *Trachurus japonicus* (character 41-0), while it is fused with the centrum in other ingroups (character 41-1).

Outgroups. The neural spine of the first abdominal vertebra is autogenous in all outgroups.

TS 42. Abdominal hemal arches (0: absent; 1: present)

Ingroups. The abdominal hemal arches are absent in *Hispidoberyx ambagiosus*, stephanoberycids, *Gibberichthys pumilus*, *Rondeletia loricata*, *Barbourisia rufa*, *Cetostoma regani* and *Hoplobrotula armata* (character 42-0), whereas they are present on the posterior abdominal vertebrae in other ingroups (character 42-1).

Outgroups. The abdominal hemal arches are absent in all outgroups.

TS 43. First epineural (0: slender; 1: expanded)

Ingroups. The first epineural is expanded and plate-like shaped in *Trachichthys australis* and *Paratrachichthys trailli* (character 43-1), while it is slender in other ingroups (character 43-0).

Outgroups. The first epineural is slender in all outgroups.

TS 44. Epipleurals (0: present; 1: absent)

Ingroups. The epipleurals are present in *Polymixia japonica* (character 44-0), while they are absent in other ingroups (character 44-1).

Outgroups. All outgroups have the epipleurals.

TS 45. Proximal insertion of Baudelot's ligament (0: first abdominal vertebra; 1: basioccipital)

Ingroups. The Baudelot's ligament is proximally inserted onto the first abdominal vertebra in *Hispidoberyx ambagiosus*, stephanoberycids, *Gibberichthys pumilus*, *Barbourisia rufa*, melamphaids, *Polymixia japonica* and *Velifer hypselopterus* (character 45-0), and onto the basioccipital in other ingroups (character 45-1). *Cetostoma regani*, *Monocentris japonica* and *Anoplogaster cornuta* are coded as "?" due to absence of the ligament.

Outgroups. The Baudelot's ligament is proximally inserted onto the first abdominal vertebra in all outgroups.

TS 46. Dorsal-fin spines (0: absent; 1: present)

Ingroups. Dorsal-fin spines are absent in *Acanthochaenus luetkenii*, *Rondeletia loricata*, *Barbourisia rufa*, *Cetostoma regani*, *Anoplogaster cornuta*, *Diretmus argenteus* and *Hoplobrotula armata* (character 46-0), whereas they are present in other ingroups (character 46-1).

Outgroups. All outgroups lack dorsal-fin spines.

TS 47. Chain-link articulation of dorsal-fin spines (0: absent; 1: present)

Ingroups. The chain-link articulations of dorsal-fin spines (sensu Johnson & Patterson,

1993) are absent in *Hispidoberyx ambagiosus*, *Stephanoberyx monae*, *Gibberichthys pumilus*, melamphaids, *Polymixia japonica* and *Velifer hypselopterus* (character 47-0), whereas they are present in trachichthyids, *Anomalops katoptron*, *Monocentris japonica*, berycids, holocentrids, *Lateolabrax japonicus*, *Lates mariae* and *Trachurus japonicus* (character 47-1). *Acanthochaenus luetkenii*, *Rondeletia loricata*, *Barbourisia rufa*, *Cetostoma regani*, *Anoplogaster cornuta*, *Diretmus argenteus* and *Hoplobrotula armata* are coded as "?" due to absence of dorsal-fin spines.

Outgroups. All outgroups are coded as "?" due to absence of dorsal-fin spines.

TS 48. Anal-fin spines (0: absent; 1: present)

Ingroups. Anal-fin spines are absent in *Acanthochaenus luetkenii*, *Rondeletia loricata*, *Barbourisia rufa*, *Cetostoma regani*, *Monocentris japonica*, *Anoplogaster cornuta*, *Diretmus argenteus* and *Hoplobrotula armata* (character 48-0), while they are present in other ingroups (character 48-1).

Outgroups. All outgroups lack anal-fin spines.

Other variations

Number of vertebrae. Moore (1993) recognized the increased number of the vertebrae as a synapomorphy of Barbourisiidae + Cetomimidae (38 or more vs. 34 or less in other ingroups of his study). In this study, however, the numbers of the vertebrae in *Hispidoberyx* (33–35) and *Lateolabrax* (36) made the gap between Barbourisiidae + Cetomimidae and other ingroups (except for *Hoplobrotula* with 54 vertebrae) obscure. Accordingly, because it is difficult to recognize these mostly serial conditions as discrete characters, the numbers of the vertebrae are not used for the analysis.

Position of epineural. Johnson & Patterson (1993) recognized a difference on the positons of the anterior epineurals (except for those on first two vertebrae) between Stephanoberyciformes and Beryciformes defined by them. According to them, most

stephanoberyciforms have these bones on the parapophyses, while beryciforms have them on the pleural ribs. In this study, however, intermediate conditions between them were observed among ingroups. For example, some anterior epineurals originate from the dorsal tip of the pleural ribs and attached to both ribs and parapophyses (or the centra when the parapophyses are absent) in *Anomalops katoptron*, *Poromitra unicornis* and *Gibberichthys pumilus*. These conditions make the variations of the positions of the epineurals serial, and then it is difficult to separate them into clearly defined characters. Consequently, the conditions of the positions of the epineurals are not used for the analysis.

Number of supraneurals. Among ingroups, the numbers of the supraneurals are various and ranging from zero in *Cetostoma regani* to six in *Barbourisia rufa*. However, because the positions of their insertion to the neural spines also include various conditions, the homology of the supraneurals among ingroups is unclear. Therefore, the number of the supraneurals is not used for the analysis.

Position of insertion of first dorsal-fin proximal pterygiophore. Regarding to the position of the insertion of the first dorsal-fin proximal pterygiophore, Moore (1993) recognized the following four conditions among his trachichthyiforms: (1) somewhere anterior to fourth neural spine; (2) between fourth and fifth neural spines; (3) anterior to eighth or ninth neural spines; and (4) posterior to fourteenth neural spine. Among ingroups in this study, the following three additional conditions were also found: (1) between the sixth and seventh neural spines in *Gibberichthys pumilus*; (2) between the ninth and tenth neural spines in *Rondeletia loricata*; and (3) between the 12th and 13th neural spines in *Acanthochaenus luetkenii*. However, the change of the positions of the anteriormost dorsal-fin proximal pterygiophore can be assumed to occur by various reasons (e.g., sift of the dorsal fin, and addition or loss of the proximal pterygiophores and/or vertebrae). Accordingly, because the homology of the “first” dorsal-fin proximal pterygiophore among ingroups is unclear, the position of the first dorsal proximal pterygiophore is not used for the analysis.

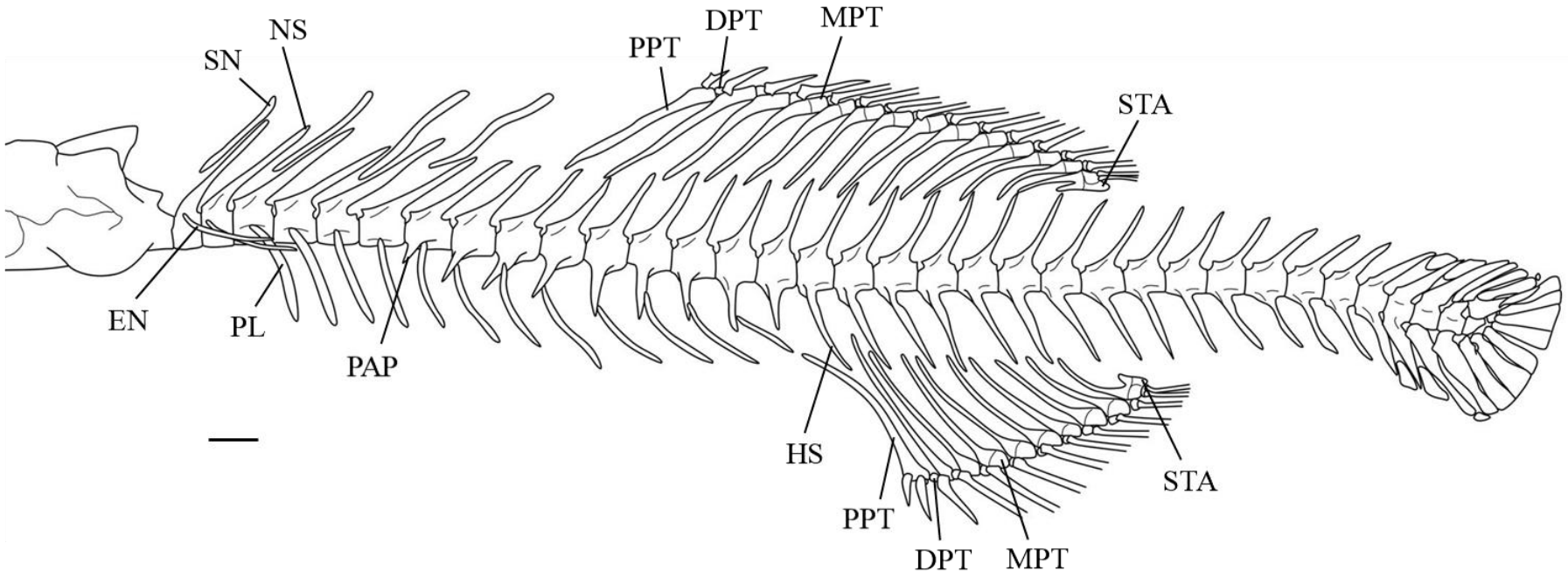

Figure 24. Lateral aspect of axial skeleton and median-fin supports in *Hispidoberyx ambagiosus*. DPT, distal pterygiophore; EN, epineural; HS, hemal spine; MPT, medial pterygiophore; NS, neural spine; PAP, parapophysis; PL, pleural rib; PPT, proximal pterygiophore; SN, supraneural; STA, stay. Scale indicates 5 mm.

4-1-10. Caudal skeleton (Figs. 25–27)

Description

The caudal skeleton comprises the ural centra, preural centra, parhypural, hypurals, epurals and uroneurals.

The ural centra are situated on the central portion of the caudal skeleton. The first ural centrum is fused with the first preural centrum. This compound bone anteriorly articulates with the second preural centrum and attached to the first uroneural dorsally, the second ural centrum posterodorsally, and the parhypural and first to second hypurals posteroventrally via a cartilage or directly. The second ural centrum is autogenous, and attached to the first uroneural anterodorsally and the third to fourth hypurals posteriorly.

The preural centra, located anterior to the ural centra, possess the neural and hemal spines dorsally and ventrally, respectively. The second preural centrum articulates with the compound bone formed by the first ural and preural centra posteriorly and the third preural centrum anteriorly. The neural spine of the second preural centrum is short and ventrally fused with the centrum. A long and autogenous hemal spine of the third preural centrum is posteroventrally capped with a cartilage and supports caudal-fin rays ventrally. The third preural centrum articulates with the second preural centrum posteriorly and the fourth preural centrum anteriorly. A long neural spine of the third preural centrum has a cartilaginous cap on its posterodorsal tip and is fused with the centrum. The post-hemal spine cartilage of the third preural centrum, inter-neural spine cartilages of the fourth and fifth preural centra, and inter-hemal spine cartilages of the fourth and fifth preural centra are present. These cartilages are composed of a single element, respectively, in HUMZ 194634, 180.7 mm SL, whereas the inter-neural spine cartilages of the fourth preural centrum comprises one anterior large element and one posterior small element, the inter-neural spine cartilages of the fifth preural centrum comprises two anterior small elements and one posterior large element, and the inter-hemal spine cartilages of the fifth preural centrum comprises one anterior small element and

one posterior large element in HUMZ 193670, 178.8 mm SL. The post-neural spine cartilage of the fourth preural centrum is present in HUMZ 193670, 178.8 mm SL, while it is absent in HUMZ 194634, 180.7 mm SL.

The parhypural, a slender plate-like bone, is attached to the hemal spine of the preural centrum anteroventrally, the first hypural posterodorsally and the compound bone formed by the first ural and preural centra dorsally. The anterodorsal portion of the bone has a hypurapophysis. The posteroventral margin of the bone has a cartilage supporting caudal-fin rays.

The hypurals, comprising six slender plate-like bones, are located on the posterior portion of the caudal skeleton and posteriorly have cartilaginous margins supporting caudal-fin rays. The first to second hypurals are attached to the compound bone formed by the first ural and preural centra anterodorsally via a cartilage or directly. The third and fourth hypurals are anteriorly attached to the second ural centrum. The fifth and sixth hypurals are anteriorly attached to the first and second uroneurals, respectively.

The epurals are composed of three rod-like bone, situated on the dorsal portion of the caudal skeleton. The posterodorsal tip of each bone is capped with a cartilage. The first, second and third epurals are anteroventrally attached to the neural spine of the second preural centrum, neural spine of the second preural centrum and first uroneural, and first uroneural, respectively. These bones are autogenous in HUMZ 194634, 180.7 mm SL, while the second and third elements are dorsally fused with each other in HUMZ 193670, 178.8 mm SL. The post-epural 3 cartilage is situated posterior to the tip of the third epural.

The uroneurals, comprising two elements, are located on the dorsal portion of the caudal skeleton. The first uroneural is attached to the second and third epurals dorsally, the second uroneural and fifth hypural posteriorly, and the compound bone formed by the first ural and preural centra, and second ural centrum ventrally. The second uroneural is attached to the first uroneural anteriorly and the sixth hypural posteriorly.

The branched caudal-fin rays are nine and eight in the upper and lower lobes, respectively (based on six specimens examined). The procurrent spines are nine and nine to ten in the upper and lower lobes, respectively (based on six specimens examined). The second ventral procurrent spine is not shortened proximally.

Character recognition

TS 49. Second ural centrum, and compound bone formed by first ural and preural centra (0: autogenous; 1: fused)

Ingroups. The second ural centrum is fused with the compound bone formed by the first ural and preural centra in melamphaids, berycids, *Holocentrus adscensionis*, *Neoniphon sammara*, *Hoplobrotula armata*, *Lateolabrax japonicus*, *Lates mariae* and *Trachurus japonicus* (Fig. 26A) (character 49-1), while these bones are autogenous in other ingroups (character 49-0). Because both conditions are observed in *Cetostoma regani* and *Trachichthys australis*, “0” and “1” are coded for them.

Outgroups. These bones are autogenous in all outgroups.

Remarks. Zehren (1979) reported that *T. australis* has the autogenous second ural centrum. In this study, the second ural centrum of the species is autogenous in one specimen (HUMZ 40221, 111.0 mm SL), but fused with the compound bone formed by the first ural and preural centra in the other specimen (AMS I.15912-007, 96.7 mm SL).

In *C. regani*, the second ural centrum is autogenous in one specimen examined in this study (one of BMNH 1996.2.14.40–43, 89.2 mm SL), while this bone is fused with the compound bone formed by the first ural and preural centra in the other specimen in BMNH 1996.2.14.40–43 (129.0 mm SL).

TS 50. Second ural centrum, and third and fourth hypurals (0: autogenous; 1: fused)

Ingroups. The second ural centrum is fused with the third and fourth hypurals in *Anoplogaster cornuta*, *Diretmus argenteus* and *Velifer hypselopterus* (Fig. 26B) (character 50-

1), while these bones are autogenous in other ingroups (character 50-0).

Outgroups. These bones are autogenous in all outgroups.

TS 51. Neural spine of second preural centrum (0: autogenous; 1: fused with centrum)

Ingroups. The neural spine of the second preural centrum is autogenous in trachichthyids and *Anomalops katoptron* (character 51-0), and fused with the centrum in other ingroups (character 51-1). As both conditions are observed in *Monocentris japonica*, "0" and "1" are coded for the species.

Outgroups. All outgroups have the autogenous hemal spine of the second preural centrum.

Remarks. Zehren (1979) and Moore (1993) reported that *M. japonica* has the autogenous neural spine of the second preural centrum. In this study, the neural spine of the second preural centrum is autogenous in one specimen of the species (HUMZ 40406, 108.9 mm SL), while it is fused with the centrum in the other specimen (HUMZ 33613, 136.0 mm SL).

TS 52. Hemal spine of third preural centrum (0: autogenous; 1: fused with centrum)

Ingroups. The hemal spine of the third preural centrum is fused with the centrum in *Melamphaes typhlops*, *Scopelogadus mizolepis* and *Hoplobrotula armata* (character 52-1), while it is autogenous in other ingroups (character 52-0).

Outgroups. The hemal spine of the third preural centrum is autogenous in all outgroups.

TS 53. Fourth and fifth hypurals (0: autogenous; 1: anteriorly fused; 2: completely fused) (ordered as 0-1-2)

Ingroups. The fourth and fifth hypurals are anteriorly fused in *Melamphaes typhlops* and *Poromitra unicornis* (character 53-1), completely fused in *Scopelogadus mizolepis* and *Hoplobrotula armata* (character 53-2), and autogenous in other ingroups (character 53-0).

Outgroups. The fourth and fifth hypurals are autogenous in all outgroups.

TS 54. First uroneural (0: autogenous; 1: fused with underlying centra)

Ingroups. The first uroneural is fused with underlying centra in melamphaids, *Anoplogaster cornuta*, *Diretmus argenteus*, berycids, *Holocentrus adscensionis*, *Neoniphon sammara*,

Hoplobrotula armata and *Trachurus japonicus* (Fig. 26) (character 54-1), while it is autogenous in other ingroups (character 54-0). As *Rondeletia loricata* and *Barbourisia rufa* have both conditions, “0” and “1” are coded for them.

Outgroups. The first uroneural is autogenous in all outgroups.

Remarks. Kotlyar (1995, 1996a) described that the first uroneural is fused with underlying centra in *R. loricata* and *B. rufa*, whereas this bone is autogenous in specimens examined in this study.

TS 55. Number of branched caudal-fin rays (0: 17; 1: 16; 2: 15; 3: 9) (ordered as 0-1-2-3)

Ingroups. The numbers of branched caudal-fin rays are nine in *Hoplobrotula armata* (character 55-3), 15 in *Cetostoma regani*, *Lateolabrax japonicus*, *Lates mariae* and *Trachurus japonicus* (character 55-2), 16 in *Polymixia japonica* (character 55-1), and 17 in other ingroups (character 55-0).

Outgroups. All outgroups have 17 branched caudal-fin rays.

Remarks. Specimens of *Stephanoberyx monae* and *Anoplogaster cornuta* examined in this study have 16 branched caudal-fin rays. However, these genera are well known to have usually 17 branched caudal-fin rays by other studies based on a lot of specimens (e.g., Ebeling & Weed, 1973; Kotlyar, 1987, 1996b). Therefore, because the fewer numbers of branched caudal-fin rays in these species observed in this study are considered to be abnormality, “0” are coded for them based on previous studies.

TS 56. Second ventral procurrent caudal-fin ray (0: not shortened proximally; 1: proximally shortened)

Ingroups. The second ventral procurrent caudal-fin ray is not shortened in *Hispidoberyx ambagiosus*, stephanoberycids, *Gibberichthys pumilus*, *Rondeletia loricata*, *Barbourisia rufa*, *Cetostoma regani*, *Polymixia japonica*, *Velifer hypselopterus* and *Trachurus japonicus* (character 56-0), while it is proximally shortened so that its base is set back from the bases of the adjacent rays in other ingroups (Fig. 27) (character 56-1). Due to absence of the second

ventral procurrent ray, "?" is coded for *Hoplobrotula armata*.

Outgroups. The second ventral procurrent ray is not shortened in *Neoscopelus microchir* and *Trachinocephalus trachinus*, whereas it is proximally shortened in *Hime japonica*.

Remarks. Although Johnson (1975) reported that melamphaids have the shortened second ventral procurrent ray, Johnson & Patterson (1993) subsequently corrected it and recognized that melamphaids lack such a condition. In this study, however, obviously shortened second ventral procurrent ray was found in melamphaids. In this family, the second ventral procurrent ray is closely attached to the first ventral procurrent ray, and the two elements look like a single ray in some case. Therefore, it is assumed that Johnson & Patterson (1993) mistakenly recognized the two rays as the first procurrent ray, and the third procurrent ray as the second.

Other variations

Fusions of parhypural and first hypural, first and second hypurals, and third and fourth hypurals. Other than the fourth and fifth hypurals, fusions were also observed between the parhypural and first hypural, the first and second hypurals, and the third and fourth hypurals in caudal elements in several taxa. In these cases, however, the extent of the fusion serially varies among ingroups, and distinct characters cannot be clearly defined. Therefore, the conditions of the fusions between the parhypural and first hypural, the first and second hypurals, and the third and fourth hypurals are not used for the analysis.

Number of hypurals. Johnson & Patterson (1993) recognized the following two conditions on the number of the hypurals among Acanthomorpha: (1) six hypurals and (2) five or fewer. In taxa lacking an autogenous sixth hypural, however, it is unclear whether the absence of the sixth hypural is caused by the fusion to the fifth hypural or loss of the bone. Accordingly, the number of the hypurals is not used for the analysis due to uncertainty of the homology.

Cartilaginous elements in caudal skeleton. Different conditions of the cartilaginous elements in the caudal skeleton were observed among ingroups. However, regarding to each

of particular cartilages defined by Fujita (1990), the size, shape and number of the elements are quite various, and then the homology of those elements is unclear. Therefore, the conditions of the cartilaginous elements in the caudal skeleton are not used for the analysis.

Number of procurrent spines. Moore (1993) recognized nine to eleven procurrent spines in both upper and lower lobes as a synapomorphy shared by Hispidoberycidae and Stephanoberycidae. Although previous works reported that the number of procurrent spines in *Hispidoberyx ambagiosus* was 9–10 (Kotlyar, 1981, 1991a; Yang et al., 1988), reexamination of the holotype of the species in this study revealed that it has eight procurrent spines in the upper caudal lobe (and nine in lower lobe as in previous studies). In addition, this study found that *Anomalops katoptron* has nine and eight procurrent spines in upper and lower lobes, respectively, and previous studies reported that *Gibberichthys pumilus* has six to eight and five to seven procurrent spines in upper and lower lobes, respectively (Ebeling & Weed, 1973; Kotlyar, 1996b). These numbers make the variation of the number of procurrent spines serial among ingroups (seven or fewer in other ingroups). Accordingly, because it is difficult to separate them into discrete characters, the number of the procurrent spines is not used for the analysis.

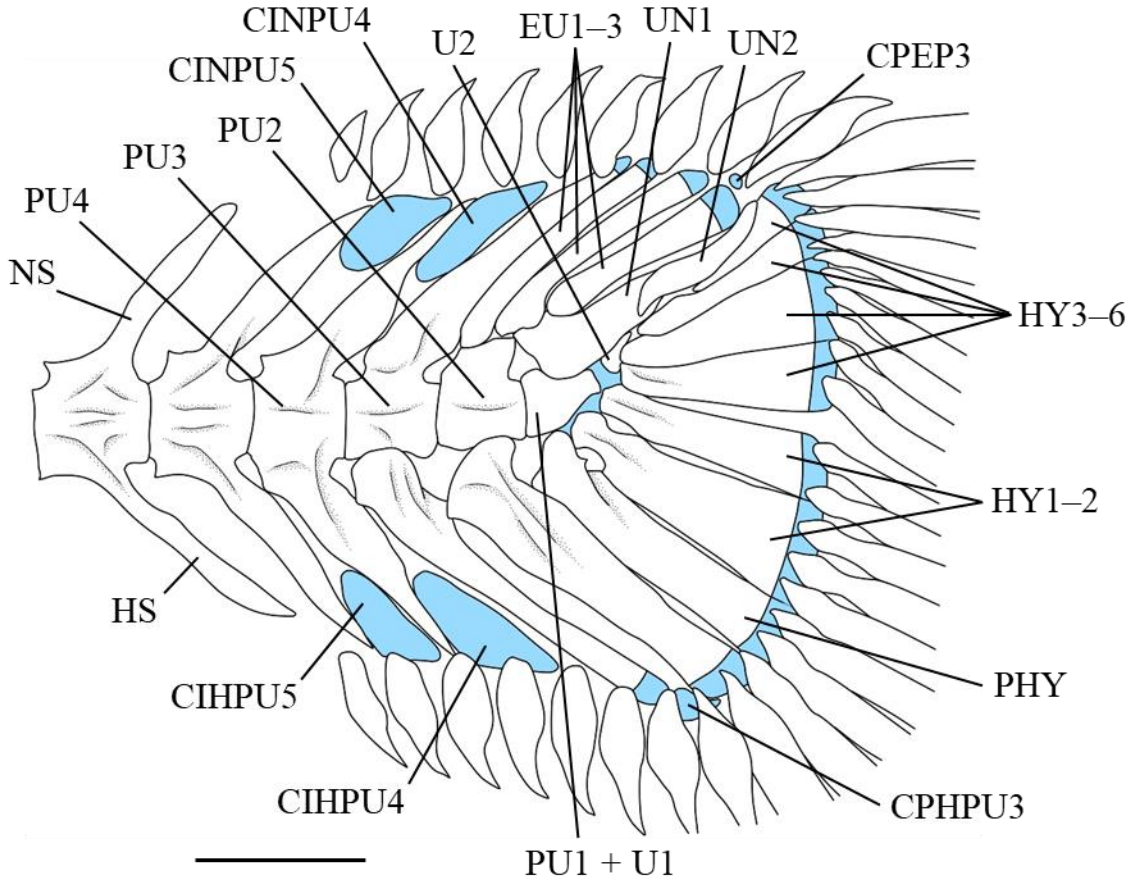

Figure 25. Lateral aspect of caudal skeleton in *Hispidoberyx ambagiosus*. CIHPU4–5, inter-hemal spine cartilage of PU4–5; CINPU4–5, inter-neural spine cartilage of PU4–5; CPEP3, post-epural 3 cartilage; CPHPU3, post-hemal spine cartilage of PU3; EU1–3, first to third epurals; HS, hemal spine; HY1–6, first to sixth hypurals; NS, neural spine; PHY, parhypural; PU1–4, first to fourth preural centra; U1–2, first to second ural centra; UN1–2, first to second uroneurals. Scale indicates 5 mm.

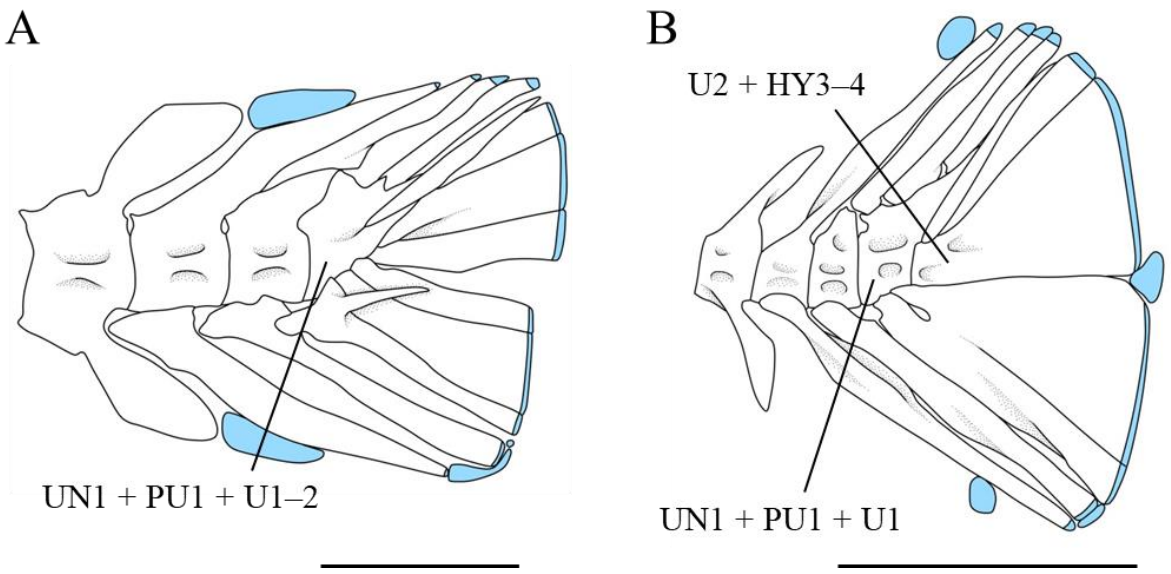

Figure 26. Lateral aspects of caudal skeleton in (A) *Holocentrus adscensionis* and (B) *Diretmus argenteus*. HY3–4, third to fourth hypurals; PU1, first preural centrum; U1–2, first to second ural centra; UN1, first uroneural. A is shown as mirror image. Scales indicate 5 mm.

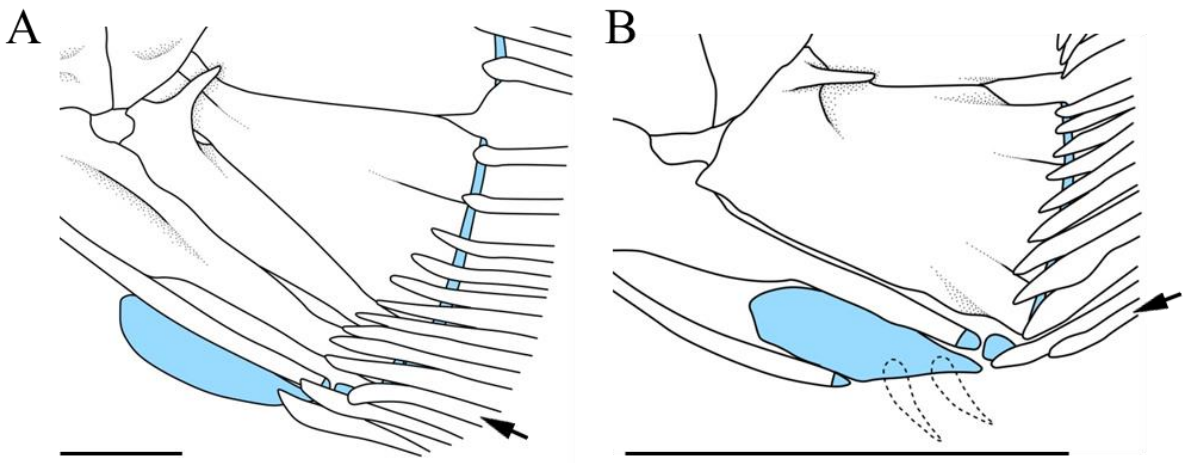

Figure 27. Lateral aspects of caudal skeleton in (A) *Beryx decadactylus* and (B) *Melamphaes typhlops*. Arrows indicate second ventral procurrent ray. B is shown as mirror image. Scales indicate 5 mm.

4-2. Myology

4-2-1. Cheek muscles (Figs. 28, 29)

Description

The cheek muscle is composed only of the adductor mandibulae, which is subdivided into four sections, A1, A2, A3 and A ω.

The section A1 is situated on the dorsolateral portion of the cheek muscles. This muscle originates from the hyomandibula and inserts onto the ligamentum primordium. The ligamentum primordium anteriorly bifurcates and inserts onto the lateral and medial surfaces of the anterior portion of the maxillary shaft, and posteroventrally inserts onto the posterior portion of the anguloarticular. This ligament lacks a posteroventral extension and insertion onto the preopercle. Subsections of this muscle are absent.

The section A2 is located on the ventrolateral portion of the cheek muscles. This muscle is medially almost fused with the section A3, and detached from the section A ω. This muscle originates from the hyomandibula, metapterygoid, preopercle, and quadrate, and inserts onto the medial surface of the lower jaw via a strong tendon. The posteroventral portion of the muscle has a distinctly separated tendon inserting onto the quadrate.

The section A3 is a medial subdivision of the adductor mandibulae and almost fused with the section A2 laterally. This muscle originates from the metapterygoid and symplectic, and inserts onto the medial surface of the lower jaw via a strong tendon.

The section A ω is located on the medial surface of the lower jaw, originating from the dentary, anguloarticular and Meckelian cartilage. This muscle is posterodorsally connected with the sections A2 and A3 via a strong tendon.

Character recognition

TS 57. Insertion of ligamentum primordium onto preopercle (0: absent; 1: present)

Ingroups. The ligamentum primordium is posteroventrally extended, passing lateral to the

section A2, and inserts onto the preopercle in trachichthyids (Fig. 29A) (character 57-1), while its extension and insertion onto the preopercle are absent in other ingroups (character 57-0).

Outgroups. The insertion of the ligament onto the preopercle is absent in all outgroups.

TS 58. Separated tendon on posteroventral portion of section A2 inserting onto quadrate (0: absent or indistinct; 1: distinct)

Ingroups. A distinctly separated tendon on the posteroventral portion of the section A2 inserting onto the quadrate is present in *Hispidoberyx ambagiosus*, stephanoberycids, *Gibberichthys pumilus* and *Rondeletia loricata* (Figs. 28, 29C) (character 58-1), whereas the tendon is absent or indistinct in other ingroups (character 58-0).

Outgroups. This tendon is absent or indistinct in all outgroups.

TS 59. Sections A2 and A ω (0: detached; 1: attached via raphe)

Ingroups. The sections A2 and A ω are attached via a raphe in *Holocentrus adscensionis*, *Neoniphon sammara*, *Lateolabrax japonicus*, *Lates mariae* and *Trachurus japonicus* (Fig. 29B) (character 59-1), whereas they are detached in other ingroups (character 59-0).

Outgroups. These muscles are detached in all outgroups.

Other variations

Subsections of section A1. The section A1 has two subsections, an anterodorsal A1 β and posteroventral A1 α, in stephanoberycids, *Cetostoma regani*, *Melamphaes typhlops*, *Anoplogaster cornuta*, *Polymixia japonica* and *Hoplobrotula armata*. Among these taxa, however, the A1 β includes various conditions. For example, this muscle in stephanoberycids originates from the metapterygoid and inserts onto the ligamentum primordium (Fig. 29C). In *C. regani*, it originates from the metapterygoid and directly inserts onto the maxilla (Fig. 29D). This muscle in *A. cornuta* originates from the palatine (some fibers originates from the first and second infraorbitals) and inserts onto the maxilla via a short tendon which is

separated from the ligamentum primordium (Fig. 29E). Due to such many variations of A1 β, the homology between the muscles in these taxa is unclear. Accordingly, the subsections of the A1 are not used for the analysis.

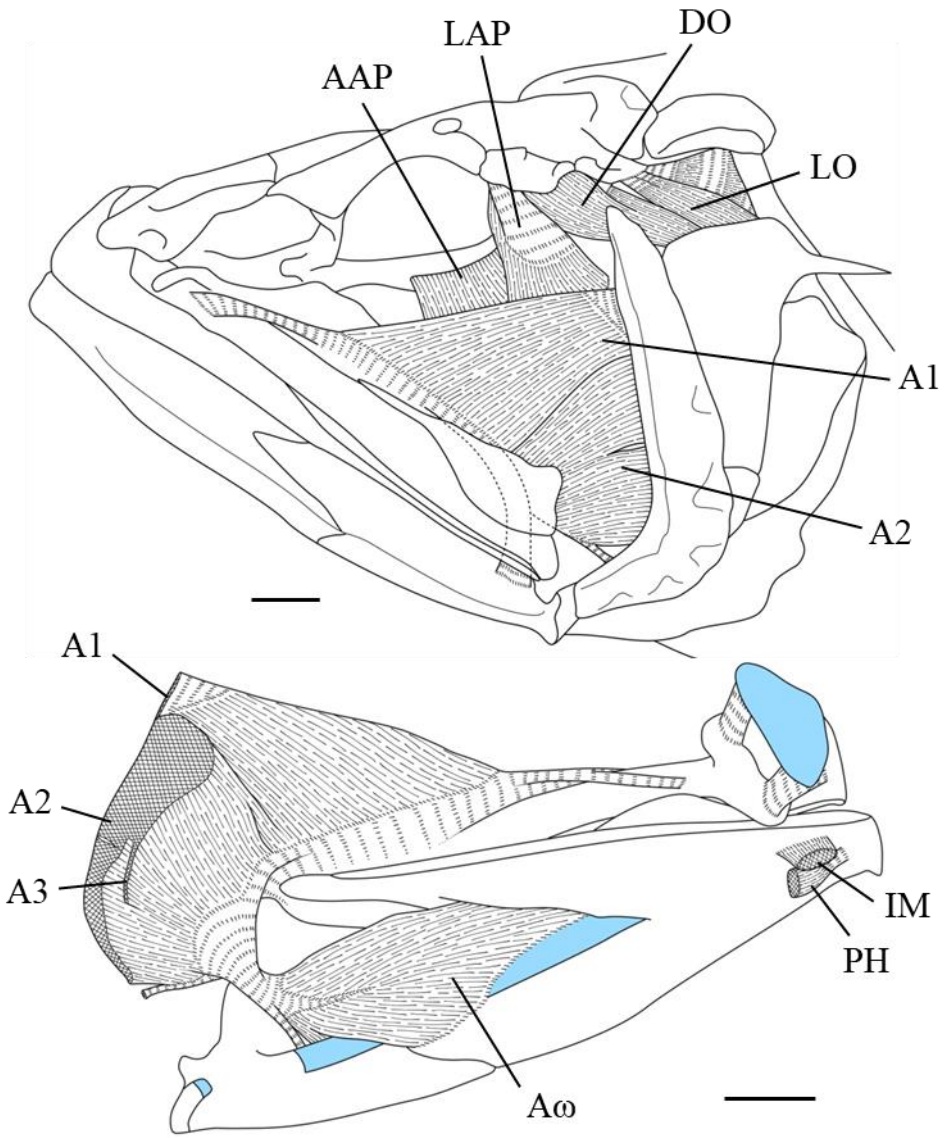

Figure 28. Lateral (upper) and medial (lower) aspects of cheek muscles in *Hispidoberyx*. A, sections of adductor mandibulae; AAP, adductor arcus palatini; DO, dilatator operculi; IM, intermandibularis; LAP, levator arcus palatini; LO, levator operculi; PH, protractor hyoidei. Scale indicates 5 mm.

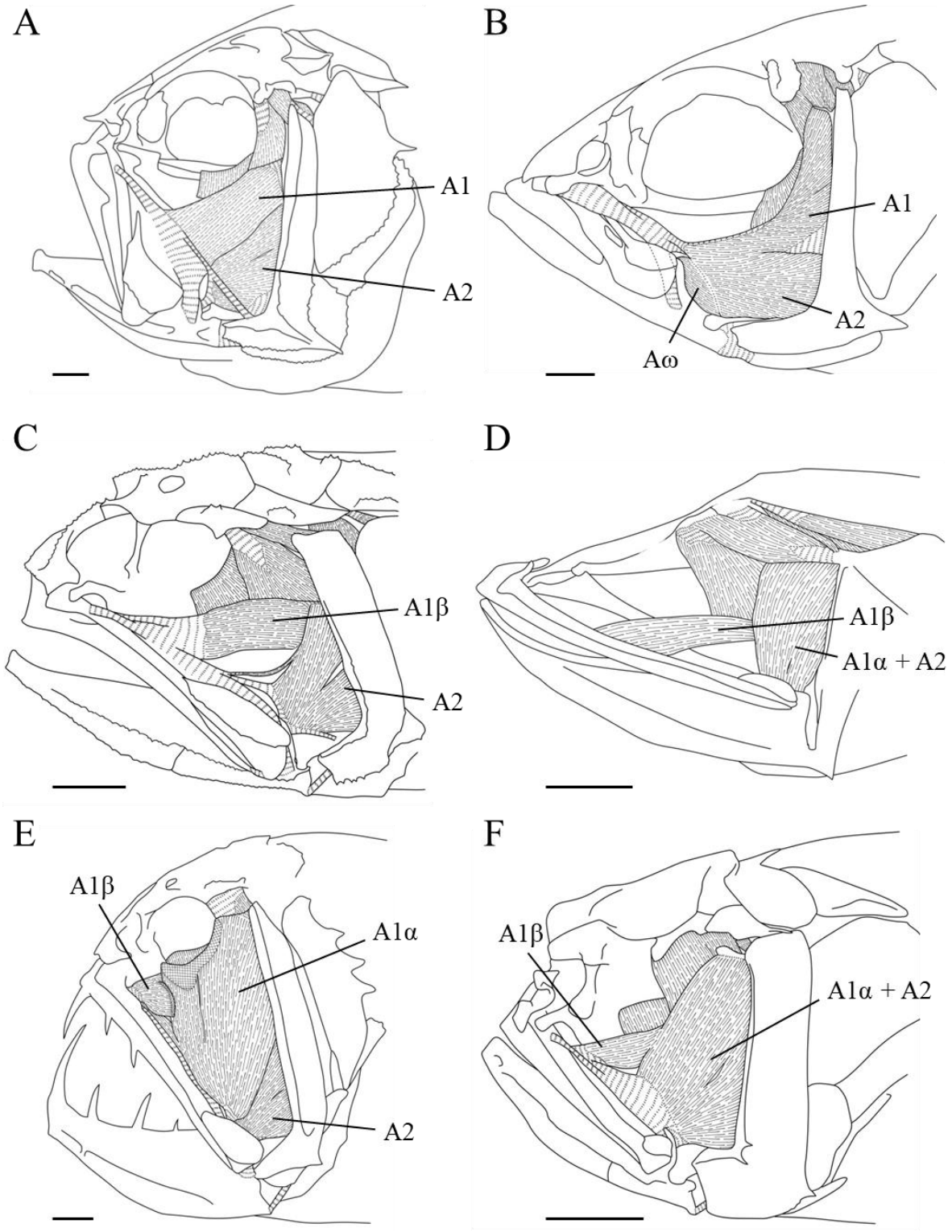

Figure 29. Lateral aspects of cheek muscles in (A) *Paratrachichthys trailli*, (B) *Neoniphon sammara* (C) *Stephanoberyx monae*, (D) *Cetostoma regani*, (E) *Anoplogaster cornuta* and (F) *Melamphaes typhlops*. A, sections of adductor mandibulae. F is shown as mirror image. Scales indicate 5 mm.

4-2-2. Cephalic muscles between neurocranium and suspensorium-opercular bones (Fig. 30)

Description

The cephalic muscles between the neurocranium and suspensorium-opercular bones include the adductor arcus palatini, levator arcus palatini, dilatator operculi, adductor hyomandibulae, adductor operculi and levator operculi.

The adductor arcus palatini is located on the posteroventral portion of the orbit. This muscle dorsomedially originates from the parasphenoid and prootic, and ventrolaterally inserts onto the endopterygoid, metapterygoid and hyomandibula. This muscle is posteriorly continuous with the adductor hyomandibulae via a thin laminate muscle.

The levator arcus palatini is situated posterior to the orbit. This muscle dorsally originates from the sphenotic, and ventrally inserts onto the hyomandibula and metapterygoid.

The dilatator operculi anterodorsally originates from the sphenotic, pterotic and hyomandibula, and posteroventrally inserts onto the anterodorsal corner of the opercle.

The adductor hyomandibulae dorsomedially originates from the pterotic, intercalar and exoccipital, and ventrolaterally inserts onto the posteromedial portion of the hyomandibula. This muscle is anteriorly continuous with the adductor arcus palatini via a thin laminate muscle.

The adductor operculi dorsomedially originates from the intercalar and exoccipital, and ventrolaterally inserts onto the anterodorsal portion of the opercle.

The levator operculi anterodorsally originates from the posterolateral corner of the pterotic and posteroventrally inserts onto the dorsomedial portion of the opercle.

Character recognition

TS 60. Origin of levator operculi (0: pterotic; 1: pterotic and posttemporal)

Ingroups. The levator operculi anterodorsally originates from the pterotic and posttemporal

in trachichthyids, *Monocentris japonica*, *Anoplogaster cornuta* and *Diretmus argenteus* (Fig. 30B) (character 60-1), whereas it originates only from the pterotic in other ingroups (character 60-0).

Outgroups. This muscle originates only from the pterotic in all outgroups.

Other variations

None.

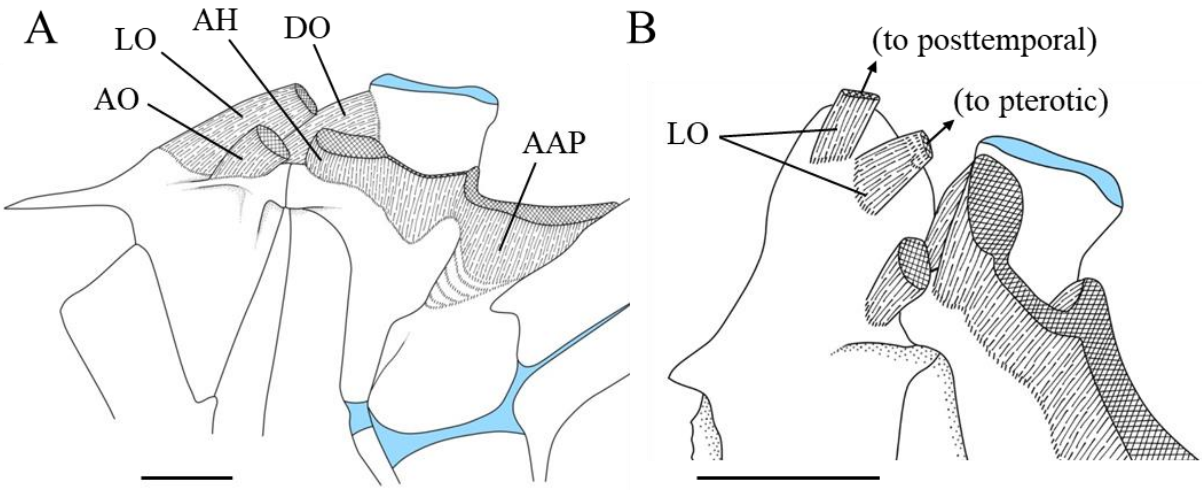

Figure 30. Medial aspects of suspensorium and opercular bones in (A) *Hispidoberyx ambagiosus* and (B) *Trachichthys australis*. AAP, adductor arcus palatini; AH, adductor hyomandibulae; AO, adductor operculi; DO, dilatator operculi; LO, levator operculi. Scales indicate 5 mm.

4-2-3. Ventral muscles of head (Figs. 31, 32)

Description

The ventral muscles of the head include the intermandibularis, protractor hyoidei, hyohyoidei abductores, hyohyoidei adductores and hyohyoides inferioris.

The intermandibularis is a small element, interconnecting the anteromedial portion of the dentary on each side.

The protractor hyoidei is a large band-like element, originating from the anteromedial portion of the dentary and inserting onto the lateral aspect of the ceratohyal.

The hyohyoidei abductores comprise two sections. The section 1 originates from the proximal portion of the branchiostegal rays (or the anteroventral portion of the ceratohyal in the anteriormost bundle) and inserts onto the distal portion of the succeeding branchiostegal rays. The section 2 originates from a raphe on the midline and inserts onto anterior several branchiostegal rays. This raphe on the midline anteriorly inserts onto the lateral aspect of the ventral hypohyal on each side via a tendon.

The hyohyoidei adductores are sheet-like elements, connecting the posterior branchiostegal rays, and the medial aspects of the opercle and subopercle.

The hyohyoides inferioris, a thin band like element, originates from a raphe on the midline and inserts onto the posteroventral portion of the ceratohyal.

Character recognition

TS 61. Hyohyoides inferioris (0: absent; 1: originating from ventral hypohyal on opposite side; 2: originating from raphe on midline) (unordered)

Ingroups. The hyohyoides inferioris originates from a raphe on the midline in *Hispidoberyx* and *Velifer hypselopterus* (character 61-2), and the ventral hypohyal on the opposite side in stephanoberycids, *Gibberichthys pumilus*, *Rondeletia loricata*, *Trachichthys australis*, *Anomalops katoptron*, *Monocentris japonica*, *Beryx decadactylus* and *Trachurus japonicus*

(character 61-1), while it is absent in other ingroups (character 61-0). In *Anoplogaster cornuta*, this muscle is absent in HUMZ 197375, 132.9 mm SL, while it is present in HUMZ 130183, 135.9 mm SL, but its origin was unable to be confirmed due to its feeble condition. Therefore, "?" is coded for the species.

Outgroups. This muscle originates from the ventral hypohyal on the opposite side in *Hime japonica*, whereas it is absent in *Neoscopelus microchir* and *Trachinocephalus trachinus*.

Other variations

Origin of hyohyoidei abductores section 2. In *Hispidoberyx ambagiosus*, the hyohyoidei abductores section 2 originates from a raphe on the midline which inserts onto the lateral aspect of the ventral hypohyal on each side. On the other hand, this muscle anteriorly originates from the ventral hypohyal on the opposite side tendinously and crosses over its antimere in other ingroups, except for *Polymixia japonica* lacking the muscle and *Velifer hypselopterus* in which it originates from the urohyal. Because all outgroups have the muscle originating from the ventral hypohyal on the opposite side, the condition in *H. ambagiosus* is considered to be an autapomorphy of the species.

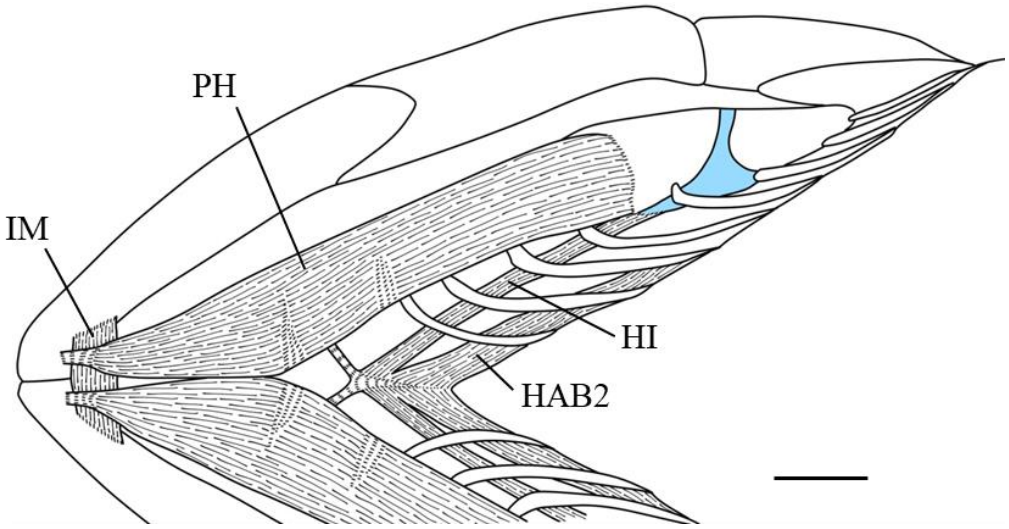

Figure 31. Ventral aspect of ventral muscles of head in *Hispidoberyx ambagiosus*. HAB2, hyohyoidei abductores section 2; HI, hyohyoides inferioris; IM, intermandibularis; PH, protractor hyoidei. Scale indicates 5 mm.

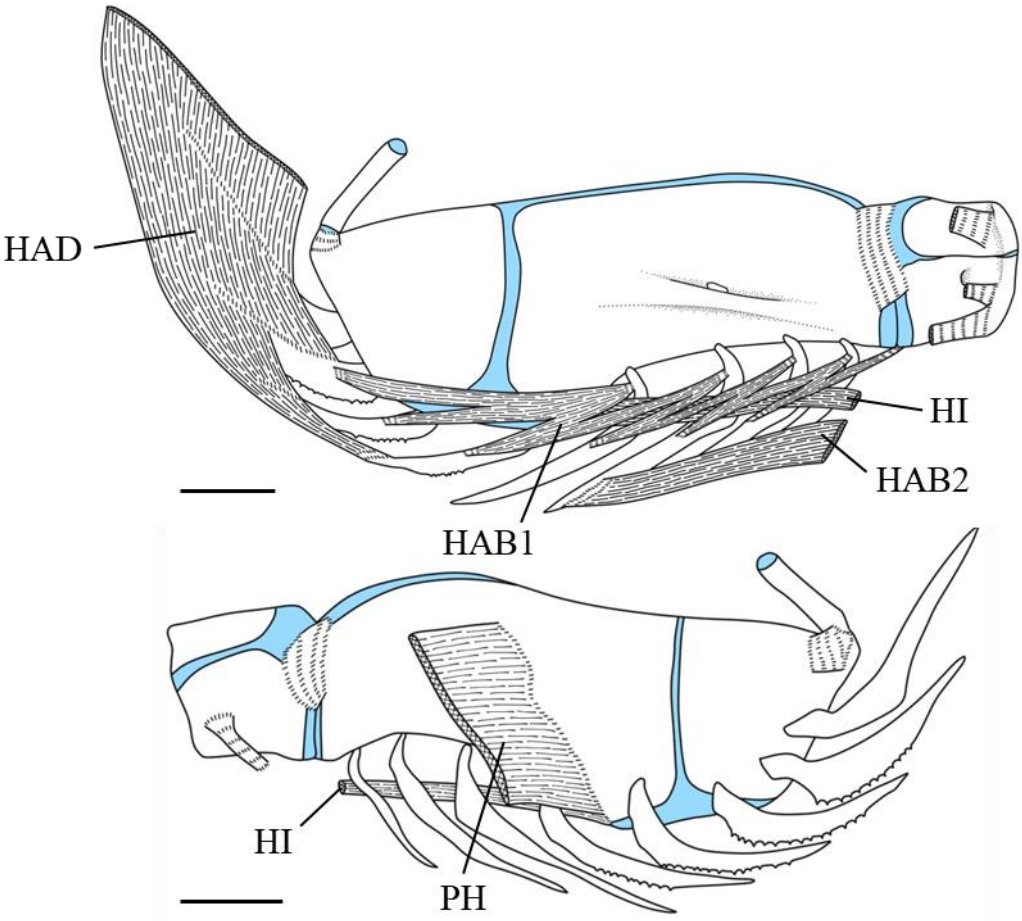

Figure 32. Medial (upper) and lateral (lower) aspects of hyoid arch and its related muscles in *Hispidoberyx ambagiosus*. HAB1–2, hyohyoidei abductores sections 1–2; HAD, hyohyoidei adductores; HI, hyohyoides inferioris; PH, protractor hyoidei. Scales indicate 5 mm.

4-2-4. Branchial muscles (Figs. 33–36)

Description

The branchial muscles consist of the levatores externi, levatores interni, levator posterior, obliquus dorsalis, transversi dorsales, retractor dorsalis, sphincter oesophagi, obliquus posterior, adductores, obliqui ventrales, rectus ventralis, rectus communis, transversi ventrales and pharyngoclaviculares.

The levatores externi, comprising four band-like elements, are connecting the upper branchial arches and neurocranium. The first to fourth elements dorsally originate from the prootic and pterotic, and ventrally insert onto the first to fourth epibranchials, respectively.

The levatores interni are composed of two band-like elements, connecting the upper branchial arches and neurocranium. The first and second elements dorsally originate from the pterotic and prootic, respectively, and ventrally insert onto the second and third pharyngobranchials, respectively.

The levator posterior, a thin band-like element, originates from the exoccipital just posterior to the origin of the adductor operculi, and inserts onto the fourth epibranchial.

The obliquus dorsalis, a robust and elongate muscle, anteriorly originates from the dorsal surface of the third pharyngobranchial, and posteriorly inserts onto the third and fourth epibranchials. This muscle is anteriorly covered with the transversus dorsalis anterior.

The transversi dorsales are sheet-like muscles, composed of the transversus dorsalis anterior and transversus dorsalis posterior. The transversus dorsalis anterior interconnects the second pharyngobranchial and second epibranchial on each side. The transversus dorsalis posterior interconnects the third pharyngobranchial and third epibranchial on each side. Some fibers of the muscle are anteriorly confluent with the transversus dorsalis anterior, and posteriorly with the sphincter oesophagi.

The retractor dorsalis is an elongate muscle, connecting the posteromedial margin of the third pharyngobranchial and the ventral surface of the third abdominal vertebra.

The sphincter oesophagi is a thin muscle encircling the anterior portion of the esophagus. Some fibers of the muscle anteriorly originate from the fourth epibranchial, third pharyngobranchial and fifth ceratobranchial. The sphincter esophagi division (sensu Springer & Johnson, 2004) is present and passes dorsal to the retractor dorsalis.

The obliquus posterior vertically interconnects the upper and lower branchial arches. This muscle is dorsomedially fused with the sphincter oesophagi. This muscle dorsally originates from the fourth epibranchial. Ventrally, the medial part of the muscle inserts on to the fifth ceratobranchial, and the lateral part of the muscle is attached to the adductor V via a raphe.

The adductores consist of two elements, the adductores IV and V. The adductor IV is situated on the anterolateral portion of the obliquus posterior, and connects the fourth epibranchial and fourth ceratobranchial. The adductor V is dorsally attached to the obliquus posterior via a raphe and ventrally inserts onto the fifth ceratobranchial.

The obliqui ventrales comprise three elements, the obliqui ventrales I to III. These elements connect the first to third hypobranchials and the first to third hypobranchials, respectively.

The rectus ventralis originates from the third hypobranchial and semicircular ligament (sensu Springer & Johnson, 2004), and inserts onto the fourth ceratobranchial. Some fibers of the muscle are laterally confluent with the rectus communis.

The rectus communis is an elongate muscle and connects the third hypobranchial and fifth ceratobranchial. Some fibers of the muscle are medially confluent with the rectus ventralis.

The transversi ventrales are composed of two elements, the transversus ventralis anterior and transversus ventralis posterior. The transversus ventralis anterior consists of unpaired and paired elements; the former interconnecting the fourth ceratobranchial on each side, and the latter interconnecting the fourth basibranchial and the fourth ceratobranchial. The transversus ventralis posterior is an unpaired element with a raphe on its midline, and interconnects the fifth ceratobranchial on each side. The anterior portion of the muscle has a tendon inserting onto the fifth ceratobranchial. The anterior portion of the tendon is bifurcated and Y-shaped in

HUMZ 193670, 178.8 mm SL, while it is not bifurcated in HUMZ 194634, 180.7 mm SL.

The pharyngoclaviculares are composed of two elements, the pharyngoclavicularis externus and pharyngoclavicularis internus. The former anterodorsally originates from the fifth ceratobranchial and posteroventrally inserts onto the cleithrum. The insertion of the muscle onto the cleithrum is situated lateral to the sternohyoideus (HUMZ 194634, 180.7 mm SL) or slightly medial to it (HUMZ 193670, 178.8 mm SL). The pharyngoclavicularis internus anteriorly originates from the fifth ceratobranchial and posteriorly inserts onto the cleithrum via a thin tendon.

Character recognition

TS 62. Levator posterior (0: absent; 1: present)

Ingroups. The levator posterior is absent in trachichthyids, *Monocentris japonica*, *Anoplogaster cornuta*, *Ostichthys japonicus* and *Velifer hypselopterus* (character 62-0), whereas it is present in other ingroups (character 62-1).

Outgroups. All outgroups lack this muscle.

TS 63. Insertion of transversus dorsalis anterior onto second epibranchial (0: present; 1: absent)

Ingroups. The insertion of the transversus dorsalis anterior onto the second epibranchial is absent in *Gibberichthys pumilus* and *Rondeletia loricata* (character 63-1), while it is present in other ingroups (character 63-0). Because both conditions are observed in *Anoplogaster cornuta*, “0” and “1” are coded for the species.

Outgroups. The insertion of the muscle onto the second epibranchial is present in all outgroups.

Remarks. In *A. cornuta*, the insertion of the transversus dorsalis anterior onto the second epibranchial is absent in one specimen examined in this study (HUMZ 130183, 113.0 mm SL), whereas it is present in the other specimen (HUMZ 197375, 132.9 mm SL).

TS 64. Sphincter oesophagi division (0: present; 1: absent)

Ingroups. The sphincter oesophagi division is absent in melamphaids and *Anoplogaster cornuta* (character 64-1), whereas it is present in other ingroups (character 64-0).

Outgroups. The sphincter oesophagi division is present in all outgroups.

TS 65. Semicircular ligament (0: absent; 1: present)

Ingroups. The semicircular ligament is absent in *Cetostoma regani*, *Poromitra unicornis*, *Scopelogadus mizolepis*, *Hoplostethus mediterraneus*, *Anoplogaster cornuta*, *Diretmus argenteus*, berycids, holocentrids and *Hoplobrotula armata* (character 65-0), whereas it is present in other ingroups (character 65-1).

Outgroups. All outgroups lack the ligament.

TS 66. Transversus ventralis anterior (0: unpaired element; 1: unpaired and paired elements; 2: paired elements) (ordered as 0-1-2)

Ingroups. The transversus ventralis anterior is composed of paired elements in *Cetostoma regani* (character 66-2), an unpaired element in melamphaids, *Diretmus argenteus*, *Holocentrus armata*, *Neoniphon sammara*, *Lateolabrax japonicus*, *Lates mariae* and *Trachurus japonicus* (character 66-0), and both unpaired and paired elements in other ingroups (character 66-1). As both second and third conditions are observed in *Rondeletia loricata* and *Anoplogaster cornuta*, “0” and “1” are coded for them.

Outgroups. This muscle comprises an unpaired element in *Neoscopelus microchir* and *Trachinocephalus trachinus*, and both unpaired and paired elements in *Hime japonica*.

Remarks. In *R. loricata*, the transversus ventralis anterior is composed of paired elements in one specimen examined in this study (HUMZ 192726, 74.9 mm SL), whereas it comprises both unpaired and paired elements in the other specimen (HUMZ 130180, 76.8 mm SL).

In *A. cornuta*, this muscle consists of paired element in one specimen examined in this study (HUMZ 197375, 132.9 mm SL), whereas it is composed of both unpaired and paired elements in the other specimen (HUMZ 130183, 113.0 mm SL).

The paired elements of the transversus ventralis anterior variously develop among ingroups. For instance, these elements are well developed in *Barbourisia rufa* (Fig. 34B), while they are moderately developed in *Hispidoberyx ambagiosus* (Fig. 33C), and weakly developed in *Hoplostethus mediterraneus* (Fig. 34C). However, the degree of development of these elements varies serially among ingroups, and clearly defined characters cannot be discerned. Consequently, the conditions of the paired elements are not included for the analysis.

TS 67. Anterior tendon of transversus ventralis posterior (0: present; 1: absent)

Ingroups. The anterior tendon of the transversus ventralis posterior is absent in *Hoplobrotula armata*, *Lateolabrax japonicus*, *Lates mariae* and *Trachurus japonicus* (character 67-1), while it is present in other ingroups (character 67-0). Because both conditions are observed in *Anomalops katoptron*, “0” and “1” are coded for the species.

Outgroups. All outgroups have the tendon.

Remarks. In *A. katoptron*, the anterior tendon of the transversus ventralis posterior is present in one specimen examined in this study (KPM-NI 10182, 87.1 mm SL), whereas it is absent in the other specimen (HUMZ 40200, unmeasured).

Various shapes of the anterior tendon of the transversus ventralis posterior are observed among ingroups. For example, *Cetostoma regani* and *Barbourisia rufa* have the tendon which is deeply bifurcated and V-shaped (Fig. 34A, B), while one specimen of *Hispidoberyx ambagiosus* has the tendon which is anteriorly bifurcated and Y-shaped. On the other hand, this tendon is simple or slightly spread anteriorly in many other taxa. However, the shape of the tendon serially varies among ingroups, and then it is difficult to be separated into clearly defined characters. Therefore, the shape of the tendon is not used for the analysis.

Other variations

Anterior origin of rectus communis. Regarding to the anterior origin of the rectus

communis, the following three conditions were observed among ingroups: (1) originating from the third hypobranchial; (2) from the third hypobranchial and urohyal; and (3) from the urohyal. However, the proportion of areas of both bones as the origin of the rectus communis includes large variation among the second condition, and then the anterior origin of the muscle serially varies among ingroups. Moreover, in several taxa, because the anterior portion of the rectus communis is fused with the rectus ventralis, it is difficult to specify the precise origination site of the muscle. Accordingly, as it is difficult to separate the conditions of the anterior origin of the rectus communis into clearly defined characters, they are not used for the analysis.

Position of ventral insertion of pharyngoclavicularis externus. The ventral insertion of the pharyngoclavicularis externus is situated medial to the sternohyoideus in *Barbourisia rufa* and *Cetostoma regani* (Fig. 36A), while it is situated lateral to sternohyoideus in many other ingroups (Fig. 36D). On the other hand, it is situated slightly medial to the sternohyoideus in *Acanthochaenus luetkenii* (Fig. 36B), and sandwiched by the latter in *Stephanoberyx monae* (Fig. 36C). These conditions make the variations of the position of the ventral insertion of this muscle serial among ingroups, and then it is difficult to separate them into discrete characters. Accordingly, the position of the ventral insertion of the pharyngoclavicularis externus is not used for the analysis.

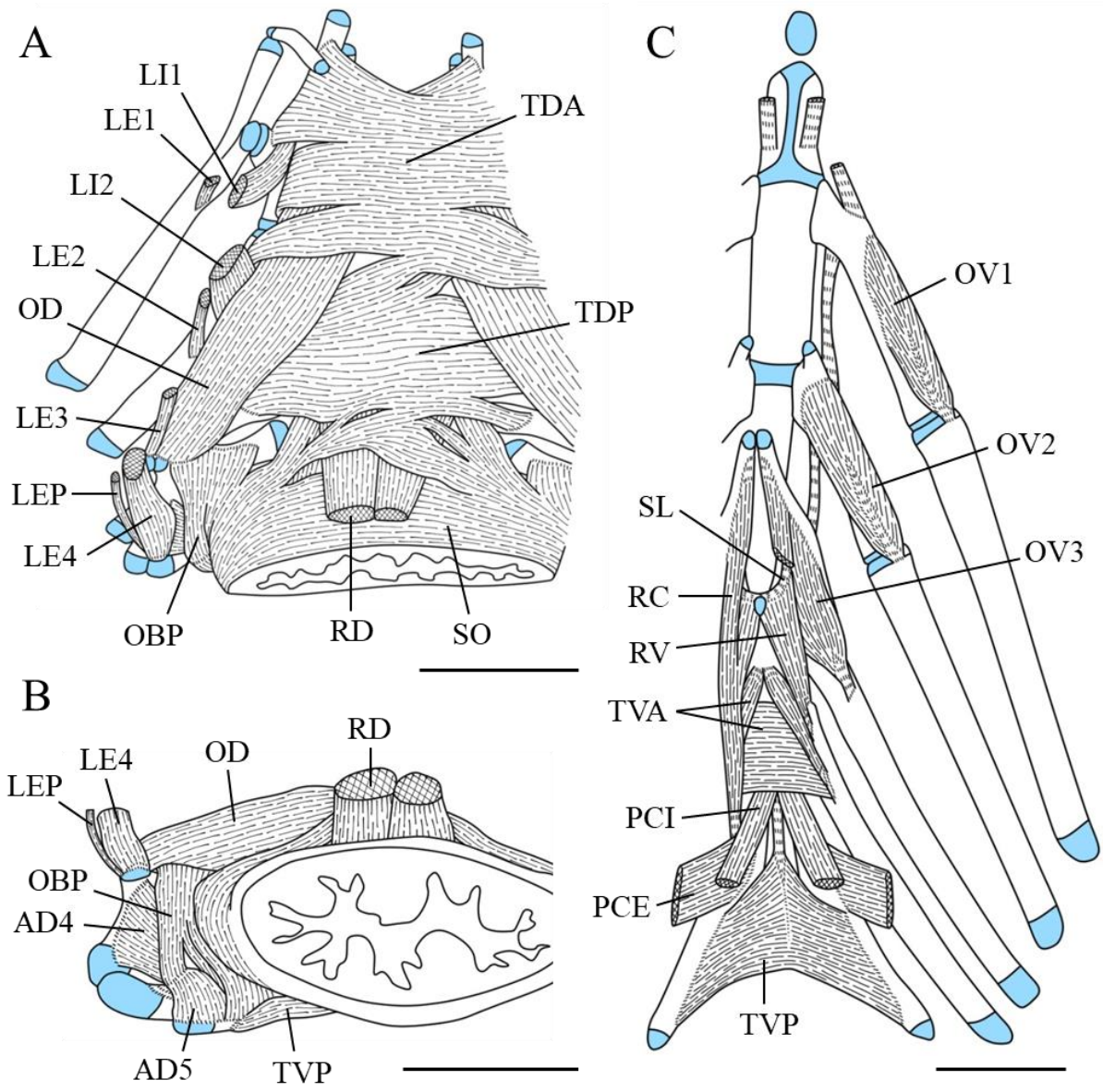

Figure 33. Dorsal (A) and posterior (B) aspects of upper branchial muscles and ventral aspect (C) of lower branchial muscles in *Hispidoberyx ambagiosus*. AD4–5, adductores IV–V; LE1–4, levatores externi I–IV; LI1–2, levatores interni I–II; LEP, levator posterior; OBP, obliquus posterior; OD, obliquus dorsalis; OV1–3, obliqui ventrales I–III; PCE, pharyngoclavicularis externus; PCI, pharyngoclavicularis internus; RC, rectus communis; RD, retractor dorsalis; RV, rectus ventralis; SL, semicircular ligament; SO, sphincter oesophagi; TDA, transversus dorsalis anterior; TDP, transversus dorsalis posterior; TVA, transversus ventralis anterior; TVP, transversus ventralis posterior. Scales indicate 5 mm.

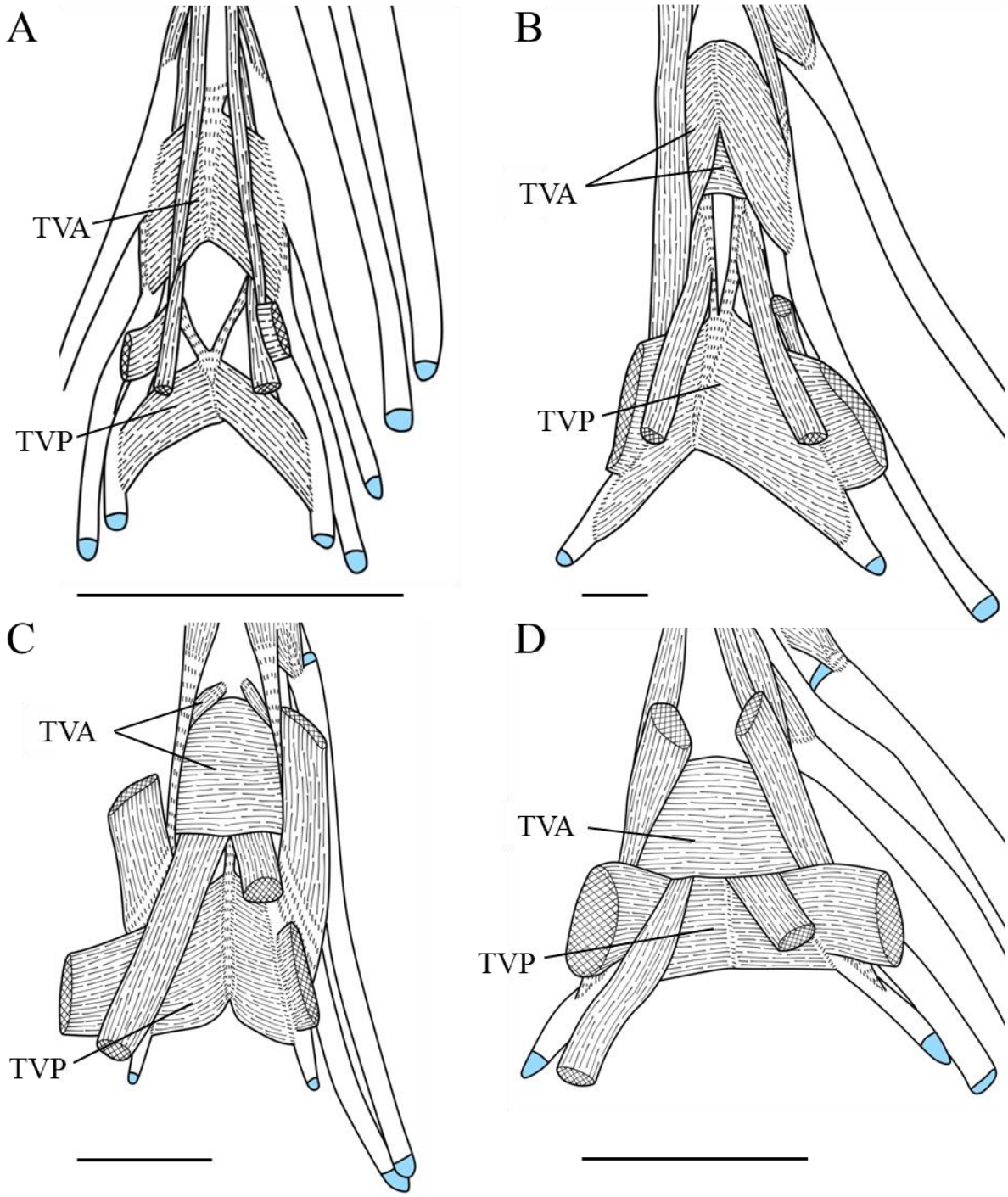

Figure 34. Ventral aspects of posterior portion of lower branchial arches in (A) *Cetostoma regani*, (B) *Barbourisia rufa*, (C) *Hoplostethus mediterraneus* and (D) *Neoniphon sammara*. TVA, transversus ventralis anterior; TVP, transversus ventralis posterior. Scales indicate 5 mm.

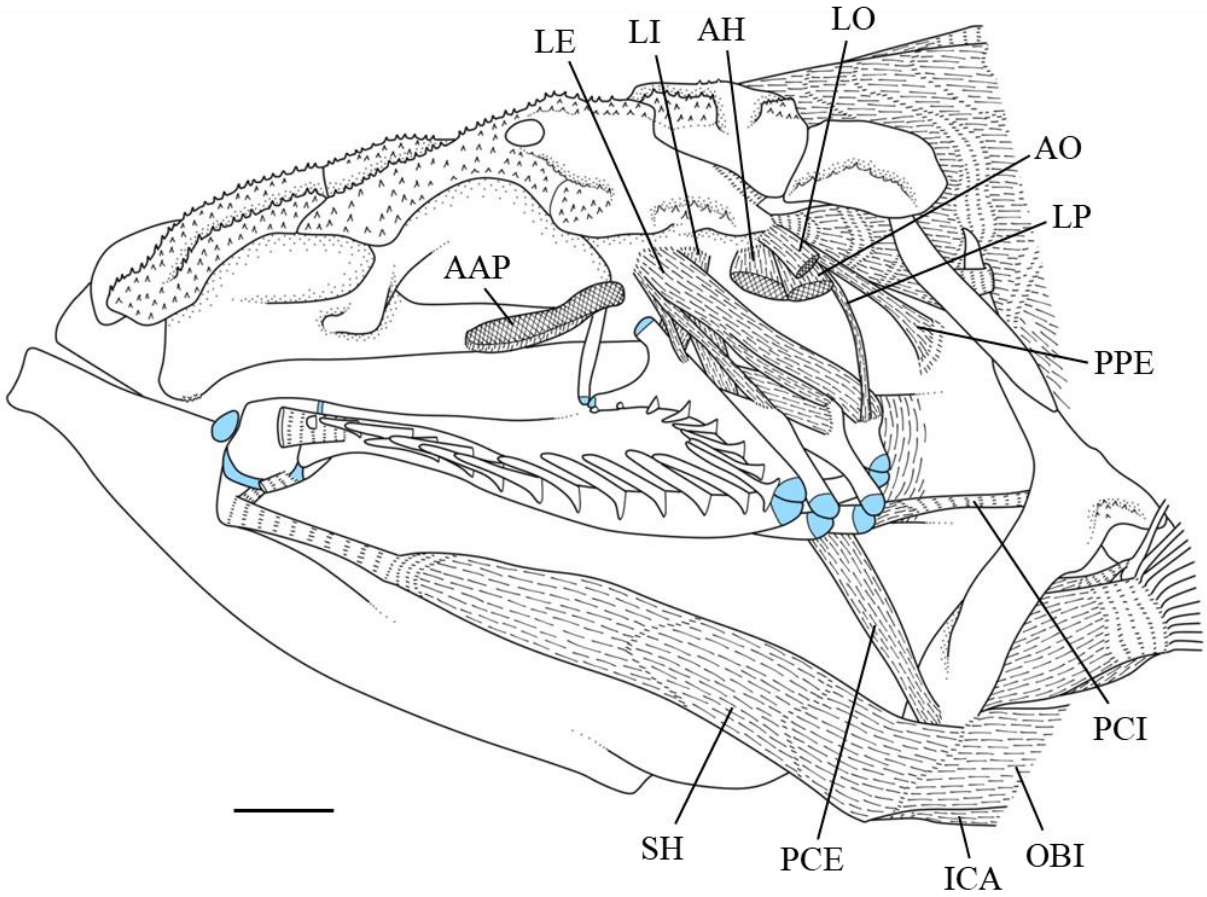

Figure 35. Lateral aspect of head region in *Hispidoberyx ambagiosus* after removal of infraorbitals, jaws, suspensorium, opercular bones and hyoid arch. AAP, adductor arcus palatini; AH, adductor hyomandibular; AO, adductor operculi; ICA, infracarinalis anterior; LE, levator externus; LI, levator internus; LO, levator operculi; LP, levator posterior; OBI, obliquus inferioris; PCE, pharyngoclavicularis externus; PCI, pharyngoclavicularis internus; PPE, protractor pectoralis; SH, sternohyoideus. Scale indicates 5 mm.

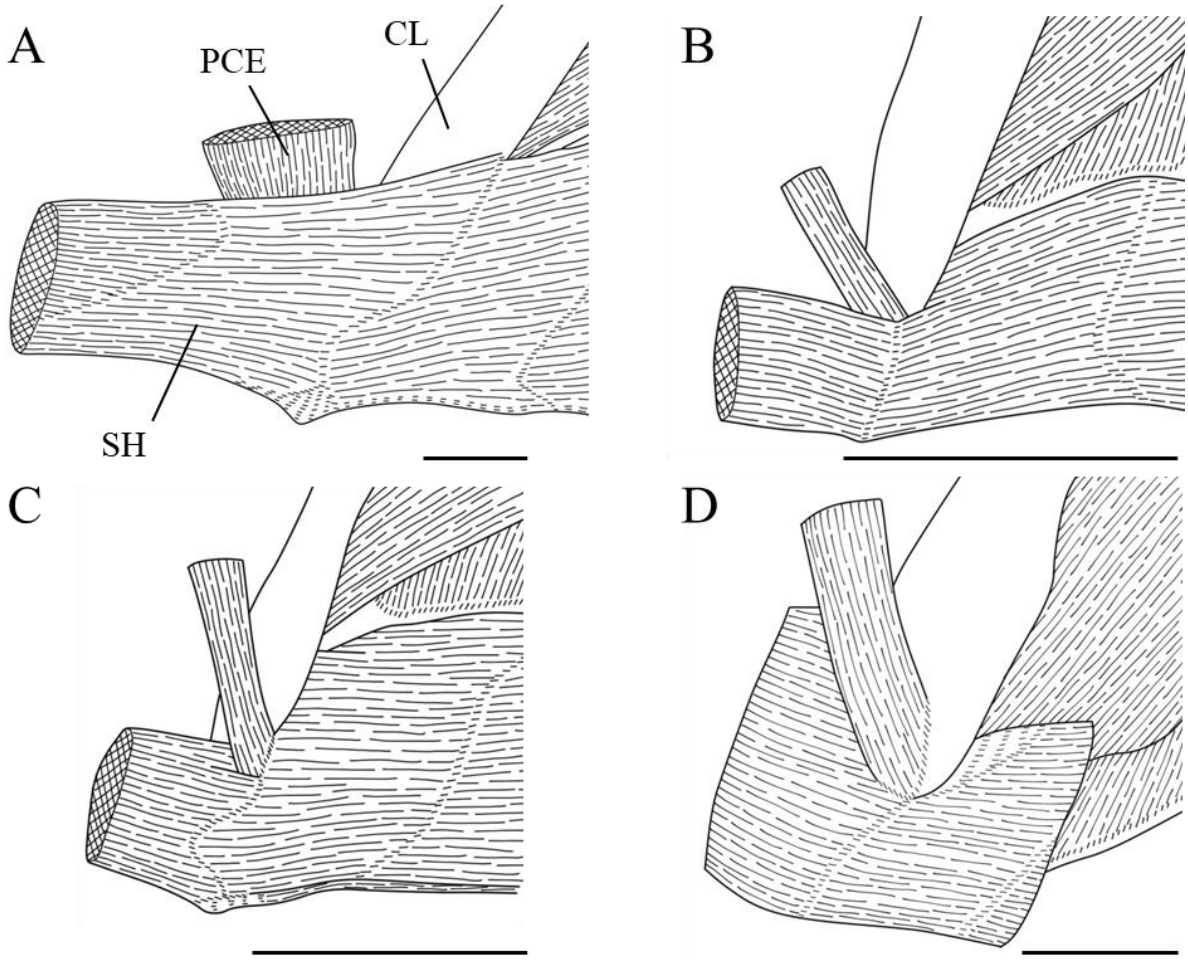

Figure 36. Lateral aspects of ventral portion of pectoral girdle in (A) *Barbourisia rufa*, (B) *Acanthochaenus luetkenii*, (C) *Stephanoberyx monae* and (D) *Trachichthys australis*. CL, cleithrum; PCE, pharyngoclavicularis externus; SH, sternohyoideus. B is shown as mirror image. Scales indicate 5 mm.

4-2-5. Pectoral-fin muscles (Figs. 37, 38)

Description

The pectoral-fin muscles are composed of the abductor superficialis, abductor profundus, arrector ventralis, adductor superficialis, adductor profundus, arrector dorsalis and adductor radialis. The protractor pectoralis and sternohyoideus are also described in this section.

The abductor superficialis is a superficial muscle of the lateral aspect of the pectoral girdle. This muscle originates from the posterior surface of the anterolateral flange of the cleithrum and inserts onto the bases of all pectoral-fin rays except for the uppermost.

The abductor profundus is a medial muscle of the lateral aspect of the pectoral girdle. This muscle originates from the coracoid and inserts onto the bases of all pectoral-fin rays.

The arrector ventralis, situated above the abductor profundus, originates from the cleithrum and coracoid, and inserts onto the base of the uppermost ray.

The adductor superficialis is located on the dorsal portion of the medial pectoral-fin muscles. This muscle originates from the cleithrum and inserts onto the anteromedial portions of all fin rays except for the uppermost.

The adductor profundus is located on the ventral portion of the medial pectoral-fin muscles. This muscle originates from the cleithrum and coracoid, and inserts onto the bases of all fin rays except for the uppermost.

The arrector dorsalis, situated on the central portion of the medial pectoral-fin muscles, originates from the cleithrum and coracoid, and inserts onto the base of the uppermost ray.

The adductor radialis is a small element, located on the medial surface of the actinosts. This muscle originates from the third and fourth actinosts, and inserts onto the base of the ventralmost ray.

The protractor pectoralis is a thin muscle, situated anterior to the pectoral girdle. This muscle originates from the pterotic and merges into a connective tissue anterior to the supracleithrum.

The sternohyoideus, a long and robust element, connects the pectoral girdle with the hyoid arch. This muscle anteriorly originates from the urohyal and posteriorly inserts onto the anteroventral portion of the cleithrum. Some fibers of the muscle are confluent with the obliquus inferioris.

Character recognition

TS 68. Adductor radialis (0: absent; 1: moderately developed; 2: well developed) (ordered as 0-1-2)

Ingroups. The adductor radialis is absent in stephanoberycids, *Rondeletia loricata*, *Barbourisia rufa*, *Cetostoma regani* and *Hoplobrotula armata* (character 68-0), while it is well developed in melamphaids (Fig. 38) (character 68-2) and moderately developed in other ingroups (character 68-1).

Outgroups. This muscle is moderately developed in *Neoscopelus microchir* and *Hime japonica*, whereas it is absent in *Trachinocephalus trachinus*.

Remarks. The well developed adductor radialis in melamphaids originates from the anteroventral portion of the coracoid and inserts onto several lower pectoral-fin rays. This muscle is anteriorly fused with the adductor profundus partially, but separated from it posteriorly and centrally. This melamphaid condition is quite different from that in other ingroups, in which this muscle is a small element originating mainly from the actinosts, and inserts onto several lower pectoral-fin rays. In this study, the muscular element observed in melamphaids was considered to be homologous with the adductor radialis in other ingroups because both of them are located ventrolateral to the adductor profundus and insert onto several lower pectoral-fin rays.

Other variations

None.

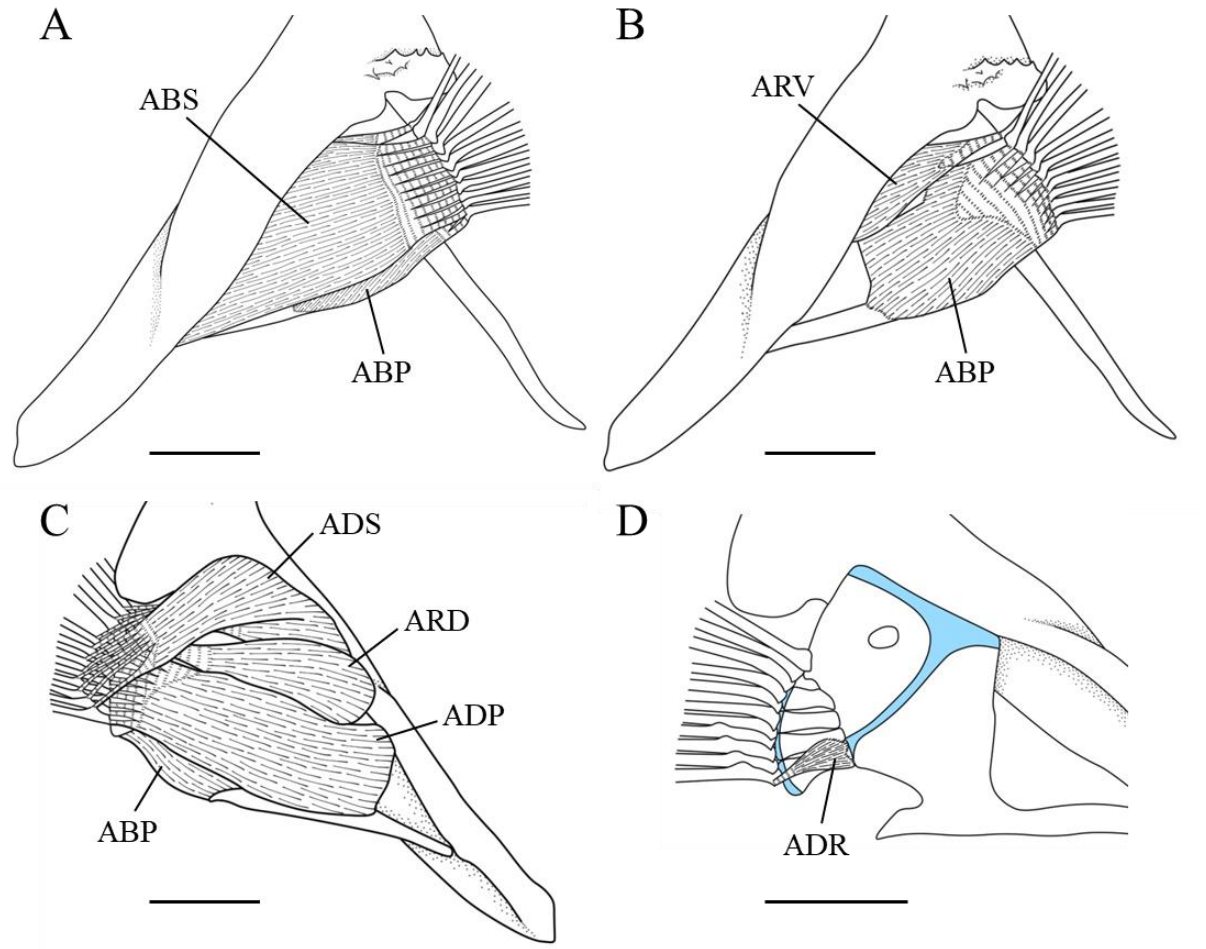

Figure 37. Lateral (A and B) and medial (C) aspects of pectoral-fin muscles in *Hispidoberyx ambagiosus*. ABP, abductor profundus; ABS, abductor superficialis; ADP, adductor profundus; ADR, adductor radialis; ADS, adductor superficialis; ARD, arrector dorsalis; ARV, arrector ventralis. B, after removal of ABS; D, after removal of ADP, ADS and ARD. Scales indicate 5 mm.

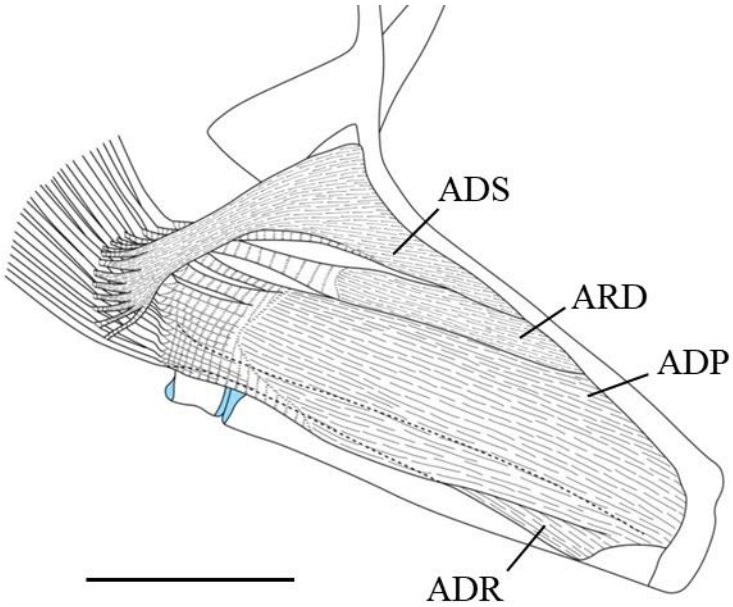

Figure 38. Medial aspect of pectoral-fin muscles in *Scopelogadus mizolepis*. ADP, adductor profundus; ADR, adductor radialis; ADS, adductor superficialis; ARD, arrector dorsalis. Scale indicates 5 mm.

4-2-6. Pelvic-fin muscles (Fig. 39)

Description

The pelvic-fin muscles comprise the abductor superficialis pelvicus, abductor profundus pelvicus, arrector ventralis pelvicus, extensor proprius, adductor superficialis pelvicus, adductor profundus pelvicus and arrector dorsalis pelvicus.

The abductor superficialis pelvicus is a superficial muscle of the ventral aspect of the pelvic girdle. This muscle originates from the ventromedial portion of the pelvic bone and a median septum in the midline, and inserts onto the bases of the spine and all soft rays except for the innermost ray.

The abductor profundus pelvicus is a medial muscle of the ventral aspect of the pelvic girdle. This muscle originates from the ventromedial portion of the pelvic bone and inserts onto the bases of all soft rays.

The arrector ventralis pelvicus is located on the ventrolateral portion of the pelvic-fin muscles. This muscle originates from the anteroventral portion of the pelvic bone and inserts onto the base of the spine.

The extensor proprius is a small element situated on the posterodorsal portion of the pelvic-fin muscles. This muscle originates from the posterolateral portion of the pelvic bone and inserts onto the bases of two or three innermost rays.

The adductor superficialis pelvicus is a superficial muscle of the dorsal aspect of the pelvic girdle. This muscle originates from the dorsomedial portion of the pelvic bone and inserts onto the bases of the spine and all soft rays.

The adductor profundus pelvicus is a medial muscle of the dorsal aspect of the pelvic girdle. This muscle originates from the dorsomedial portion of the pelvic bone and inserts onto the bases of all soft rays.

The arrector dorsalis pelvicus is located on the dorsolateral portion of the pelvic-fin muscles. This muscle originates from the central portion of the dorsal aspect of the pelvic

bone and inserts onto the base of the spine.

Character recognition

TS 69. Abductor superficialis pelvicus (0: present; 1: absent)

Ingroups. The abductor superficialis pelvicus is absent in stephanoberycids (character 69-1), whereas it is present in other ingroups (character 69-0). Due to absence of the pelvic girdle, "?" is coded for *Cetostoma regani*.

Outgroups. All outgroups have the abductor superficialis pelvicus.

TS 70. Extensor proprius (0: present; 1: absent)

Ingroups. The extensor proprius is absent in stephanoberycids, *Gibberichthys pumilus*, *Rondeletia loricata*, *Barbourisia rufa* and *Hoplobrotula armata* (character 70-1), while it is present in other ingroups (character 70-0). Because of absence of the pelvic girdle, "?" is coded for *Cetostoma regani*.

Outgroups. All outgroups have the extensor proprius.

Other variations

None.

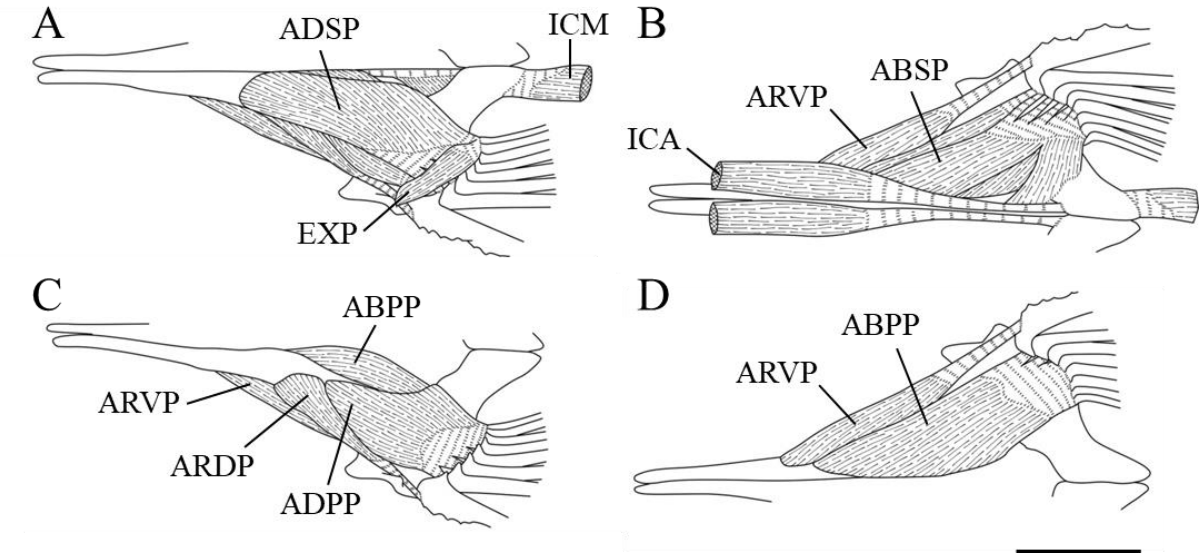

Figure 39. Dorsal (A and C) and ventral (B and D) aspects of pelvic-fin muscles in *Hispidoberyx ambagiosus*. ABPP, abductor profundus pelvicus; ABSP, abductor superficialis pelvicus; ADPP, adductor profundus pelvicus; ADSP, adductor superficialis pelvicus; ARDP, arrector dorsalis pelvicus; ARVP, arrector ventralis pelvicus; EXP, extensor proprius; ICA, infracarinalis anterior; ICM, infracarinalis medius. C, after removal of ADSP and EXP; D, after removal of ABSP and ICA. Scale indicates 5 mm.

4-2-7. Caudal-fin muscles (Fig. 40)

Description

The caudal-fin muscles include the interradialis, hypochordal longitudinalis, flexor dorsalis, flexor dorsalis superior, flexor ventralis externus, flexor ventralis and flexor ventralis inferior. The flexor dorsalis and flexor dorsalis superior are fused with each other. The adductor dorsalis is absent.

The interradialis, comprising dorsal and ventral elements, interconnects the anterior portions of caudal-fin rays. A small additional bundle separated from the dorsal element is present, connecting the first dorsal procurrent ray and several subsequent principal rays.

The hypochordal longitudinalis originates from the parhypural and first to third hypurals, and tendinously inserts onto the posteriormost upper procurrent ray and several upper principal rays.

A muscular element formed by fusion of the flexor dorsalis and flexor dorsalis superior originates from the neural spines of the first to sixth preural centra, first uroneural and first to third epurals, and inserts onto the bases of several principal rays on the upper lobe.

The flexor ventralis externus originates from the hemal spines of the third to fifth preural centra, and tendinously inserts onto the bases of several upper principal rays on the lower lobe.

The flexor ventralis originates from the hemal spine of the second preural centrum, parhypural and first hypural, and inserts onto the bases of all principal rays on the lower lobe.

The flexor ventralis inferior originates from the hemal spines of the second and third preural centra, and inserts onto the bases of two posteriormost procurrent rays on the lower lobe.

Character recognition

TS 71. Insertion of flexor ventralis onto ventralmost principal ray on upper lobe (0: absent; 1:

present)

Ingroups. The flexor ventralis inserts onto principal rays on the lower lobe and the ventralmost principal ray on the upper lobe in melamphaids and *Beryx decadactylus* (character 71-1), whereas it inserts only onto principal rays on the lower lobe in other ingroups (character 71-0).

Outgroups. This muscle inserts only onto principal rays on the lower lobe in all outgroups.

Other variations

Fusion of flexor dorsalis and flexor dorsalis superior. The autogenous flexor dorsalis superior is absent in many ingroups including *Hispidoberyx ambagiosus*, while this muscle is present and clearly separable from the flexor dorsalis in melamphaids. In the former condition, the dorsal portion of the flexor dorsalis occupies the almost same region with the flexor dorsalis superior in melamphaids. In addition, Winterbottom (1974) noted that the separation of the flexor dorsalis superior from the flexor dorsalis may not be complete in some cases. Therefore, in taxa without the autogenous flexor dorsalis superior, this muscle was considered to be fused with the flexor dorsalis. On the other hand, the flexor dorsalis superior is incompletely fused with the flexor dorsalis and the degree of the fusion is various in some taxa (e.g., berycids and holocentrids). Such a variation in these muscles makes their fusion and separation serial among ingroups, and it cannot be separated into clearly defined characters. Consequently, the conditions of the flexor dorsalis and flexor dorsalis superior are not used for the analysis.

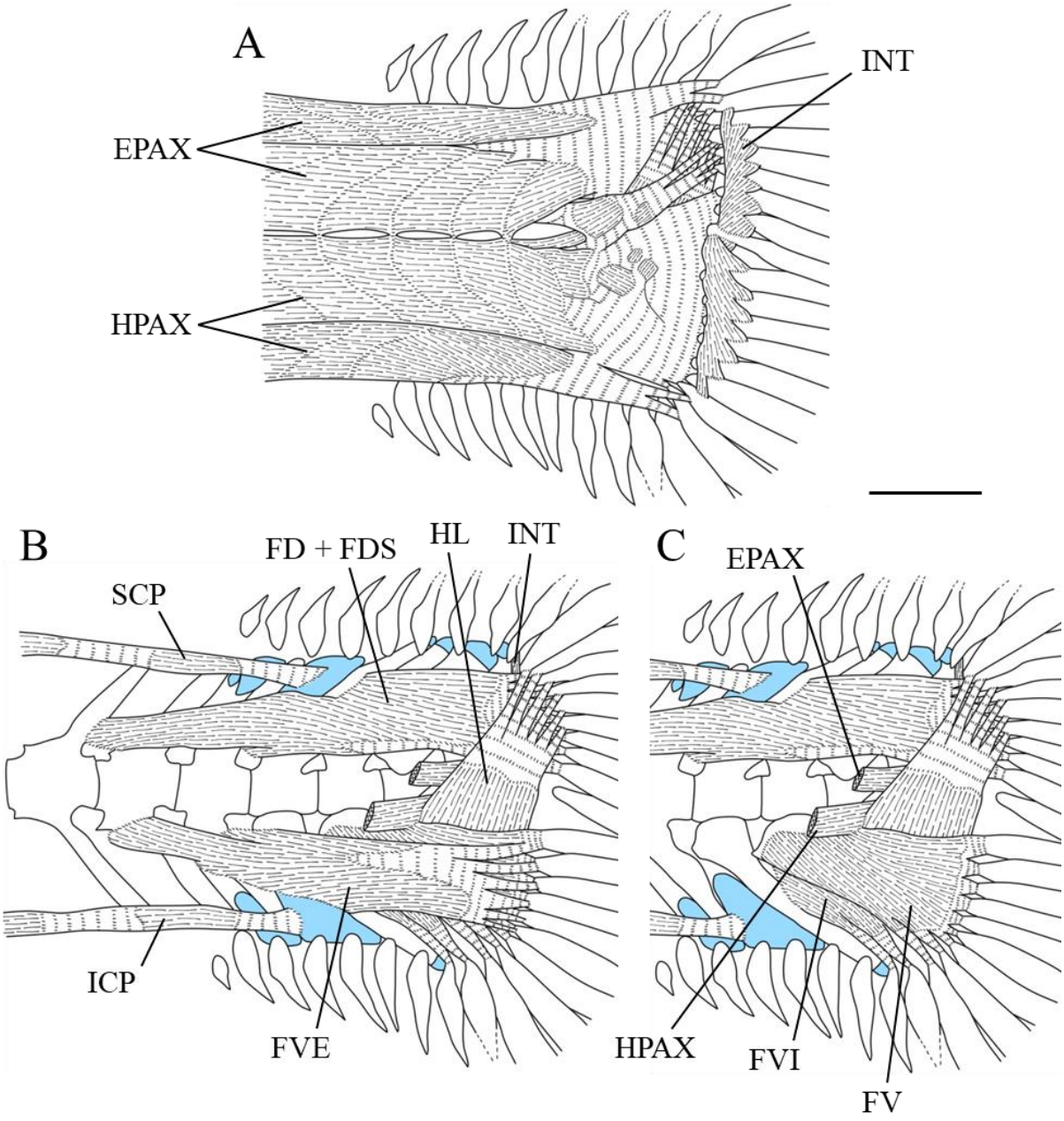

Figure 40. Lateral aspects of caudal-fin muscles in *Hispidoberyx ambagiosus*. EPAX, epaxialis; FD, flexor dorsalis; FDS, flexor dorsalis superior; FV, flexor ventralis; FVE, flexor ventralis externus; FVI, flexor ventralis inferior; HL, hypochordal longitudinalis; HPAX, hypaxialis; ICP, infracarinalis posterior; INT, interradialis; SCP, supracarinalis posterior. B, after removal of EPAX and HPAX; C, after removal of FVE. Scale indicates 5 mm.

4-2-8. Muscles of median fin and their supportive elements (Figs. 41, 42)

Description

The muscles of the dorsal fin consist of the inclinatores dorsales, erectores dorsales and depressores dorsales.

The inclinatores dorsales originate from the fascia between the skin and epaxialis, and insert onto the lateral surface of the bases of the dorsal-fin rays. The erectores dorsales originate from the anterolateral surfaces of the proximal pterygiophores and insert onto the anterolateral bases of the dorsal-fin rays. The depressores dorsales originate from the posterolateral surfaces of the proximal pterygiophores and insert onto the posterolateral bases of the dorsal-fin rays.

The muscles of the anal fin comprise the inclinatores anales, erectores anales and depressores anales.

The inclinatores anales originate from the fascia between the skin and hypaxialis, and insert onto the lateral surface of the bases of the anal-fin rays. The erectores anales originate from the anterolateral surfaces of the proximal pterygiophores and insert onto the anterolateral bases of the anal-fin rays. The depressores anales originate from the posterolateral surfaces of the proximal pterygiophores and insert onto the posterolateral bases of the anal-fin rays.

The carinal muscles are slender band-like elements and composed of the supracarinalis anterior, supracarinalis posterior, infracarinalis anterior, infracarinalis medius and infracarinalis posterior.

The supracarinalis anterior is located on the dorsal midline between the neurocranium and dorsal fin, connecting the supraoccipital and the first proximal pterygiophore of the dorsal fin. The supracarinalis posterior is situated on the dorsal midline between the dorsal and caudal fins, connecting the stay of the dorsal fin and the inter-neural spine cartilage of the fourth preural centrum. The infracarinalis anterior lies on the ventral midline between pectoral and pelvic fins, and interconnects the ventral tip of the cleithrum and the posteroventral portion of

the pelvic bone. The infracarinalis medius is located on the ventral midline between the pelvic and anal fins, connecting the posterior process of the pelvic bone and the first proximal pterygiophore of the anal fin. The infracarinalis posterior lies on the ventral midline between the anal and caudal fins, and interconnects the stay of the anal fin and the inter-hemal spine cartilage of the fourth preural centrum.

An unnamed muscle is present lateral to the supracarinalis anterior. This muscle is a pair of thin band-like elements, and posteromedially originates from the supracarinalis anterior and anterolaterally inserts onto the tip of the dorsal limb of the posttemporal tendinously.

Character recognition

TS 72. Unnamed muscle on lateral portion of supracarinalis anterior (0: absent; 1: thin and band-like; 2: wide and sheet-like) (unordered)

Ingroups. A thin band-like unnamed muscle is present in *Hispidoberyx ambagiosus*, *Gibberichthys pumilus*, *Rondeletia loricata*, *Barbourisia rufa* and *Cetostoma regani* (Fig. 42A) (character 72-1), while a wide sheet-like element is present in holocentrids (Fig. 42B) (character 72-2). Other ingroups lack such a muscle element (character 72-0).

Outgroups. All outgroups lack this unnamed muscle.

Remarks. Teleosts, except for most ostariophysan and ctenosquamates, usually have the craniotemporalis muscle which is a well differentiated anterior slip subdivided from the epaxialis, passing anterolaterally from the dorsal midline and inserting onto the posterodorsal margin of the dorsal limb of the posttemporal (Stiassny, 1986, 1996; de Pinna, 1996). The unnamed muscle found in this study is superficially similar to the craniotemporalis. However, because the former is completely separated from the epaxialis and lie on the surface of it, and it posteromedially originates from the supracarinalis anterior, it is assumed to be derived from the supracarinalis anterior rather than the epaxialis, and not homologous with the craniotemporalis in basal teleosts.

In addition, the unnamed muscle in holocentrids is different from that in *H. ambagiosus*, *G. pumilus*, *R. loricata*, *B. rufa* and *C. regani* because the former is a wide sheet-like element and its posteromedial origin also includes the anterior proximal and distal pterygiophores of the dorsal fin (vs. a thin band-like element and originated only form the supracarinalis anterior in the latter). Therefore, as the homology between the unnamed muscles observed in holocentrids and the others is uncertain, this transformation series is assumed as "unordered", including non-homologous character evolution of the two the type muscles.

Other variation

None.

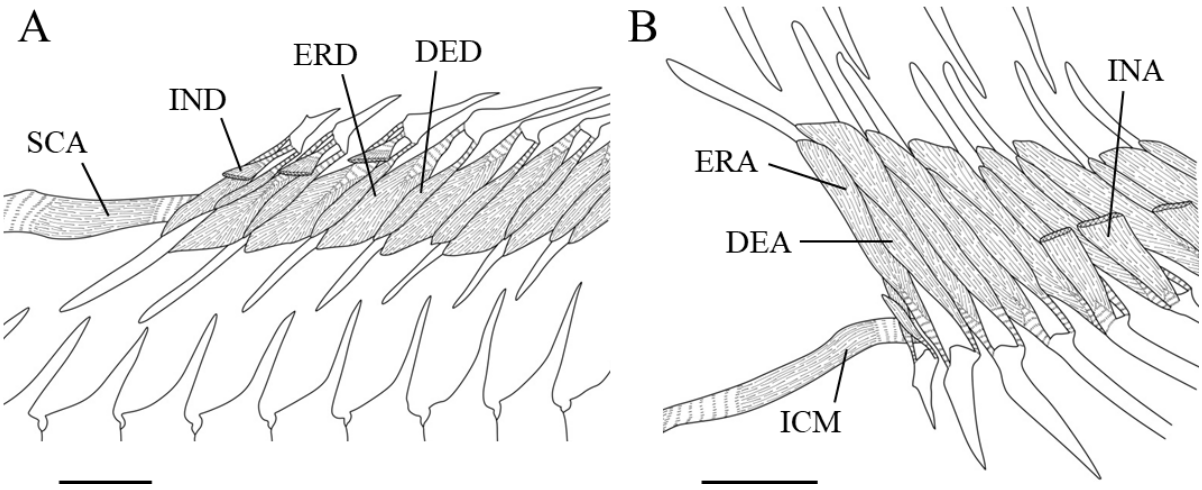

Figure 41. Lateral aspects of (A) dorsal and (B) anal-fin muscles in *Hispidoberyx ambagiosus*. DEA, depressores anales; DED, depressores dorsales; ERA, erectores anales; ERD, erectores dorsales; ICM, infracarinalis medius; INA, inclinatores anales; IND, inclinatores dorsales; SCA, supracarinalis anterior. Scales indicate 5 mm.

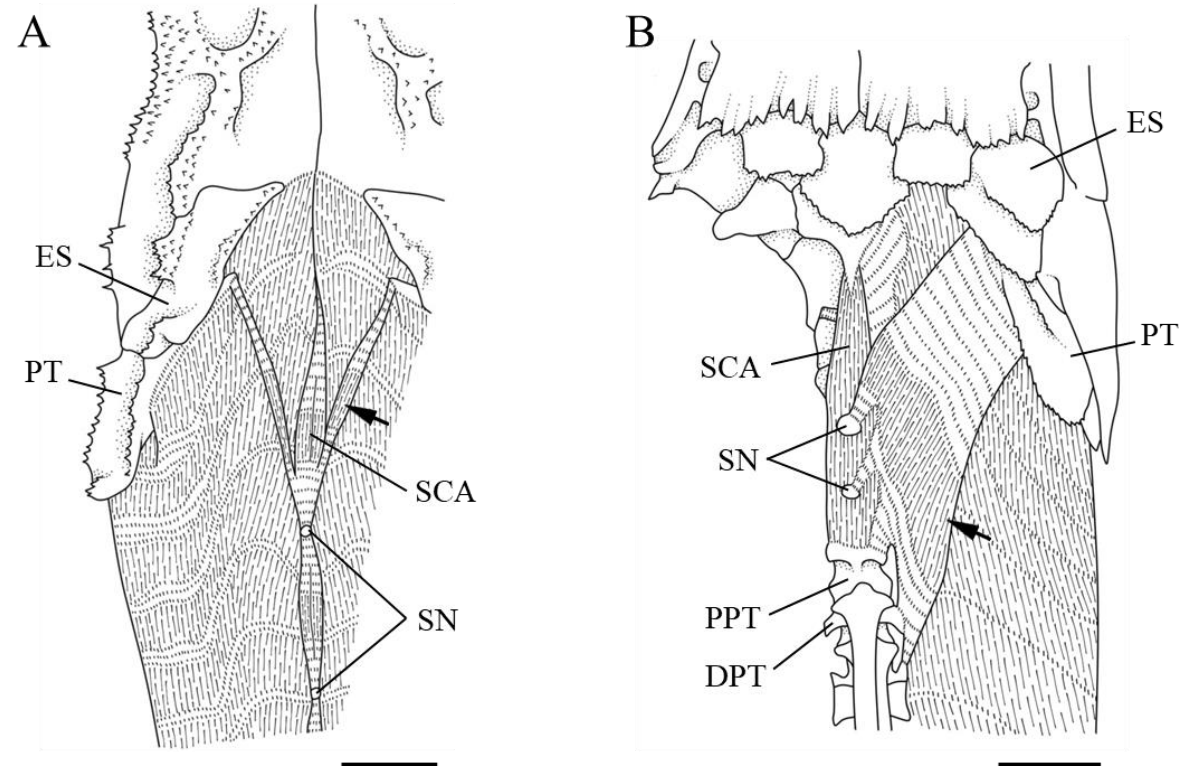

Figure 42. Dorsal aspects of anterior portions of body and carinal muscles in (A) *Hispidoberyx ambagiosus* and (B) *Neoniphon sammara*. DPT, distal pterygiophore; ES, extrascapular; PPT, proximal pterygiophore; PT, posttemporal; SCA, supracarinalis anterior; SN, supraneurals. Arrows indicate unnamed muscles. Scales indicate 5 mm.

4-2-9. Body muscles (Fig. 43)

Description

The body muscles consist of three major divisions, the epaxialis, hypaxialis and lateralis superficialis.

The epaxialis occupies the dorsal large part of the body muscles above the horizontal septum. Fibers on the dorsal portion course posteroventrally, while fibers on the ventral portion course anteroventrally. The anterior portion of the muscle is attached to the posterodorsal portion of the neurocranium and the dorsal portion of the pectoral girdle.

The hypaxialis lies on the ventral large part of the body muscles below the horizontal septum. This muscle is composed of two subdivisions, the obliquus superioris and obliquus inferioris. The obliquus superioris is situated just below the horizontal septum and courses posteroventrally. The anterior portion of the muscle is attached to the posteroventral portion of the neurocranium. The obliquus inferioris is located ventral to the obliquus superioris and courses anteroventrally. The anterior portion of the muscle is attached to the ventral portion of the pectoral girdle; some fibers being confluent with the sternohyoideus.

The lateralis superficialis, a thin sheet-like element with longitudinally directed fibers, is situated on the middle and superficial portions of the body muscles. This muscle widely covers the ventral portion of the epaxialis and the dorsal portion of the hypaxialis. The anterior portion of the muscle is fused with the epaxialis and hypaxialis.

Character recognition

No variations available for the phylogenetic analysis were recognized.

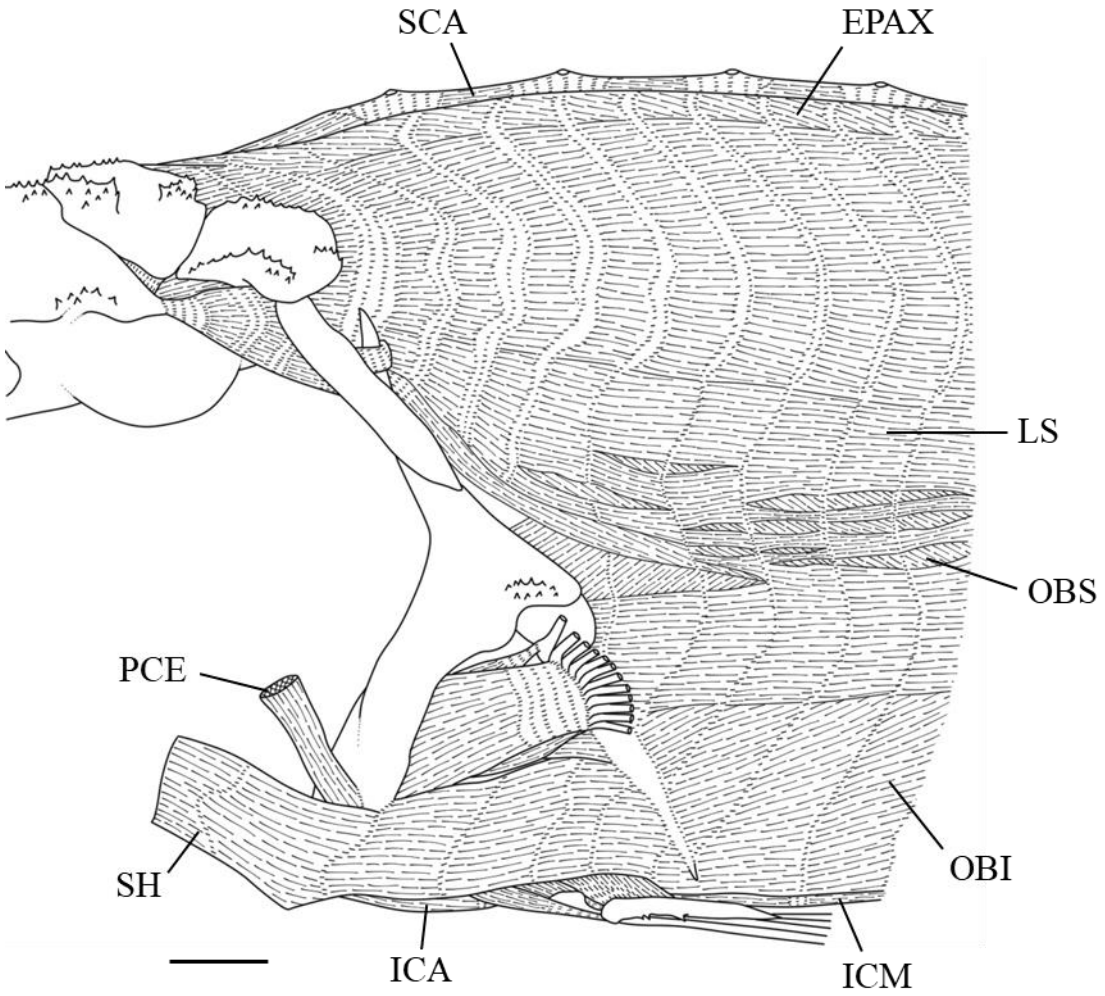

Figure 43. Lateral aspect of anterior body muscles in *Hispidoberyx ambagiosus*. EPAX, epaxialis; ICA, infracarinalis anterior; ICM, infracarinalis medius; LS, lateralis superficialis; OBI, obliquus inferioris; OBS, obliquus superioris; PCE, pharyngoclavicularis externus; SCA, supracarinalis anterior; SH, sternohyoideus. Scale indicates 5 mm.

4-3. Other internal and external morphology (Figs. 44–47)

Description

The sclera, Tominaga's organ, prepectoral organ, Jakubowski's organ, dorsal fin, abdominal scutes and lateral line system on trunk, which are considered to be available for the analysis, are described and discussed in this section.

Sclera. The sclera is a thin cartilaginous ring encircling the eyeball and lacks its ossification.

Tominaga's organ (Fig. 44). The Tominaga's organ (sensu Paxton et al., 2001) is present and situated anterior to the orbit and medial to the nasal cavity in which the nasal rosette lies. This organ is oval and dorso-ventrally depressed, and not divided into any distinct lobes. This organ is hollow and its thick wall has a globular structure. The olfactory nerve runs posteroventral to the organ, and reaches the floor of the nasal cavity and the nasal rosette without distinct innervation of the Tominaga's organ. Several small pores are present on the posterior floor of the nasal cavity posterior to the nasal rosette. Blind pockets posteriorly extend from these pores, but not reach the Tominaga's organ. A thin-walled duct posteriorly runs from the posteromedial portion of the organ, and abruptly curves anterolaterally. Subsequently, the duct turns posteroventrally, and reaches the dorsal margin of the third infraorbital. The posterior end of the duct turns laterally and protrudes externally. The tapered tip of the duct has a quite tiny opening.

Prepectoral organ. The prepectoral organ (see Remarks of TS 75) is absent.

Jakubowski's organ. The Jakubowski's organ (sensu Johnson & Patterson, 1993) is absent.

Dorsal fin. The dorsal fin is composed of one element; the anterior spiny-rays part being not separated from the posterior soft-rays part.

Abdominal scutes. The abdominal scutes are absent on the ventral midline of the belly.

Lateral line system on trunk (Fig. 47). The lateral line system on the trunk comprises papillate neuromasts and a canal supported by pored lateral line scales. The lateral line scales

are arrowhead-shaped and have Y-shaped spinulose ridges. External openings of the trunk canal are located on the anterior tip of the anterior ridge, and the area posterior to the conjunction of the ridges. The posterior portion of the canal extending beyond the posterior margin of the scale is supported by epidermis. The papillate neuromasts are almost regularly placed on each lateral line scale; the numbers of them are 0–2 (usually 2) above the ridges, 0–2 (usually 2) below the ridges and 0–1 (usually 1) posterior to the lateral line scale. The last neuromast is placed slightly dorsal to the midline of the lateral line scales.

Character recognition

TS 73. Ossifications of sclera (0: present; 1: absent)

Ingroups. Two ossifications of sclera are present on the anterior and posterior portions of the eyeball in berycids, holocentrids, *Polymixia japonica*, *Velifer hypselopterus*, *Lateolabrax japonicus*, *Lates mariae* and *Trachurus japonicus* (character 73-0), while they are absent in other ingroups (character 73-1).

Outgroups. *Neoscopelus microchir* lacks ossifications of sclera, whereas *Trachinocephalus trachinus* and *Hime japonica* have them.

TS 74. Tominaga's organ (0: absent; 1: present)

Ingroups. Tominaga's organ is present in *Hispidoberyx ambagiosus*, *Stephanoberyx monae*, *Gibberichthys pumilus* and *Rondeletia loricata* (character 74-1), whereas it is absent in other ingroups (character 74-0).

Outgroups. All outgroups lack this organ.

Remarks. Paxton et al. (2001) found that species of *Rondeletia* and *Gibberichthys* exclusively have a unique globular organ near the nasal rosette, which were termed Tominaga's organ. In these genera, the conditions of the Tominaga's organ observed in this study were almost same as Paxton et al. (2001) described. They found thin-walled ducts running from pores at the posterior end of raphe of the nasal rosette to the anteromedial

portions of two lobes of the Tominaga's organ in *Rondeletia*. Although these pores and ducts were also observed in this study, it could not be confirmed if the ducts entered into the organ due to the feeble conditions.

Although Paxton et al. (2001) reported that *H. ambagiosus* lacks this organ based on only one specimen of the species (MNHN unregistered, 175 mm SL), this study found the organ in four specimens (130.1–191.2 mm SL) including males and females. It is assumed that they failed to find the organ in *H. ambagiosus*, due to the different condition of the organ in the species from those in *Gibberichthys* and *Rondeletia*.

In addition, this study found the Tominaga's organ in *Stephanoberyx monae* which was not examined by Paxton et al. (2001). The organ in this species (Fig. 45) is much smaller than those in *H. ambagiosus*, *G. pumilus* and *R. loricata*. This organ is elliptical and has a few globular structures, located anterior to the orbit and posteromedial to the nasal rosette. The olfactory nerve runs ventral to the organ; some branches of the nerve enter the organ. The posterior floor of the nasal cavity has four pores, from which blind pockets posteromedially extend and enter the organ.

The organs found in *H. ambagiosus* and *S. monae* exhibit different features from the Tominaga's organs in *Gibberichthys* and *Rondeletia*. However, because these organs share distinct similarities, its location near the olfactory organ and the presence of the globular structures, they are considered to be homologous with the Tominaga's organ in this study.

TS 75. Prepectoral organ (0: absent; 1: present)

Ingroups. The prepectoral organ is present in stephanoberycids (character 75-1), while it is absent in other ingroups (character 75-0).

Outgroups. All outgroups lack this organ.

Remarks. In two genera of Stephanoberycidae examined in this study, a peculiar organ was found on the region anterior to the supracleithrum and posterior to the upper branchial arches (Fig. 46). As this organ has not been reported by previous studies, it is herein tentatively

called as “prepectoral organ” and its morphology is described in detail as below.

The prepectoral organ comprises an anterodorsal main part and posteroventral duct, which are entirely covered with the epidermis and hidden by the opercle externally. The posteroventral end of the duct has a slit-like external opening which is situated anterior to the ventral tip of the supracleithrum. The wall of the duct is quite thin and has many longitudinally running fibers which appear to be muscular. The duct anterodorsally runs along the supracleithrum and abruptly curves ventrally just posterior to the connection with the main part. The main part is a bean-shaped element and its concave portion is directed posterodorsally and laterally. The dorsomedial portion of the ventral swelling is connected with the duct. The main part is hollow and has a much thicker wall than the duct. The wall of it has a globular structure. The surface of the concave portion has parallelly lined fibers which appear to be muscular. Some flocculent materials are present in the duct and main part.

The globular structure of the main part and flocculent materials found in the duct and main part suggest a secretory function of the prepectoral organ. In addition, putative muscular fibers on this organ suggest a possibility that it has an ability to discharge secreted materials actively from the external opening on the posteroventral end of the duct. However, to confirm this assumption, histological examination is needed.

TS 76. Jakubowski’s organ (0: absent; 1: present)

Ingroups. The Jakubowski’s organ is present in trachichthyids, *Anomalops katoptron*, *Monocentris japonica*, *Diretmus argenteus*, *Anoplogaster cornuta*, berycids and holocentrids (character 76-1), while it is absent in other ingroups (character 76-0).

Outgroups. This organ is absent in all outgroups.

Remarks. The Jakubowski’s organ is the buccal-innervated terminal supraorbital neuromast(s) with the associated modification of the nasal bone and contact between the tips of the supraorbital and infraorbital canals (Johnson & Patterson, 1993). Although the buccal-innervated terminal supraorbital neuromast was not able to be confirmed in *Diretmus*

argenteus due to the poor condition of the specimen examined in this study, "1" is coded for the species following Johnson & Patterson (1993) who recognized the organ in it.

TS 77. Separate anterior dorsal fin (0: absent; 1: present)

Ingroups. A separate anterior dorsal fin is present in *Anomalops katoptron*, *Monocentris japonica*, holocentrids, *Lateolabrax japonicus*, *Lates mariae* and *Trachurus japonicus* (character 77-1), whereas it is absent in other ingroups (character 77-0).

Outgroups. All outgroups lack a separate anterior dorsal fin.

TS 78. Abdominal scutes (0: absent; 1: present)

Ingroups. Abdominal scutes are present in trachichthyids, *Anomalops katoptron*, *Monocentris japonicus* and *Diretmus argenteus* (character 78-1), while they are absent in other ingroups (character 78-0).

Outgroups. Abdominal scutes are absent in all outgroups.

TS 79. Papillate lateral line system on trunk (0: absent; 1: present)

Ingroups. The lateral line system formed by papillate neuromasts on the trunk is present in *Hispidoberyx ambagiosus*, stephanoberycids, *Gibberichthys pumilus*, *Rondeletia loricata*, *Barbourisia rufa* and *Cetostoma regani* (character 79-1), whereas it is absent in other ingroups (character 79-0).

Outgroups. All outgroups lack the papillate lateral line system on trunk.

Remarks. In this study, the papillate lateral line system on the trunk was not able to be confirmed in *G. pumilus* and *C. regani* because of the poor conditions of the specimens examined. However, "1" is coded for them following to previous studies reporting the presence of papillae on the trunk (Ebeling & Weed, 1973; Rosen, 1973; Paxton, 1989; Paxton et al., 2001).

TS 80. Trunk canal (0: canal supported by scales; 1: dermal canal; 2: groove supported by scales; 3: absent) (unordered)

Ingroups. The trunk canal is present as a dermal canal in *Barbourisia rufa*, *Cetostoma*

regani and *Hoplobrotula armata* (character 80-1), and a groove supported by scales in *Anoplogaster cornuta* (character 80-2). The trunk canal is absent in stephanoberycids, *Gibberichthys pumilus*, *Rondeletia loricata*, melamphaids and *Diretmus argenteus* (character 80-3), while it is present as a canal supported by scales in other ingroups (character 80-0).

Outgroups. The trunk canal is present as a canal supported by scales in all outgroups.

Other variations

None.

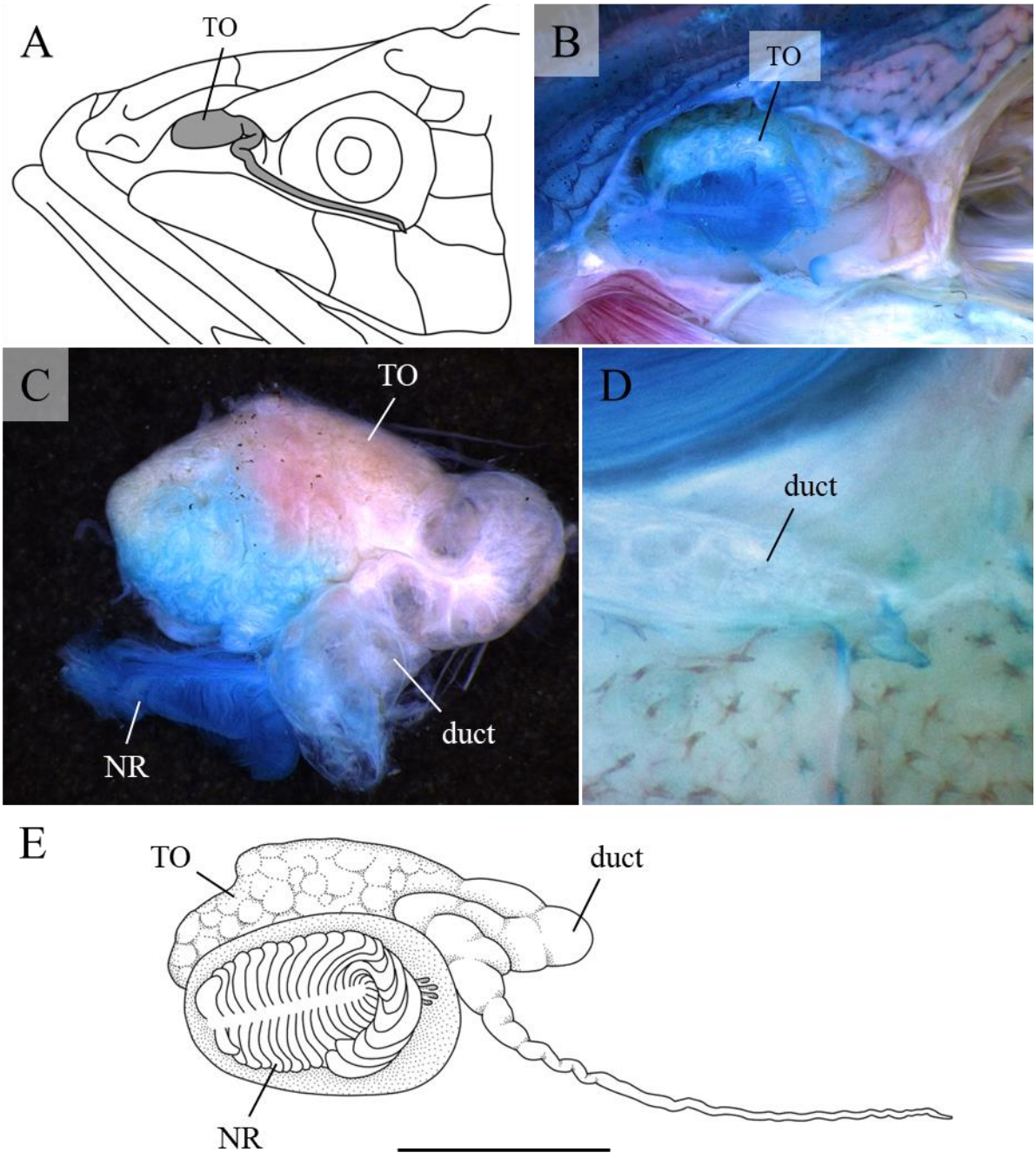

Figure 44. Tominaga's organ in *Hispidoberyx ambagiosus*. A, diagrammatic illustration indicating position of Tominaga's organ. B, lateral aspect of preorbital region after removal of epidermis. C, dorsal aspect of Tominaga's organ. D, posterior tip of duct after removal of epidermis. E, line drawing of lateral aspect of Tominaga's organ. NR, nasal rosette; TO, Tominaga's organ. B and C, posterior portion of duct is damaged. D is shown as mirror image. Scale indicates 5 mm.

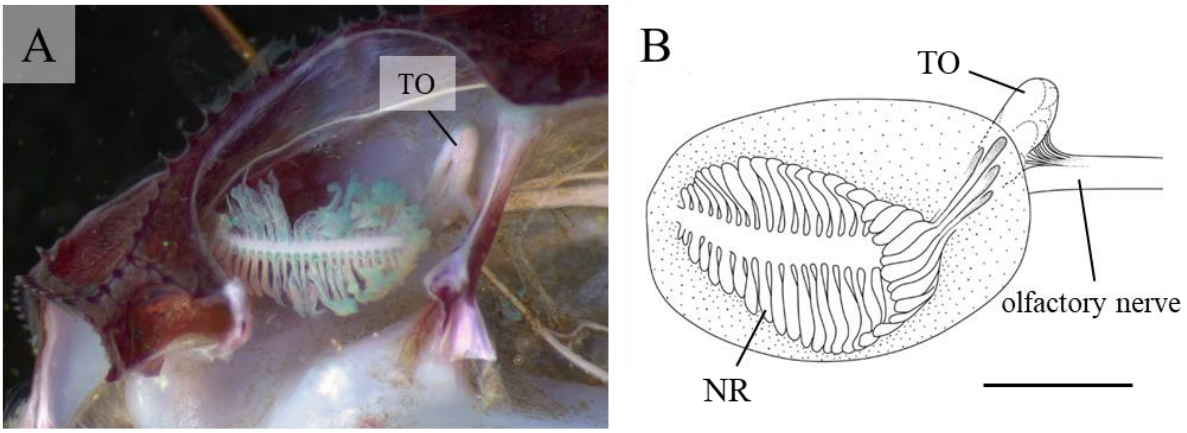

Figure 45. Tominaga's organ in *Stephanoberyx monae*. A, lateral aspect of preorbital region after removal of epidermis. B, line drawing of lateral aspect of Tominaga's organ. NR, nasal rosette; TO, Tominaga's organ. Scale indicates 5 mm.

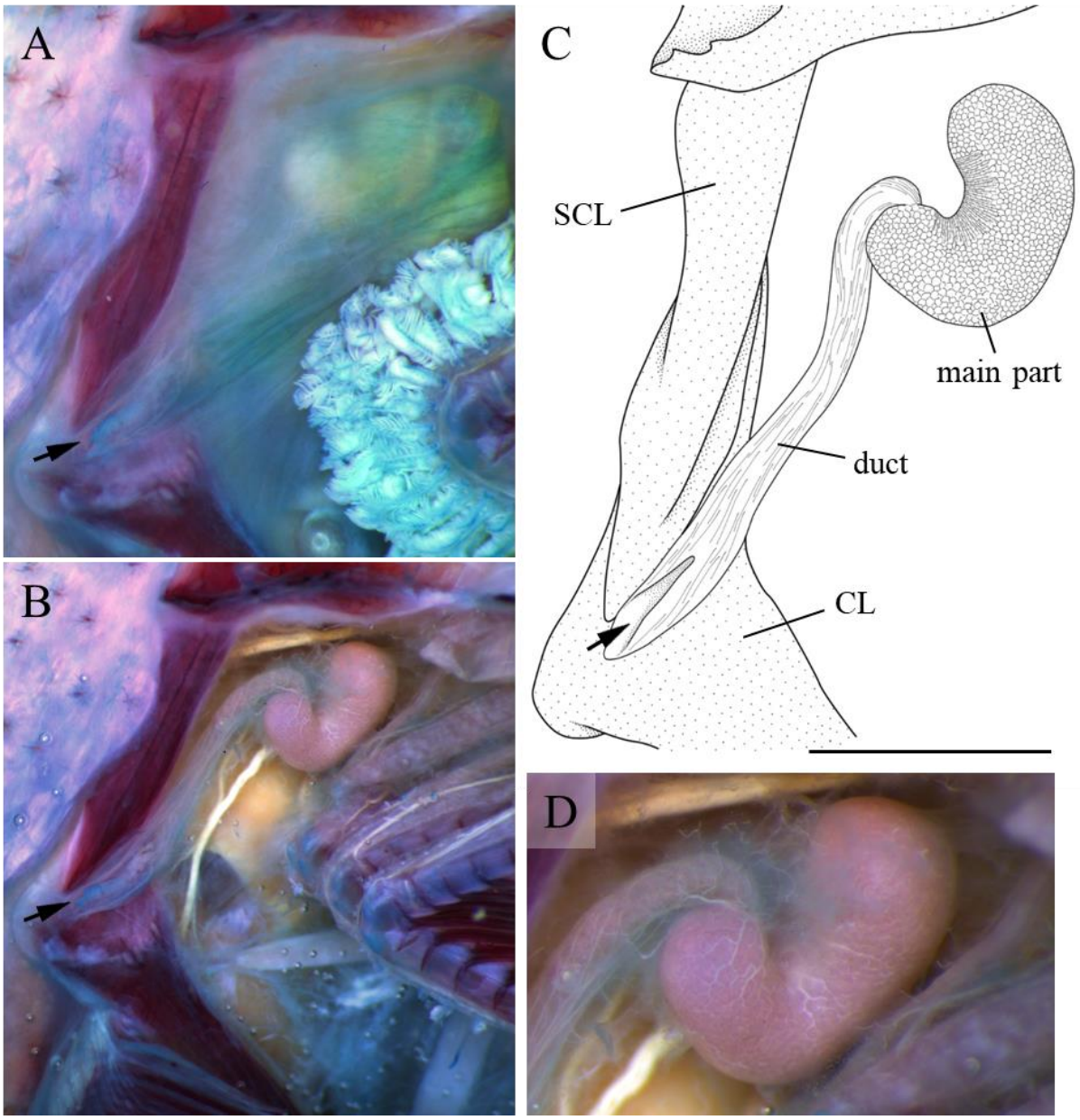

Figure 46. Lateral aspect of prepectoral organ on right side in *Acanthochaenus luetkenii*. A, prepectoral region medial to opercle. B, after removal of epidermis, connective tissue and gill filaments. C, line drawing of prepectoral organ. D, enlarged view of main part. CL, cleithrum; SCL, supracleithrum. Arrows indicates external openings. Scale indicates 3 mm.

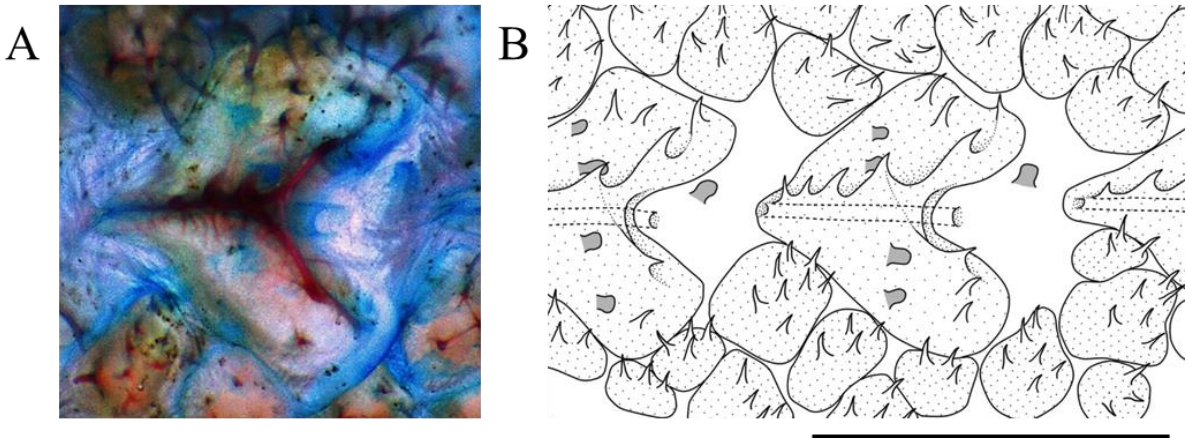

Figure 47. Photograph (A) and line drawing (B) of lateral line scales in *Hispidoberyx ambagiosus*. Gray colored processes and dashed lines indicate papillate neuromasts and trunk canals, respectively. Scale indicates 5 mm.

V. Phylogenetic relationships of *Hispidoberyx ambagiosus* and related taxa

Characters in 80 transformation series were used for the analysis to infer the phylogenetic relationships of *Hispidoberyx ambagiosus* and its related taxa. These transformation series and the character matrix are shown in Tables 1 and 2, respectively. As the result of the phylogenetic analysis, three equally most parsimonious trees (consistency index 0.42, rescaled consistency index 0.29, tree length 267) were obtained. A strict consensus tree constructed from these three most parsimonious trees is shown in Figures 48–50.

In the cladogram, *Hispidoberyx ambagiosus* was inferred to form a monophyletic group (clade D2) thirdly branched off from the ingroup with Stephanoberycidae, Gibberichthyidae, Rondeletiidae, Barbourisiidae and Cetomimidae, and to be a sister group of clade F1 including the former three families.

5-1. Description of the obtained phylogenetic relationships

Contained taxa and supporting characters of each clade are shown below. Asterisk and "r" indicate autapomorphic characters and reversals, respectively.

Clade A. Includes all ingroups. This clade is unambiguously supported by five synapomorphies, characters 46-1, 48-1, 51-1, 65-1 and 66-1. It is also supported by three synapomorphies, characters 9-1, 21-2 and 62-1 according to ACCTRAN, and one synapomorphy, character 21-1 according to DELTRAN. This clade is divided into clades B1 and B2.

Clade B1. Includes all ingroups except for *Polymixia japonica*. This clade is unambiguously supported by seven synapomorphies, characters 4-1*, 13-1*, 15-1*, 16-1*, 18-1*, 41-1 and 44-1*. It is also supported by two synapomorphies, characters 14-1 and 25-1 according to ACCTRAN. This clade is divided into clades C1 and C2.

Clade B2. Includes only *Polymixia japonica*. This clade unambiguously has three apomorphies, characters 1-1, 12-2 and 55-1*. It also has three apomorphies, characters 9-1,

21-2 and 62-1 according to DELTRAN.

Clade C1. Includes all ingroups except for *Polymixia japonica* and *Velifer hypselopterus*. This clade is unambiguously supported by two synapomorphies, characters 20-1* and 73-1*. It is also supported by three synapomorphies, characters 9-0r, 21-1 and 32-1 according to ACCTRAN, and one synapomorphy, character 62-1 according to DELTRAN. This clade is divided into clades D1 and D2.

Clade C2. Includes only *Velifer hypselopterus*. This clade unambiguously has six apomorphies, characters 5-1, 6-1, 12-0, 21-3*, 50-1 and 61-2. It also has one apomorphy, character 62-0r according to ACCTRAN, and three apomorphies, characters 9-1, 14-1 and 25-1 according to DELTRAN.

Clade D1. Includes species of Berycida except for stephanoberycoids, and percomorphs. This clade is unambiguously supported by six synapomorphies, characters 37-1, 39-1, 49-1, 54-1, 56-1* and 65-0r. It is also supported by two synapomorphies, characters 25-0r and 28-1 according to ACCTRAN. This clade is divided into clades K1 and K2.

Clade D2. Includes stephanoberycoids. This clade is unambiguously supported by five synapomorphies, characters 11-1*, 17-1, 42-0, 72-1* and 79-1*. It is also supported by three synapomorphies, characters 27-1, 68-0 and 70-1 according to ACCTRAN, and one synapomorphy, character 32-1 according to DELTRAN. This clade is divided into clades E1 and E2.

Clade E1. Includes *Barbourisia rufa* and *Cetostoma regani*. This clade is unambiguously supported by five synapomorphies, characters 10-1, 15-0r, 46-0r, 48-0r and 80-1. It is also supported by one synapomorphy, character 68-0 according to DELTRAN. This clade is divided into clades J1 and J2.

Clade E2. Includes *Hispidoberyx ambagiosus*, stephanoberycids, *Gibberichthys pumilus* and *Rondeletia loricata*. This clade is unambiguously supported by four synapomorphies, characters 8-1*, 40-1, 58-1* and 74-1*. It is also supported by one synapomorphy, character

61-1 according to ACCTRAN, and one synapomorphy, character 27-1 according to DELTRAN. This clade is divided into clades F1 and F2.

Clade F1. Includes stephanoberycids, *Gibberichthys pumilus* and *Rondeletia loricata*. This clade is unambiguously supported by two synapomorphies, characters 5-1 and 80-3. It is also supported by one synapomorphy, character 24-1 according to ACCTRAN, and three synapomorphies, characters 14-1, 61-1 and 70-1 according to DELTRAN. This clade is divided into clades G1 and G2.

Clade F2. Includes only *Hispidoberyx ambagiosus*. This clade unambiguously has two apomorphies, characters 39-1 and 61-2. It also has three apomorphies, characters 14-0r, 68-1r and 70-0r according to ACCTRAN, and one apomorphy, character 25-1 according to DELTRAN.

Clade G1. Includes *Gibberichthys pumilus* and *Rondeletia loricata*. This clade is unambiguously supported by three synapomorphies, characters 13-0r, 23-0 and 63-1. This clade is divided into clades I1 and I2.

Clade G2. Includes stephanoberycids. This clade is unambiguously supported by six synapomorphies, characters 3-1*, 26-1*, 29-2*, 69-1*, 72-0r and 75-1*. It is also supported by two synapomorphies, characters 24-1 and 68-0 according to DELTRAN. This clade is divided into clades H1 and H2.

Clade H1. Includes only *Acanthochaenus luetkenii*. This clade unambiguously has seven apomorphies, characters 21-0r, 22-1, 28-1, 40-0r, 46-0r, 48-0r and 74-0r. It is also has one apomorphy, character 25-1 according to DELTRAN.

Clade H2. Includes only *Stephanoberyx monae*. This clade has one apomorphy, character 25-0r according to ACCTRAN.

Clade I1. Includes only *Rondeletia loricata*. This clade unambiguously has five apomorphies, characters 8-0r, 20-0r, 45-1, 46-0r and 48-0r. It also has three apomorphies, characters 24-1, 25-1 and 68-0 according to DELTRAN.

Clade I2. Includes only *Gibberichthys pumilus*. This clade unambiguously has two apomorphies, characters 21-0r and 39-1. It also has three apomorphies, characters 24-0r, 25-0r and 68-1r according to ACCTRAN.

Clade J1. Includes only *Cetostoma regani*. This clade unambiguously has seven apomorphies, characters 13-0r, 22-1, 24-1, 36-2*, 55-2, 65-0r and 66-2*. It also has one apomorphy, character 14-0r according to ACCTRAN, and two apomorphies, characters 25-1 and 27-1 according to DELTRAN.

Clade J2. Includes only *Barbourisia rufa*. This clade has two apomorphies, characters 25-0r and 27-0r according to ACCTRAN, and two apomorphies, characters 14-1 and 70-1 according to DELTRAN.

Clade K1. Includes trachichthyiforms, holocentriforms, berycids and percomorphs. This clade is unambiguously supported by two synapomorphies, characters 45-1 and 47-1*. It is also supported by four synapomorphies, characters 1-1, 14-0r, 32-0r and 41-0r according to ACCTRAN. This clade is divided into clades N1 and N2.

Clade K2. Includes melamphaids. This clade is unambiguously supported by 12 synapomorphies, characters 5-1, 7-1, 10-0, 33-1, 34-1*, 35-1*, 53-1, 64-1, 66-0r, 68-2*, 71-1 and 80-3. It is also supported by three synapomorphies, characters 14-1, 28-1 and 32-1 according to DELTRAN. This clade is divided into clades L1 and L2.

Clade L1. Includes only *Poromitra unicornis*. This clade lacks apomorphies.

Clade L2. Includes *Melamphaes typhlops* and *Scopelogadus mizolepis*. This clade is unambiguously supported by one synapomorphy, character 52-1. This clade is divided into clades M1 and M2.

Clade M1. Includes only *Scopelogadus mizolepis*. This clade unambiguously has two apomorphies, characters 12-0 and 53-2.

Clade M2. Includes only *Melamphaes typhlops*. This clade unambiguously has one apomorphy, character 65-1r.

Clade N1. Includes percomorphs. This clade is unambiguously supported by five synapomorphies, characters 18-0r, 19-1*, 30-1, 55-2 and 67-1. It is also supported by one synapomorphy, character 28-0r according to ACCTRAN, and one synapomorphy, character 41-0r according to DELTRAN. This clade is divided into clades X1 and X2.

Clade N2. Includes trachichthyiforms, holocentriforms and berycids. This clade is unambiguously supported by one synapomorphy, character 76-1*. It is also supported by one synapomorphy, character 9-1r according to ACCTRAN, and three synapomorphies, characters 1-1, 9-1 and 28-1 according to DELTRAN. This clade is divided into clades O1 and O2.

Clade O1. Includes berycids and holocentriforms. This clade is unambiguously supported by three synapomorphies, characters 12-2, 38-1* and 73-0r. It is also supported by one synapomorphy, character 41-0r according to DELTRAN. This clade is divided into clades T1 and T2.

Clade O2. Includes trachichthyiforms. This clade is unambiguously supported by four synapomorphies, characters 6-1, 22-1, 36-1* and 49-0r. It is also supported by four synapomorphies, characters 5-1, 41-1r, 60-1 and 78-1 according to ACCTRAN. This clade is divided into clades P1 and P2.

Clade P1. Includes anoplogastroids. This clade is unambiguously supported by three synapomorphies, characters 46-0r, 48-0r and 50-1. It is also supported by three synapomorphies, characters 25-1r, 66-0r and 80-2 according to ACCTRAN, and one synapomorphy, character 25-1 according to DELTRAN. This clade is divided into clades S1 and S2.

Clade P2. Includes trachichthyoids. This clade is unambiguously supported by three synapomorphies, characters 29-1*, 51-0r and 54-0r. It is also supported by one synapomorphy, character 65-1r according to ACCTRAN, and one synapomorphy, character 78-1 according to DELTRAN. This clade is divided into clades Q1 to Q3. Phylogenetic

relationships of clades Q1 to Q3 are unresolved.

Clade Q1. Includes only *Monocentris japonica*. This clade unambiguously has three apomorphies, characters 37-0r, 40-1 and 48-0r. It also has two apomorphies, characters 62-0r and 77-1 according to DELTRAN.

Clade Q2. Includes only *Anomalops katoptron*. This clade unambiguously has two apomorphies, characters 30-1 and 39-0r. It also has one apomorphy, character 60-0r according to ACCTRAN, and one apomorphy, character 77-1 according to DELTRAN.

Clade Q3. Includes trachichthyids. This clade is unambiguously supported by two synapomorphies, characters 31-1* and 57-1*. It is also supported by one synapomorphy, character 5-0r according to ACCTRAN, and one synapomorphy, character 62-0r according to DELTRAN. This clade is divided into clades R1 to R3. Phylogenetic relationships of clades R1 to R3 are unresolved.

Clade R1. Includes only *Paratrachichthys trailli*. This clade has one apomorphy, character 43-1 according to DELTRAN.

Clade R2. Includes only *Hoplostethus mediterraneus*. This clade has one apomorphy, character 65-0r according to ACCTRAN.

Clade R3. Includes only *Trachichthys australis*. This clade has two apomorphies, characters 37-0r and 43-1 according to DELTRAN.

Clade S1. Includes only *Diretmus argenteus*. This clade unambiguously has four apomorphies, characters 10-1, 17-1, 27-1 and 80-3. It also has three apomorphies, characters 14-1r, 21-2r and 32-1r according to ACCTRAN, and five apomorphies, characters 14-1, 21-2, 32-1, 66-0r and 78-1 according to DELTRAN.

Clade S2. Includes only *Anoplogaster cornuta*. This clade unambiguously has five apomorphies, characters 23-0, 37-0r, 39-0r, 40-1 and 64-1. It also has one apomorphy, character 78-0r according to ACCTRAN, and two apomorphies, characters 62-0r and 80-2 according to DELTRAN.

Clade T1. Includes holocentriforms. This clade is unambiguously supported by four synapomorphies, characters 4-0r, 18-0r, 72-2* and 77-1. This clade is divided into clades V1 and V2.

Clade T2. Includes berycids. This clade is unambiguously supported by three synapomorphies, characters 2-1, 20-2* and 7-1. This clade is divided into clades U1 and U2.

Clade U1. Includes only *Centroberyx lineatus*. This clade lacks apomorphies.

Clade U2. Includes only *Beryx decadactylus*. This clade unambiguously has two apomorphies, characters 61-1 and 71-1.

Clade V1. Includes only *Ostichthys japonicus*. This clade unambiguously has three apomorphies, characters 49-0r, 54-0r and 62-0r.

Clade V2. Includes *Holocentrus adscensionis* and *Neoniphon sammara*. This clade is unambiguously supported by three synapomorphies, characters 15-0r, 59-1 and 66-0r. This clade is divided into clades W1 and W2.

Clade W1. Includes only *Neoniphon sammara*. This clade lacks apomorphies.

Clade W2. Includes only *Holocentrus adscensionis*. This clade unambiguously has one apomorphy, character 20-0r.

Clade X1. Includes *Lateolabrax japonicus*, *Lates mariae* and *Trachurus japonicus*. This clade is unambiguously supported by six synapomorphies, characters 40-1, 59-1, 65-1r, 66-0r, 73-0r and 77-1. It is also supported by one synapomorphy, character 21-2r according to ACCTRAN, and two synapomorphies, characters 1-1 and 21-2 according to DELTRAN. This clade is divided into clades Y1 and Y2.

Clade X2. Includes only *Hoplobrotula armata*. This clade unambiguously has 13 apomorphies, characters 2-1, 10-1, 17-1, 37-0r, 42-0, 46-0r, 48-0r, 52-1, 53-2, 55-3*, 68-0, 70-1 and 80-1. It also has two apomorphies, characters 1-0r and 32-1r according to ACCTRAN, and one apomorphy, character 32-1 according to DELTRAN.

Clade Y1. Includes only *Trachurus japonicus*. This clade unambiguously has three

apomorphies, characters 20-0r, 56-0r and 61-1. It also has one apomorphy, character 25-1r according to ACCTRAN, and one apomorphy, character 25-1 according to DELTRAN.

Clade Y2. Includes *Lateolabrax japonicus* and *Lates mariae*. This clade unambiguously has one synapomorphy, character 54-0r. This clade is divided into clades Z1 and Z2.

Clade Z1. Includes only *Lates mariae*. This clade unambiguously has one apomorphy, character 15-0r.

Clade Z2. Includes only *Lateolabrax japonicus*. This clade lacks apomorphies.

Table 1. List of transformation series and characters used for the phylogenetic analysis.

TS 1.	Subocular shelf (0: absent; 1: present)
TS 2.	First and third infraorbitals (0: separated by second infraorbital; 1: attached)
TS 3.	Third and fourth infraorbitals (0: autogenous; 1: fused)
TS 4.	Antorbital (0: present; 1: absent)
TS 5.	Vomerine teeth (0: present; 1: absent)
TS 6.	Size of ethmoid (0: large; 1: small)
TS 7.	Anterolateral process of ethmoid (0: absent or weakly developed; 1: well developed)
TS 8.	Y-shaped pattern of frontal ridges (0: absent; 1: present)
TS 9.	Orbitosphenoid (0: absent; 1: present)
TS 10.	Basisphenoid (0: present; 1: absent)
TS 11.	Exoccipital condyles on both sides (0: attached; 1: detached)
TS 12.	Number of supramaxillae (0: zero; 1: one; 2: two) (ordered as 0-1-2)
TS 13.	Median palato-maxillary ligament (0: present; 1: absent)
TS 14.	Palatine teeth (0: present; 1: absent)
TS 15.	Ectopterygoid teeth (0: present; 1: absent)
TS 16.	Endopterygoid teeth (0: present; 1: absent)
TS 17.	Ethmo-maxillary and palato-premaxillary ligaments (0: separated; 1: partially confluent)
TS 18.	Number of dorsal condyles of hyomandibula (0: two; 1: one)
TS 19.	Ceratohyal and epihyal (0: separated by cartilage or shallowly sutured; 1: deeply sutured)
TS 20.	Number of ligaments connecting ventral hypohyal and branchial arch (0: zero; 1: one; 2: two) (ordered as 0-1-2)
TS 21.	Number of branchiostegal rays (0: nine or more; 1: eight; 2: seven; 3: six) (ordered as 0-1-2-3)
TS 22.	Basihyal (0: present; 1: absent)
TS 23.	Fourth basibranchial and fifth ceratobranchial (0: directly attached; 1: connected via ligament)
TS 24.	Tooth plate on fifth ceratobranchial (0: present; 1: absent)
TS 25.	Tooth plate on third epibranchial (0: present; 1: absent)

Table 1. Continued.

TS 26.	Anterior tip of fourth epibranchial (0: almost in same width or broader than third epibranchial; 1: distinctly thinner than third epibranchial)
TS 27.	Tooth plate on second pharyngobranchial (0: present; 1: absent)
TS 28.	Fourth pharyngobranchial (0: present; 1: absent)
TS 29.	Fourth pharyngobranchial tooth plate (0: autogenous; 1: fused with third pharyngobranchial tooth plate; 2: absent) (unordered)
TS 30.	Interarcual cartilage (0: absent; 1: present)
TS 31.	Posterolateral branch of temporal portion of main trunk canal on posttemporal (0: absent; 1: present)
TS 32.	Temporal portion of main trunk canal on supracleithrum (0: present; 1: absent)
TS 33.	Number of foramina on scapula (0: one; 1: two)
TS 34.	Posterior process of coracoid (0: present; 1: absent)
TS 35.	Fourth actinost (0: without notch; 1: with notch posteriorly)
TS 36.	Number of postcleithra (0: three or two; 1: one; 2: zero) (ordered as 0-1-2)
TS 37.	Anterior process of pelvic bone (0: absent; 1: present)
TS 38.	Internal wing of pelvic bone (0: not expanded; 1: anterodorsally expanded)
TS 39.	Pelvic fin-spine (0: absent; 1: present)
TS 40.	Lateral pelvic radials (0: present; 1: absent)
TS 41.	Neural spine of first abdominal vertebra (0: autogenous; 1: fused with centrum)
TS 42.	Abdominal hemal arches (0: absent; 1: present)
TS 43.	First epineural (0: slender; 1: expanded)
TS 44.	Epipleurals (0: present; 1: absent)
TS 45.	Proximal insertion of Baudelot's ligament (0: first abdominal vertebra; 1: basioccipital)
TS 46.	Dorsal-fin spines (0: absent; 1: present)
TS 47.	Chain-link articulation of dorsal-fin spines (0: absent; 1: present)
TS 48.	Anal-fin spines (0: absent; 1: present)
TS 49.	Second ural centrum, and compound bone formed by first ural and preural centra (0: autogenous; 1: fused)
TS 50.	Second ural centrum, and third and fourth hypurals (0: autogenous; 1: fused)
TS 51.	Neural spine of second preural centrum (0: autogenous; 1: fused with centrum)

Table 1. Continued.

TS 52.	Hemal spine of third preural centrum (0: autogenous; 1: fused with centrum)
TS 53.	Fourth and fifth hypurals (0: autogenous; 1: anteriorly fused; 2: completely fused) (unordered)
TS 54.	First uroneural (0: autogenous; 1: fused with underlying centra)
TS 55.	Number of branched caudal-fin rays (0: 17; 1: 16; 2: 15; 3: 9) (ordered as 0-1-2-3)
TS 56.	Second ventral procurrent caudal-fin ray (0: not shortened proximally; 1: proximally shortened)
TS 57.	Insertion of ligamentum primordium onto preopercle (0: absent; 1: present)
TS 58.	Separated tendon on posteroventral portion of section A2 inserting onto quadrate (0: absent or indistinct; 1: distinct)
TS 59.	Sections A2 and Aω (0: detached; 1: attached via raphe)
TS 60.	Origin of levator operculi (0: pterotic; 1: pterotic and posttemporal)
TS 61.	Hyohyoides inferioris (0: absent; 1: originating from ventral hypohyal on opposite side; 2: originating from raphe on midline) (unordered)
TS 62.	Levator posterior (0: absent; 1: present)
TS 63.	Insertion of transversus dorsalis anterior onto second epibranchial (0: present; 1: absent)
TS 64.	Sphincter oesophagi division (0: present; 1: absent)
TS 65.	Semicircular ligament (0: absent; 1: present)
TS 66.	Transversus ventralis anterior (0: unpaired element; 1: unpaired and paired elements; 2: paired elements) (ordered as 0-1-2)
TS 67.	Anterior tendon of transversus ventralis posterior (0: present; 1: absent)
TS 68.	Adductor radialis (0: absent; 1: moderately developed; 2: well developed) (ordered as 0-1-2)
TS 69.	Abductor superficialis pelvicus (0: present; 1: absent)
TS 70.	Extensor proprius (0: present; 1: absent)
TS 71.	Insertion of flexor ventralis onto ventralmost principal ray on upper lobe (0: absent; 1: present)
TS 72.	Unnamed muscle on lateral portion of supracarinalis anterior (0: absent; 1: thin and band-like; 2: wide and sheet-like) (unordered)

Table 1. Continued.

TS 73.	Ossifications of sclera (0: present; 1: absent)
TS 74.	Tominaga's organ (0: absent; 1: present)
TS 75.	Prepectoral organ (0: absent; 1: present)
TS 76.	Jakubowski's organ (0: absent; 1: present)
TS 77.	Separate anterior dorsal fin (0: absent; 1: present)
TS 78.	Abdominal scutes (0: absent; 1: present)
TS 79.	Papillate lateral line system on trunk (0: absent; 1: present)
TS 80.	Trunk canal (0: canal supported by scales; 1: dermal canal; 2: groove supported by scales; 3: absent) (unordered)

Table 2. Matrix of characters in transformation series for phylogenetic analysis.

	Transformation series and characters																																						
	1	**2**	**3**	**4**	**5**	**6**	**7**	**8**	**9**	**10**	**11**	**12**	**13**	**14**	**15**	**16**	**17**	**18**	**19**	**20**	**21**	**22**	**23**	**24**	**25**	**26**	**27**	**28**	**29**	**30**	**31**	**32**	**33**	**34**	**35**	**36**	**37**	**38**	**39**	**40**
Hispidoberyx ambagiosus	0	0	0	1	0	0	0	1	0	0	1	1	1	0	1	1	1	1	0	1	1	0	A	0	1	0	1	0	0	0	0	1	0	0	0	0	A	0	1	1
Stephanoberyx monae	0	0	1	1	1	0	0	1	0	0	1	1	1	1	1	1	1	1	0	1	1	0	1	1	0	1	1	0	2	0	0	1	0	0	0	0	0	0	0	1
Acanthochaenus luetkenii	0	0	1	1	1	0	0	1	0	0	1	1	1	1	1	1	1	1	0	1	0	1	1	1	1	1	1	1	2	0	0	1	0	0	0	0	0	0	0	0
Gibberichthys pumilus	0	0	0	1	1	0	0	1	0	0	1	1	0	1	1	1	1	1	0	1	0	0	0	0	0	0	1	0	0	0	0	1	0	0	0	0	0	0	1	1
Rondeletia loricata	0	0	0	1	1	0	0	0	0	0	1	1	0	1	1	1	1	1	0	0	1	0	0	1	1	0	1	0	0	0	0	1	0	0	0	0	0	0	0	1
Barbourisia rufa	0	0	0	1	0	0	0	0	0	1	1	1	1	1	0	1	1	1	0	1	1	0	1	0	0	0	0	0	0	0	0	1	0	0	0	0	0	0	0	0
Cetostoma regani	0	0	0	1	0	0	0	0	0	1	1	1	0	0	0	1	?	1	0	1	1	1	A	1	1	0	1	0	0	0	0	1	0	0	0	2	?	?	?	?
Melamphaes typhlops	0	0	0	1	1	0	1	0	0	1	0	1	1	1	1	1	0	1	0	1	1	0	1	0	0	0	0	1	0	0	0	1	1	1	1	0	1	0	1	0
Poromitra unicornis	0	0	0	1	1	0	1	0	0	1	0	1	1	1	1	1	0	1	0	1	1	0	1	0	0	0	0	1	0	0	0	1	1	1	1	0	1	0	1	0
Scopelogadus mizolepis	0	0	0	1	1	0	1	0	0	1	0	0	1	1	1	1	0	1	0	1	1	0	1	0	0	0	0	1	0	0	0	1	1	1	1	0	1	0	1	0
Trachichthys australis	1	0	0	1	0	1	0	0	1	0	0	1	1	0	1	1	0	1	0	1	1	1	1	0	0	0	0	1	1	0	1	0	0	0	0	1	0	0	1	0
Hoplostethus mediterraneus	1	0	0	1	0	1	0	0	1	0	0	1	1	0	1	1	0	1	0	1	1	1	1	0	0	0	0	1	1	0	1	0	1	0	0	1	1	0	1	0
Paratrachichthys trailli	1	0	0	1	0	1	0	0	1	0	0	1	1	0	1	1	0	1	0	1	1	1	1	0	0	0	0	1	1	0	1	0	1	0	0	1	1	0	1	0
Anomalops katoptron	1	0	0	1	1	1	0	0	1	0	0	1	1	0	A	A	0	1	0	1	1	1	1	0	0	0	0	1	1	1	0	0	0	0	0	1	1	0	0	0
Monocentris japonica	1	0	0	1	1	1	0	0	1	0	0	1	1	0	A	A	0	1	0	1	1	1	1	0	0	0	0	1	1	0	0	0	0	0	0	1	0	0	1	1
Anoplogaster cornuta	1	0	0	1	1	1	0	0	1	0	0	1	1	0	1	1	0	1	0	1	1	1	0	0	1	0	0	1	0	0	0	0	0	0	0	1	0	0	0	1
Diretmus argenteus	1	0	0	1	1	1	0	0	1	1	0	1	1	1	1	1	1	1	0	1	2	1	1	0	1	0	1	1	0	0	0	1	0	0	0	1	1	0	1	0
Beryx decadactylus	1	1	0	1	0	0	1	0	1	0	0	2	1	0	1	1	0	1	0	2	1	0	1	0	0	0	0	1	0	0	0	0	0	0	0	0	1	1	1	0
Centroberyx lineatus	1	1	0	1	0	0	1	0	1	0	0	2	1	0	1	1	0	1	0	2	1	0	1	0	0	0	0	1	0	0	0	0	0	0	0	0	1	1	1	0
Holocentrus adscensionis	1	0	0	0	0	0	0	0	1	0	0	2	1	0	0	1	0	0	0	0	1	0	1	0	0	0	0	1	0	0	0	0	0	0	0	0	1	1	1	0
Neoniphon sammara	1	0	0	0	0	0	0	0	1	0	0	2	1	0	0	1	0	0	0	1	1	0	1	0	0	0	0	1	0	0	0	0	0	0	0	0	1	1	1	0
Ostichthys japonicus	1	0	0	0	0	0	0	0	1	0	0	2	1	0	1	1	0	0	0	1	1	0	1	0	0	0	0	1	0	0	0	0	0	0	0	0	1	1	1	0
Polymixia japonica	1	0	0	0	0	0	0	0	1	0	0	2	0	0	0	0	0	0	0	0	2	0	1	0	0	0	0	0	0	0	0	0	0	0	0	0	0	0	0	0
Velifer hypselopterus	0	0	0	1	1	1	0	0	1	0	0	0	1	1	1	1	?	1	0	0	3	0	1	0	1	0	0	0	0	0	0	0	0	0	0	0	0	0	0	0
Hoplobrotula armata	0	1	0	1	0	0	0	0	0	1	0	1	1	0	1	1	1	0	1	1	1	0	1	0	0	0	0	0	0	1	0	1	0	0	0	0	0	0	1	0
Lateolabrax japonicus	1	0	0	1	0	0	0	0	0	0	0	1	1	0	1	1	0	0	1	1	2	0	1	0	0	0	0	0	0	1	0	0	0	0	0	1	0	1	1	1
Lates mariae	1	0	0	1	0	0	0	0	0	0	0	1	1	0	0	1	0	0	1	1	2	0	1	0	0	0	0	0	0	1	0	0	0	0	0	1	0	1	1	1
Trachurus japonicus	1	0	0	1	0	0	0	0	0	0	0	1	1	0	1	1	0	0	1	0	2	0	1	0	1	0	0	0	0	1	0	0	0	0	0	1	0	1	1	1
OUTGROUPS																																								
Neoscopelus microchir	0	0	0	0	0	0	0	0	0	1	0	1	0	0	0	0	0	0	0	0	0	0	1	0	0	0	0	0	0	0	0	0	0	0	0	0	0	0	0	0
Trachinocephalus trachinus	0	0	0	0	?	0	0	0	0	0	0	0	0	0	1	1	?	0	0	0	0	0	0	0	1	0	0	0	2	0	0	0	0	1	0	0	0	0	0	0
Hime japonica	0	0	0	0	0	0	0	0	0	0	0	2	0	0	0	0	0	0	0	0	0	0	0	0	0	0	0	0	0	0	0	0	0	0	0	0	0	0	0	0

A, 0 and 1

Table 2. Continued.

	Transformation series and characters																																						
	41	**42**	**43**	**44**	**45**	**46**	**47**	**48**	**49**	**50**	**51**	**52**	**53**	**54**	**55**	**56**	**57**	**58**	**59**	**60**	**61**	**62**	**63**	**64**	**65**	**66**	**67**	**68**	**69**	**70**	**71**	**72**	**73**	**74**	**75**	**76**	**77**	**78**	**79**	**80**
Hispidoberyx ambagiosus	1	0	0	1	0	1	0	1	0	0	1	0	0	0	0	0	0	1	0	0	2	1	0	0	1	1	0	1	0	0	0	1	1	1	0	0	0	0	1	0
Stephanoberyx monae	1	0	0	1	0	1	0	1	0	0	1	0	0	0	0	0	0	1	0	0	1	1	0	0	1	1	0	0	1	1	0	0	1	1	1	0	0	0	1	3
Acanthochaenus luetkenii	1	0	0	1	0	0	?	0	0	0	1	0	0	0	0	0	0	1	0	0	1	1	0	0	1	1	0	0	1	1	0	0	1	0	1	0	0	0	1	3
Gibberichthys pumilus	1	0	0	1	0	1	0	1	0	0	1	0	0	0	0	0	0	1	0	0	1	1	1	0	1	1	0	1	0	1	0	1	1	1	0	0	0	0	1	3
Rondeletia loricata	1	0	0	1	1	0	?	0	0	0	1	0	0	A	0	0	0	1	0	0	1	1	1	0	1	A	0	0	0	1	0	1	1	1	0	0	0	0	1	3
Barbourisia rufa	1	0	0	1	0	0	?	0	0	0	1	0	0	A	0	0	0	0	0	0	0	1	0	0	1	1	0	0	0	1	0	1	1	0	0	0	0	0	1	1
Cetostoma regani	1	0	0	1	?	0	?	0	A	0	1	0	0	0	2	0	0	0	0	0	0	1	0	0	0	2	0	0	?	?	0	1	1	0	0	0	0	0	1	1
Melamphaes typhlops	1	1	0	1	0	1	0	1	1	0	1	1	1	1	0	1	0	0	0	0	0	1	0	1	1	0	0	2	0	0	1	0	1	0	0	0	0	0	0	3
Poromitra unicornis	1	1	0	1	0	1	0	1	1	0	1	0	1	1	0	1	0	0	0	0	0	1	0	1	0	0	0	2	0	0	1	0	1	0	0	0	0	0	0	3
Scopelogadus mizolepis	1	1	0	1	0	1	0	1	1	0	1	1	2	1	0	1	0	0	0	0	0	1	0	1	0	0	0	2	0	0	1	0	1	0	0	0	0	0	0	3
Trachichthys australis	1	1	1	1	1	1	1	1	A	0	0	0	0	0	0	1	1	0	0	1	1	0	0	0	1	1	0	1	0	0	0	0	1	0	0	1	0	1	0	0
Hoplostethus mediterraneus	1	1	0	1	1	1	1	1	0	0	0	0	0	0	0	1	1	0	0	1	0	0	0	0	0	1	0	1	0	0	0	0	1	0	0	1	0	1	0	0
Paratrachichthys trailli	1	1	1	1	1	1	1	1	0	0	0	0	0	0	0	1	1	0	0	1	0	0	0	0	1	1	0	1	0	0	0	0	1	0	0	1	0	1	0	0
Anomalops katoptron	1	1	0	1	1	1	1	1	0	0	0	0	0	0	0	1	0	0	0	0	1	1	0	0	1	1	A	1	0	0	0	0	1	0	0	1	1	1	0	0
Monocentris japonica	1	1	0	1	?	1	1	0	0	0	A	0	0	0	0	1	0	0	0	1	1	0	0	0	1	1	0	1	0	0	0	0	1	0	0	1	1	1	0	0
Anoplogaster cornuta	1	1	0	1	?	0	?	0	0	1	1	0	0	1	0	1	0	0	0	1	?	0	A	1	0	A	0	1	0	0	0	0	1	0	0	1	0	0	0	2
Diretmus argenteus	1	1	0	1	1	0	?	0	0	1	1	0	0	1	0	1	0	0	0	1	0	1	0	0	0	0	0	1	0	0	0	0	1	0	0	1	0	1	0	3
Beryx decadactylus	0	1	0	1	1	1	1	1	1	0	1	0	0	1	0	1	0	0	0	0	1	1	0	0	0	1	0	1	0	0	1	0	0	0	0	1	0	0	0	0
Centroberyx lineatus	0	1	0	1	1	1	1	1	1	0	1	0	0	1	0	1	0	0	0	0	0	1	0	0	0	1	0	1	0	0	0	0	0	0	0	1	0	0	0	0
Holocentrus adscensionis	0	1	0	1	1	1	1	1	1	0	1	0	0	1	0	1	0	0	1	0	0	1	0	0	0	0	0	1	0	0	0	2	0	0	0	1	1	0	0	0
Neoniphon sammara	0	1	0	1	1	1	1	1	1	0	1	0	0	1	0	1	0	0	1	0	0	1	0	0	0	0	0	1	0	0	0	2	0	0	0	1	1	0	0	0
Ostichthys japonicus	0	1	0	1	1	1	1	1	0	0	1	0	0	0	0	1	0	0	0	0	0	0	0	0	0	1	0	1	0	0	0	2	0	0	0	1	1	0	0	0
Polymixia japonica	0	1	0	0	0	1	0	1	0	0	1	0	0	0	1	0	0	0	0	0	0	1	0	0	1	1	0	1	0	0	0	0	0	0	0	0	0	0	0	0
Velifer hypselopterus	1	1	0	1	0	1	0	1	0	1	1	0	0	0	0	0	0	0	0	0	2	0	0	0	1	1	0	1	0	0	0	0	0	0	0	0	0	0	0	0
Hoplobrotula armata	0	0	0	1	1	0	?	0	1	0	1	1	2	1	3	?	0	0	0	0	0	1	0	0	0	1	1	0	0	1	0	0	1	0	0	0	0	0	0	1
Lateolabrax japonicus	0	1	0	1	1	1	1	1	1	0	1	0	0	0	2	1	0	0	1	0	0	1	0	0	1	0	1	1	0	0	0	0	0	0	0	0	1	0	0	0
Lates mariae	0	1	0	1	1	1	1	1	1	0	1	0	0	0	2	1	0	0	1	0	0	1	0	0	1	0	1	1	0	0	0	0	0	0	0	0	1	0	0	0
Trachurus japonicus	0	1	0	1	1	1	1	1	1	0	1	0	0	1	2	0	0	0	1	0	1	1	0	0	1	0	1	1	0	0	0	0	0	0	0	0	1	0	0	0
OUTGROUPS																																								
Neoscopelus microchir	0	1	0	0	0	0	?	0	0	0	0	0	0	0	0	0	0	0	0	0	0	0	0	0	0	0	0	1	0	0	0	0	1	0	0	0	0	0	0	0
Trachinocephalus trachinus	0	0	0	0	0	0	?	0	0	0	0	0	0	0	0	0	0	0	0	0	0	0	0	0	0	0	0	0	0	0	0	0	0	0	0	0	0	0	0	0
Hime japonica	0	0	0	0	0	0	?	0	0	0	0	0	0	0	0	1	0	0	0	0	1	0	0	0	0	1	0	1	0	0	0	0	0	0	0	0	0	0	0	0

A, 0 and 1

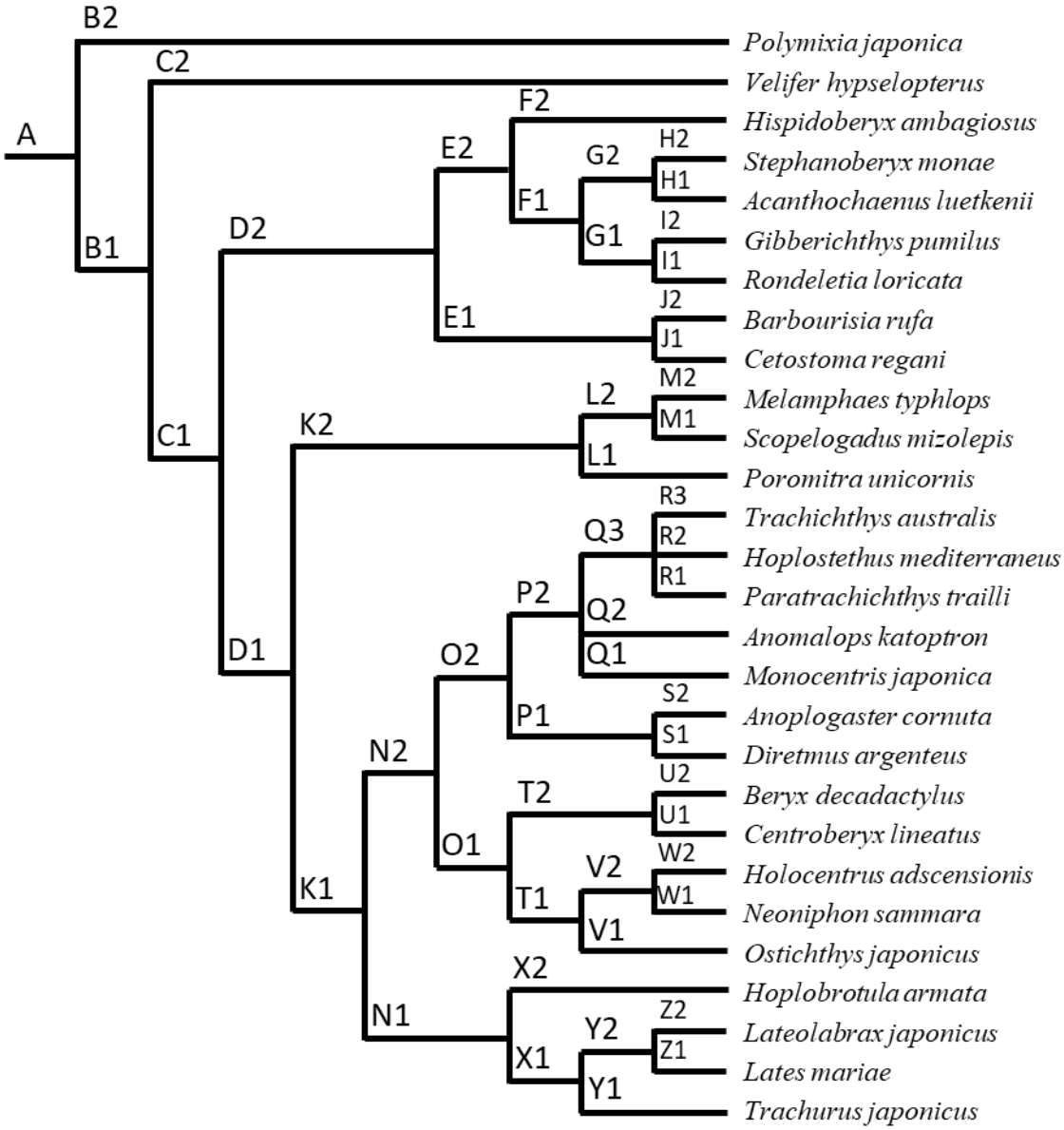

Figure 48. Strict consensus tree of three equally parsimonious trees representing phylogenetic relationships of *Hispidoberyx ambagiosus* and related taxa.

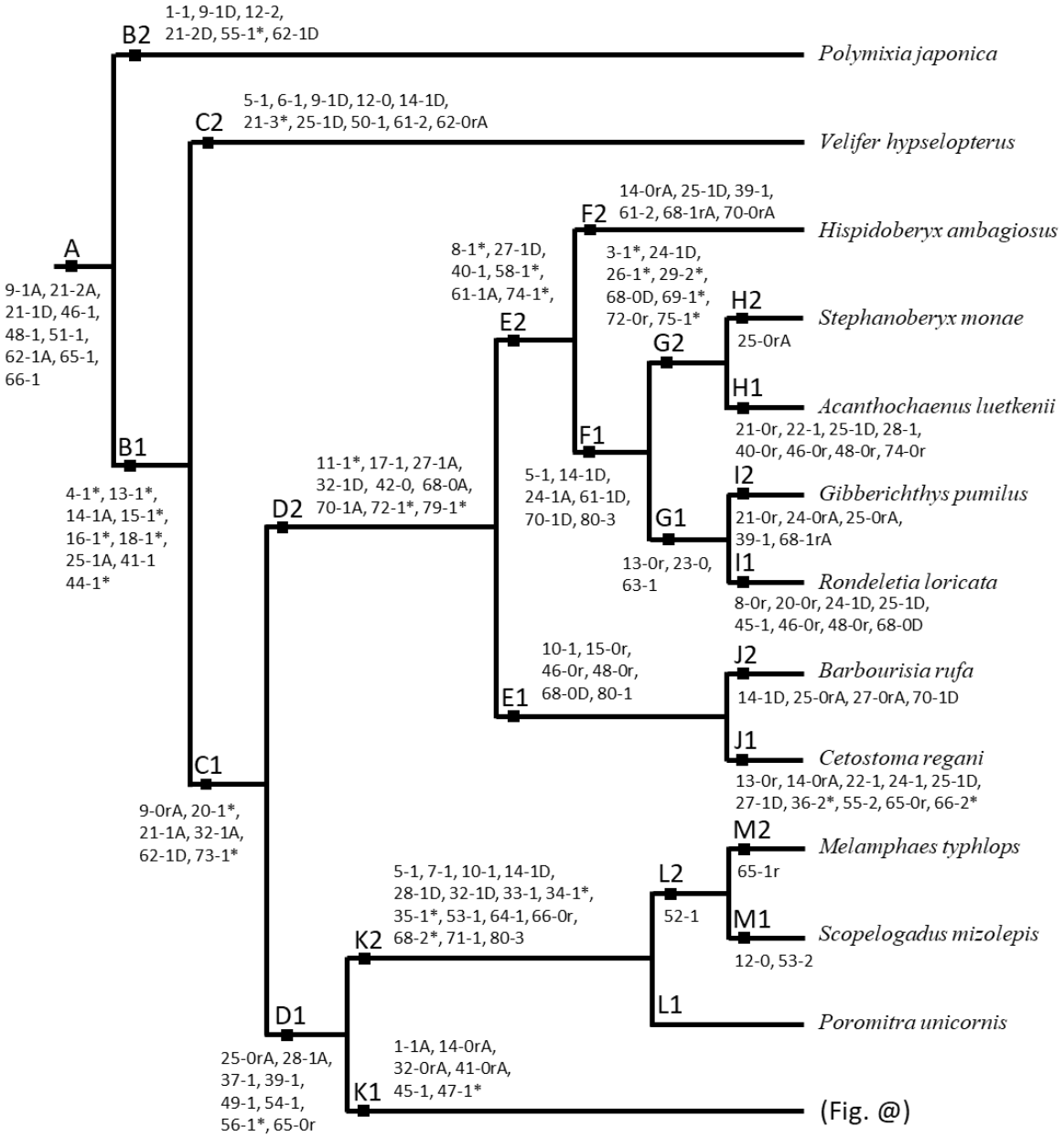

Figure 49. Cladogram and character distribution on clades A to M2. A, ACCTRAN; D, DELTRAN; r, reversal; asterisk, autapomorphy.

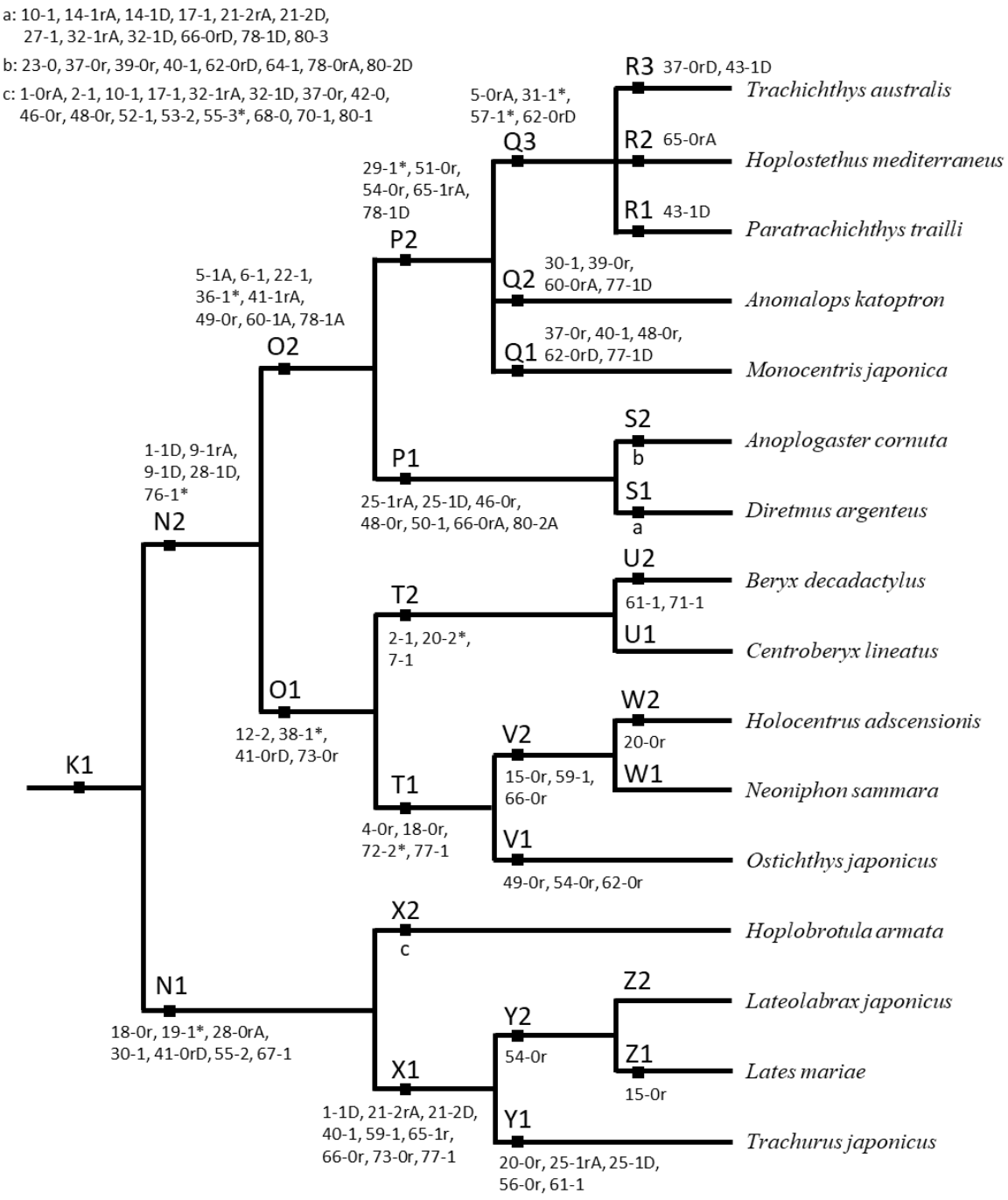

Figure 50. Cladogram and character distribution on clades N1 to Z2. A, ACCTRAN; D, DELTRAN; r, reversal; asterisk, autapomorphy.

5-2. Comparison with previous works

5-2-1. Phylogenetic position of *Hispidoberyx ambagiosus*

Moore's (1993) study is the sole previous work which conducted the phylogenetic analysis including *Hispidoberyx ambagiosus* and objectively inferred its phylogenetic position among related taxa. He carried out the phylogenetic analysis among Trachichthyiformes (sensu Moore, 1993) and inferred that Hispidoberycidae forms a monophyletic group together with Stephanoberycidae, Gibberichthyidae, Rondeletiidae, Barbourisiidae and Cetomimidae (Fig. 51B) [Megalomycteridae was also contained, which is now regarded as a junior synonym of Cetomimidae (Johnson et al., 2009)]. In his study, the monophyly of the clade including these families was supported by the following three synapomorphies: abdominal hemal arches lost; exoccipital condyles widely separated; and insertion of first dorsal pterygiophore anterior to eighth or ninth neural spine. As the result of the present study, the monophyly of the clade including these six families (clade D2) was also strongly supported by five unambiguous synapomorphies including three autapomorphies (shown by asterisks): exoccipital condyles on both sides detached (character 11-1*); ethmo-maxillary and palato-premaxillary ligaments partially confluent (character 17-1); abdominal hemal arches absent (character 42-0); unnamed muscle on lateral portion of supracarinalis anterior thin and band-like (character 72-1*); and papillate lateral line system on trunk present (character 79-1*).

Among the monophyletic group including these families, Moore (1993) inferred a sister relationship of Hispidoberycidae and Stephanoberycidae based on a single synapomorphy (9–11 procurrent caudal-fin spines on both upper and lower lobes). Previous studies (Kotlyar, 1981, 1991a; Yang et al., 1988) reported that the number of procurrent caudal-fin spines in Hispidoberycidae is 9–10. In this study, however, reexamination of the holotype of the *H. ambagiosus* revealed that it has eight procurrent spines on the upper caudal lobe, which extends the range of the number of procurrent caudal-fin spines in Hispidoberycidae to 8–10. Moreover, because some other taxa having eight to nine procurrent spines make the variation

of the number of procurrent spines serial among ingroups, the number of the procurrent spines was not able to be used for the analysis in this study (see “Other variations” in the section on the caudal skeleton). Accordingly, the character suggested by Moore (1993), 9–11 procurrent caudal-fin spines on both upper and lower lobes, cannot be a synapomorphy of Hispidoberycidae and Stephanoberycidae.

On the other hand, clade E2 which was inferred to contain Hispidoberycidae, Stephanoberycidae, Gibberichthyidae and Rondeletiidae in this study is strongly supported by four unambiguous synapomorphies including three autapomorphies: Y-shaped pattern of frontal ridges present (character 8-1*); lateral pelvic radials absent (character 40-1); separated tendon on posteroventral portion of section A2 inserting onto quadrate distinct (character 58-1*); and Tominaga’s organ present (character 74-1*). Although the last character, the presence of Tominaga’s organ, was previously known only in Gibberichthyidae and Rondeletiidae (Paxton et al., 2001), this study revealed that the organ is also present in Hispidoberycidae and stephanoberycid *Stephanoberyx monae*. Because any secretory organs located near the nasal rosette like Tominaga’s organ have never been reported in any other fish taxa, this unique character strongly characterizes the clade formed by Hispidoberycidae, Stephanoberycidae, Gibberichthyidae and Rondeletiidae. The close relationship of Hispidoberycidae with Stephanoberycidae and Gibberichthyidae is congruent with Moore’s (1993) cladogram and Kotlyar’s (1991a) hypothesis based on the osteological examination that the superfamily Hispidoberycoidea is closely related to the superfamily Stephanoberycoidea including Stephanoberycidae and Gibberichthyidae. In addition, although the sister relationship of Gibberichthyidae and Rondeletiidae was suggested by Rosen (1973) and Paxton et al. (2001) without a phylogenetic analysis, the present study inferred this relationship based on the phylogenetic analysis for the first time.

5-2-2. Non-monophyly of Berycida

As the result of the phylogenetic analysis, series Berycida (sensu Nelson et al., 2016) was inferred to be non-monophyletic and divided into three different lineages, clades D2, K2 and N2. The monophyly of Berycida is supported by some molecular studies (e.g., Miya et al., 2001, 2005; Near et al., 2012, 2013) (Fig. 52A), while many other molecular studies showed its non-monophyly (e.g., Miya et al., 2003; Betancur-R et al., 2013, 2017; Chen et al., 2014; Dornburg et al., 2017; Hughes et al., 2018) (Fig. 52B, C). Additionally, many morphology-based phylogenetic studies have shown non-monophyly of Berycida (e.g., Stiassny & Moore, 1992; Johnson & Patterson, 1993; Moore, 1993) (Fig. 51A–C). Zehren (1979), who conducted a pioneering morphological phylogenetic study of this group, inferred it to be monophyletic (Fig. 51D), but he also suggested a possibility that Holocentridae can be removed from this group by further studies and discovery of additional characters.

Stiassny & Moore's (1992) and Moore's (1993) morphological studies suggested a hypothesis that all families of Berycida except for Holocentridae and Berycidae form a monophyletic group [= Trachichthyiformes sensu Moore, 1993 (see Table 3 for its compositions)] and the latter two families are positioned in different lineages, respectively (Fig. 51A, B). In the present study, however, trachichthyiforms defined by them were divided into three clades, clades D2, K2 and O2, which are strongly supported by five, 12 and four synapomorphies, respectively. Synapomorphies of Trachichthyiformes suggested by Moore (1993) are the following three characters: ossified sclera present (character 73-1 in this study); neural spine of first vertebra fused with centrum (character 41-1); and number of supramaxillae one (character 12-1). As the result of the analysis in this study, character 73-1 was inferred to be a synapomorphy of clade C1 formed by Berycida and Percomorpha with reversals in clades N1 and O1. Character 41-1 was inferred to be a synapomorphy of clade B1 including all ingroups except Polymixiidae, with reversals in clades K1 and O2 according to ACCTRAN, or in clades N1 and O1 according to DELTRAN. Character 12-1 was inferred to be a primitive condition among ingroups in this study. Therefore, the monophyly of

Trachichthyiformes (sensu Moore, 1993) was rejected in this study as well as in Johnson & Patterson's (1993) morphological study and many molecular studies.

Johnson & Patterson (1993) proposed a different phylogenetic relationship based on morphological characters, in which Berycida was divided into two orders, Beryciformes and Stephanoberyciformes (Fig. 51C) (see Table 3 for their compositions). According to Johnson & Patterson (1993), Beryciformes was inferred to be supported by the following three synapomorphies: Jakubowski's organ present (character 76-1); second ventral procurrent caudal ray shortened proximally (character 56-1); and orbitosphenoid present (character 9-1). The analysis in the present study also inferred Beryciformes defined by them to be a monophyletic group (clade N2), which is unambiguously supported by a single synapomorphy, character 76-1. Character 9-1 also supports clade N2 according to DELTRAN (as a reversal character according to ACCTRAN), while character 56-1 was inferred to support a deeper node (clade D1) with a reversal at clade Y1. On the other hand, Stephanoberyciformes, which was inferred to be supported by a single synapomorphy (the extrascapular enlarged and covering the parietal) by Johnson & Patterson (1993), was divided into two lineages, clades D2 and K2 in this study. The character on the extrascapular suggested by them was not used for the analysis in the present study because the size of the extrascapula serially varies among ingroups and the autogenous parietal is absent in *Hispidoberyx ambagiosus*, *Acanthochaenus luetkenii* and *Gibberichthys pumilus* (see "Other variations" in the section on the pectoral girdle). As the result of the analysis in this study, Melamphaidae, which was included in Stephanoberyciformes by Johnson & Patterson (1993), formed a monophyletic group (clade D1) with clade K1 including Beryciformes defined by them and Percomorpha. Clade D1 is strongly supported by six unambiguous synapomorphies including one autapomorphy. Although the monophyly of Stephanoberyciformes was also supported by other major morphological studies (e.g., Zehren, 1979; Moore, 1993), its monophyly was morphologically rejected for the first time in this study.

In molecular phylogenetic studies including taxa of Berycida, each monophyly of major clades, Beryciformes, Trachichthyiformes and Holocentriformes (sensu Nelson et al., 2016) (see Table 3 for their compositions) is constantly supported despite different relationships among them (Fig. 52). In this study, the monophyly of the latter two orders were also supported, respectively, while Beryciformes was inferred to be non-monophyletic, being divided into clades D2, K2 and T2. The monophyly of Beryciformes (sensu Nelson et al., 2016) has never been supported by any morphological studies, and no synapomorphies have been given for the order to date. The incongruence on this order between molecular and morphological studies is one of problematic points on the phylogeny of Berycida.

Table 3. Representatives of previously recognized classifications of extant taxa at order to family levels among Berycida (sensu Nelson et al., 2016).

Authors	Moore (1993)	Johnson & Patterson (1993)	Nelson et al. (2016)
Classification	Order Trachichthyiformes	Order Beryciformes	Order Beryciformes
	Suborder Trachichthyoidei	Family Anomalopidae	Suborder Stephanoberycoidei
	Family Anomalopidae	Family Anoplogastridae	Superfamily Stephanoberycoidea
	Family Anoplogastridae	Family Berycidae	Family Gibberichthyidae
	Family Diretmidae	Family Diretmidae	Family Hispidoberycidae
	Family Monocentridae	Family Holocentridae	Family Stephanoberycidae
	Family Trachichthyidae	Family Monocentridae	Superfamily Cetomimoidea
	Suborder Stephanoberycoidei	Family Trachichthyidae	Family Barbourisiidae
	Family Barbourisiidae	Order Stephanoberyciformes	Family Cetomimidae
	Family Cetomimidae	Family Barbourisiidae	(Syn.: Megalomycteridae)
	Family Gibberichthyidae	Family Cetomimidae	Family Rondeletiidae
	Family Hispidoberycidae	Family Gibberichthyidae	Suborder Berycoidei
	Family Megalomycteridae	Family Hispidoberycidae	Family Berycidae
	Family Melamphaidae	Family Megalomycteridae	Family Melamphaidae
	Family Rondeletiidae	Family Melamphaidae	Order Trachichthyiformes
	Family Stephanoberycidae	Family Rondeletiidae	Suborder Anoplogastroidei
		Family Stephanoberycidae	Family Anoplogastridae
	(not assigned to this order)		Family Diretmidae
	Family Berycidae		Suborder Trachichthyoidei
	Family Holocentridae		Family Anomalopidae
			Family Monocentridae
			Family Trachichthyidae
			Order Holocentriformes
			Family Holocentridae

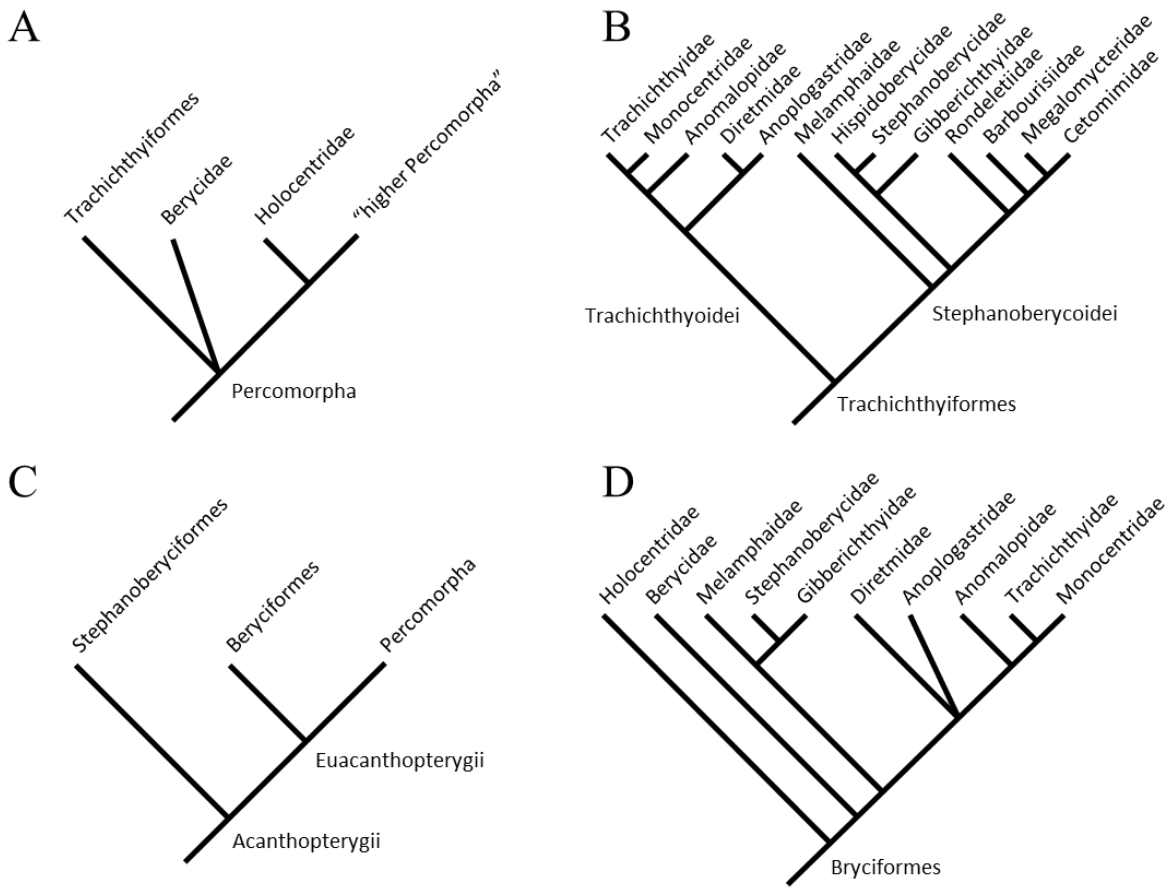

Figure 51. Previously inferred relationships of Berycida and related taxa based on morphological characters. A, Stiassny & Moore (1992); B, Moore (1993); C, Johnson & Patterson (1993); D, Zehren (1979).

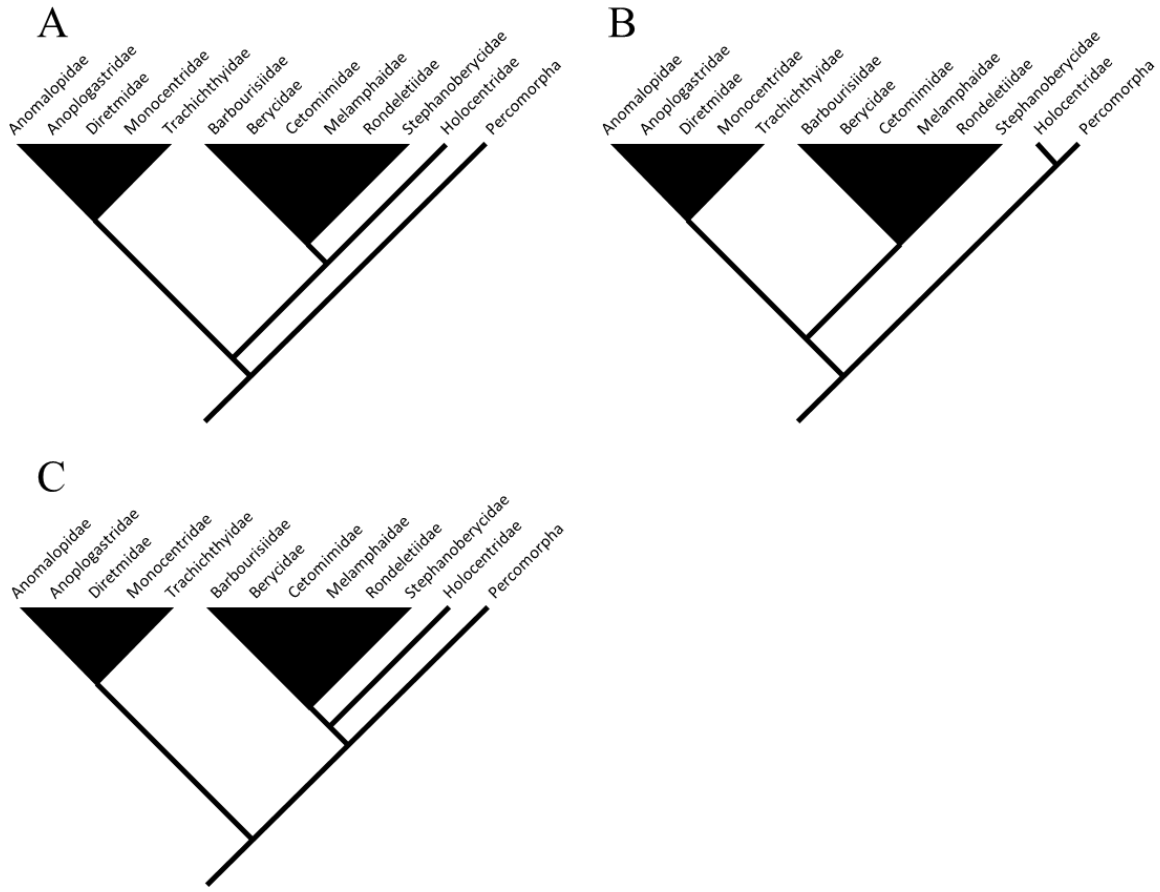

Figure 52. Previously inferred relationships of Berycida and related taxa based on molecular data. A, Miya et al. (2005) and Near et al. (2012); B, Betancur-R et al. (2013, 2017); C, Miya et al. (2003), Chen et al. (2014) and Dornburg et al. (2017).

VI. Classification

As a result of the present analysis, *Hispidoberyx ambagiosus* was placed among taxa of Berycida. In this study, a new classification based on the inferred relationships is discussed only on Berycida, because this study focused on the phylogenetic placement of *H. ambagiosus* and the number of taxa other than Berycida used in this study is insufficient for addressing their classification.

6-1. Reconstruction of classification of *Hispidoberyx ambagiosus* and related taxa

The phylogenetic analysis in this study resulted in the non-monophyly of the series Berycida (sensu Nelson et al., 2016). Although many disagreements are present on the monophyly of Berycida between previous studies as noted in the former chapter, more comprehensive study including various taxa is needed to discuss the classification of higher taxa at levels of series or division. Accordingly, the classification at levels higher than order are not discussed in this study. In addition, because the number of taxa in each family of Berycida used in this study is insufficient for discussion of the classification at generic level, the classification at order to family levels among Berycida (sensu Nelson et al., 2016) is discussed below.

The classification of Nelson et al. (2016), which was followed as the initial classification in this study, recognized the following three orders among Berycida: Beryciformes (including Hispidoberycidae, Stephanoberycidae, Gibberichthyidae, Rondeletiidae, Barbourisiidae, Cetomimidae, Melamphaidae and Berycidae); Trachichthyiformes (including Anomalopidae, Anoplogastridae, Diretmidae, Monocentridae and Trachichthyidae); and Holocentriformes (including only Holocentridae) (Table 3). Of these orders, Beryciformes including Hispidoberycidae was inferred to be divided into three different lineages, clades D2, K2 and T2, which are unambiguously supported by five, 12 and three synapomorphies, respectively, whereas the latter two orders were inferred to form well supported monophyletic groups in

this study, respectively. Most of molecular studies support the monophyly of Beryciformes (sensu Nelson et al., 2016), while previous morphological studies have never supported its monophyly to date (Zehren, 1979; Johnson & Patterson, 1993; Moore, 1993). In contrast, the monophyly of the six families included in clade D2 (Hispidoberycidae, Stephanoberycidae, Gibberichthyidae, Rondeletiidae, Barbourisiidae and Cetomimidae) is supported by previous morphological (Moore, 1993) and molecular studies (Near et al., 2013; Betancur-R et al., 2017), although Hispidoberycidae and Gibberichthyidae have never been used for molecular studies. In the present study, therefore, clade D2 is given an ordinal rank to be Stephanoberyciformes.

On the other hand, Melamphaidae was independently placed on a different lineage (clade K2) from other taxa of Beryciformes (sensu Nelson et al., 2016), and possesses 12 synapomorphies including three autapomorphies. Besides, the monophyly of Melamphaidae is also supported by both morphological and molecular studies (e.g., Zehren, 1979; Moore, 1993; Miya et al., 2005; Near et al., 2013; Betancur-R et al., 2017). Accordingly, clade K2 also should be given an ordinal rank to be Melamphaiformes (new name).

Berycidae was inferred to form a monophyletic group (clade N2) with many other taxa of "Berycida". Although clade N2 is consistent with the order Beryciformes defined by Johnson & Patterson (1993) (Table 3), this clade is unambiguously supported by only a single synapomorphy. In addition, the monophyly of Beryciformes (sensu Johnson & Patterson, 1993) has not been supported by many other morphological (e.g., Zehren, 1979; Stiassny & Moore, 1992; Moore, 1993) and molecular studies (e.g., Miya et al., 2005; Near et al., 2013; Betancur-R et al., 2017). On the other hand, clades O2 and T1 are consistent with Trachichthyiformes and Holocentriformes (sensu Nelson et al., 2016), respectively, which are supported by four synapomorphies including one autapomorphy, respectively. The monophyly of each order has been supported by other morphological (e.g., Zehren, 1979; Moore, 1993) and molecular studies (e.g., Miya et al., 2005; Near et al., 2013; Betancur-R et

al., 2017). Moreover, although clade O1 is supported by three unambiguous synapomorphies, an order including only Holocentridae and Berycidae has never been established in previous classification to date. Consequently, clades O2, T1 and T2 should be given ordinal ranks to be Trachichthyiformes, Holocentriformes and Beryciformes, respectively. As a result, these classification at order level proposed above well agrees with the theory of sequencing convention by Nelson (1973).

Stephanoberyciformes redefined in this study is consistent with the suborder Stephanoberycoidei (sensu Nelson et al., 2016), in which two superfamilies, Stephanoberycoidea (including Hispidoberycidae, Stephanoberycidae and Gibberichthyidae) and Cetomimoidea (Rondeletiidae, Barbourisiidae and Cetomimidae), were recognized by Nelson et al. (2016) (Table 3). In the cladogram of this study, Stephanoberyciformes (clade D2) is divided into clades E1 (including Barbourisiidae and Cetomimidae) and E2 (Hispidoberycidae, Stephanoberycidae, Gibberichthyidae and Rondeletiidae), which are supported by five and four unambiguous synapomorphies, respectively. Because these clades are morphologically well defined and separable from each other, they should be given taxonomic ranks. In this study, therefore, clades E1 and E2 are given subordinal names, Cetomimoidei and Stephanoberycoidei, respectively.

Trachichthyiformes was inferred to be divided into clades P1 (including Anoplogastridae and Diretmidae) and P2 (Anomalopidae, Monocentridae and Trachichthyidae) in this study. The familial compositions of clades P1 and P2 are congruent with the suborders Anoplogastroidei and Trachichthyoidei (sensu Nelson et al., 2016), respectively (Table 3). Therefore, clades P1 and P2 are given subordinal names Anoplogastroidei and Trachichthyoidei, respectively. This classification agrees with that in Nelson et al. (2016).

In this study, because all families were inferred to be monophyletic groups, no taxonomic changes are performed at familial level.

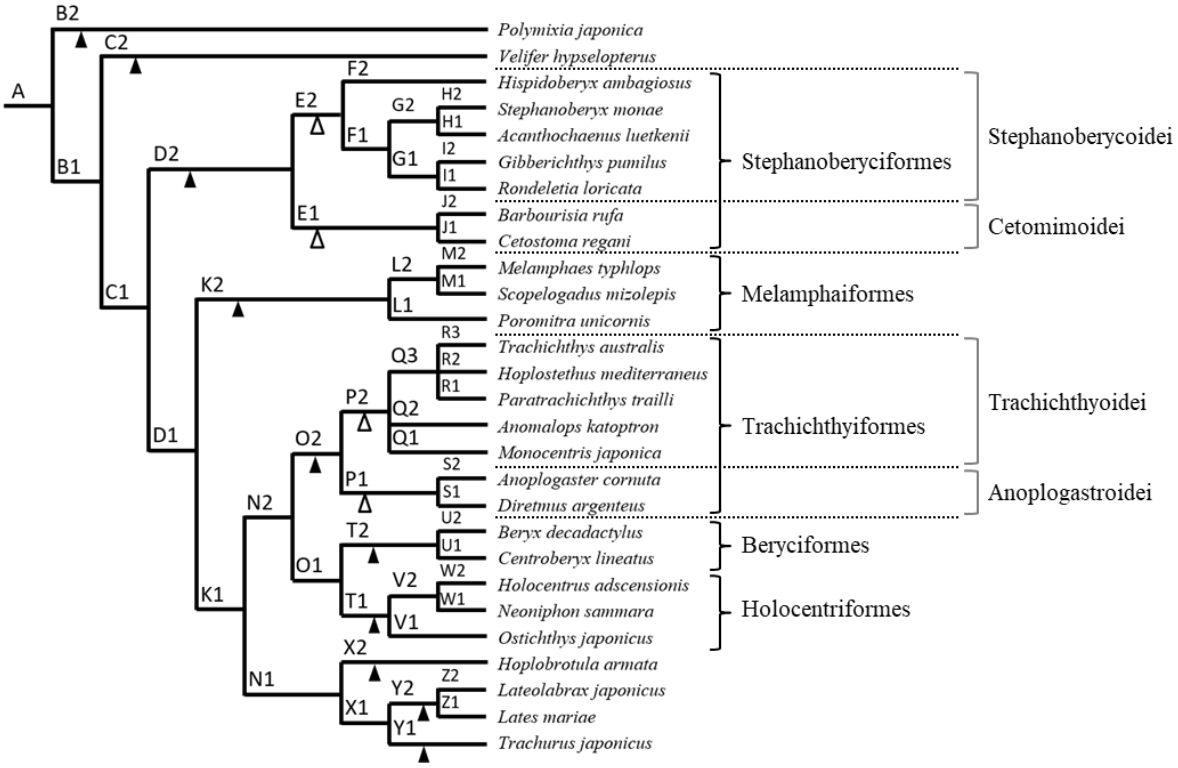

Figure 53. Phylogenetic relationships of *Hispidoberyx ambagiosus* and related taxa, with rankings at order (closed triangle) and suborder levels (open triangle).

6-2. New classification of *Hispidoberyx ambagiosus* and related taxa

A newly proposed classification of *Hispidoberyx ambagiosus* and its related taxa is shown below. In the proposed classification, Diagnosis and Remarks are given here only to Stephanoberyciformes and contained taxa including *H. ambagiosus*.

Series “Berycida” (sensu Nelson et al., 2016)

Order Stephanoberyciformes (new usage)

Suborder Stephanoberycoidei (new usage)

Family Gibberichthyidae Parr, 1933

Family Hispidoberycidae Kotlyar, 1981

Family Rondeletiidae Goode & Bean, 1895

Family Stephanoberycidae Gill, 1844

Suborder Cetomimoidei (new usage)

Family Barbourisiidae Parr, 1945

Family Cetomimidae Goode & Bean, 1895

Order Melamphaiformes (new name)

Family Melamphaidae Gill, 1893

Order Beryciformes (new usage)

Family Berycidae Lowe, 1839

Order Trachichthyiformes sensu Nelson et al., 2016

Suborder Anoplogastroidei sensu Nelson et al., 2016

Family Anoplogastridae Gill, 1893

Family Diretmidae Gill, 1893

Suborder Trachichthyoidei sensu Nelson et al., 2016

Family Anomalopidae Gill, 1889

Family Monocentridae Gill, 1859

Family Trachichthyidae Bleeker, 1856

Order Holocentriformes sensu Nelson et al., 2016

Family Holocentridae Bonaparte, 1833

Key to orders of the series "Berycida" (sensu Nelson et al., 2016)

1a. Spiny portion of dorsal fin with 10–13 spines and its base much longer than that of soft rayed portion; anal fin with four spines, the third spine often longest . . . . . Holocentriformes

1b. Spiny portion of dorsal fin with 1–10 spines and its base shorter than that of soft rayed portion, or dorsal fin spines absent; anal fin with 1–4 spines, the last spine often longest, or anal-fin spines absent 2

2a. Two supramaxillae present; pelvic fin with one spine and 7–13 soft rays . . . . . Beryciformes

2b. One supramaxilla present or absent; pelvic fin with one spine and 3–7 soft rays, or pelvic-fin spine absent 3

3a. Abdominal scutes usually present; 1–2 supraneurals present . . . . . Trachichthyiformes

3b. Abdominal scutes absent; 3–8 supraneurals present or absent 4

4a. Dorsal fin located much anterior to anal fin; sensory structures in form of epidermal embossed lines present on head . . . . . Melamphaiformes

4b. Dorsal fin located on almost opposite side of anal fin; sensory structures in form of epidermal embossed lines absent on head . . . . . Stephanoberyciformes

Order Stephanoberyciformes (new usage)

Diagnosis. Subocular shelf absent; orbitosphenoid absent; exoccipital condyles on both sides detached; one supramaxilla present or absent; ethmo-maxillary and palato-premaxillary

ligaments, when present, partially confluent; temporal portion of main trunk canal on supracleithrum absent; neural spine of first abdominal vertebra fused with centrum; abdominal hemal arches absent; second ventral procurrent caudal-fin ray not shortened proximally; thin and band-like unnamed muscle on lateral portion of supracarinalis anterior present (absent in stephanoberycids); ossification of sclera absent; Jakubowski's organ absent; papillate lateral line system on trunk present; dorsal fin located on almost opposite side of anal fin.

Remarks. This order comprises two suborders, Stephanoberycoidei with four families and Cetomimoidei with two families.

Although many previous morphological studies included Melamphaidae in this group [e.g., Stephanoberycoidei (sensu Moore, 1993) and Stephanoberyciformes (sensu Johnson & Patterson, 1993)], the analysis in this study inferred the family to be placed on the different lineage from this order. The exclusion of Melamphaidae from this group is supported by many molecular studies (e.g., Near et al., 2013; Betancur-R et al., 2017). As Moore's (1993) cladogram placed Melamphaidae at the most basal position among his stephanoberycoids (Fig. 51B), the monophyly of the remaining taxa (= Stephanoberyciformes defined by the present study) is also supported by his study.

Although the six families included in this order represent large morphological diversity, they share unique characters such as the thin and band-like unnamed muscle on the lateral portion of the supracarinalis anterior (except for stephanoberycids), and the papillate lateral line system on the trunk.

Suborder Stephanoberycoidei (new usage)

Diagnosis. Y-shaped pattern of frontal ridges present (absent in Rondeletiidae); basisphenoid present; ectopterygoid teeth absent; dorsal, anal and pelvic-fin spines present or absent;

separated tendon on posteroventral portion of section A2 inserting onto quadrate distinctly present; hyohyoides inferioris present; Tominaga's organ present; dermal canal on trunk absent; 24–35 total vertebrae. Meristic counts from Paxton et al. (2001), Kotlyar (2004a–c) and Merrett & Moore (2005).

Remarks. This suborder includes four families, Gibberichthyidae, Hispidoberycidae, Rondeletiidae and Stephanoberycidae.

The families included in this suborder share a remarkable autapomorphic character, the presence of Tominaga's organ, with the absence of the organ in stephanoberycid *Acanthochaenus luetkenii* as a reversal character. Although two stephanoberycids, *Abyssoberyx levisquamosus* Merrett & Moore, 2005 and *Malacosarcus macrostoma* (Günther, 1878) were not examined in this study, the absence of Tominaga's organ in the former species was reported by Paxton et al. (2001). The condition in the latter species is unknown.

This suborder is clearly separable from Cetomimoidei by the absence of the dermal canal on the trunk and 24–35 total vertebrae (vs. present and 38–59 in cetomimoids).

Suborder Cetomimoidei (new usage)

Diagnosis. Y-shaped pattern of frontal ridges absent; basisphenoid absent; ectopterygoid teeth present; dorsal, anal and pelvic-fin spines absent; separated tendon on posteroventral portion of section A2 inserting onto quadrate absent; hyohyoides inferioris absent; Tominaga's organ absent; dermal canal on trunk present; 38–59 total vertebrae. Meristic counts from Paxton (1989) and Paxton et al. (2001).

Remarks. This suborder consists of two families, Barbourisiidae and Cetomimidae.

Although previous classifications traditionally included so-called "whale fishes", Rondeletiidae, Barbourisiidae and Cetomimidae, into a single taxonomic group (e.g., Nelson, 1976, 1984, 2006; Nelson et al., 2016), the analysis in this study inferred that Rondeletiidae is

included in Stephanoberycoidei as a sister family of Gibberichthyidae. The non-monophyly of "whale fishes" and the sister relationship of Rondeletiidae and Gibberichthyidae are also supported by Paxton et al. (2001).

This suborder is clearly distinguishable from Stephanoberycoidei by the presence of the dermal canal on the trunk and 38–59 total vertebrae (vs. absent and 24–35 in stephanoberycoids).

VII. General discussion

7-1. Morphological specificity of *Hispidoberyx ambagiosus*

In the original description of *Hispidoberyx ambagiosus* by Kotlyar (1981), this species was described as a new species belonging to a new genus and family based on its unique combination of morphological characters different from all other beryciform families. However, although the present study conducted detailed morphological examinations of *H. ambagiosus* including osteology, myology, and other internal and external characters, only one autapomorphy of the species among ingroups was found. The hyohyoidei abductores section 2 originates from a raphe on the midline was considered to be an autapomorphy of the species (see "Other variations" in the section on the ventral muscle of the head), but such a condition in the muscle is recognized in various other groups [e.g., scorpaeniforms (Yabe, 1985), gadiforms (Endo, 2002) and perciform uranoscopids (Vilasri, 2013)]; and thus it cannot be a rare condition in acanthomorphs. On the other hand, although *H. ambagiosus* was inferred to have two unambiguous synapomorphies (character 39-1, pelvic-fin spine present; character 61-2, hyohyoides inferioris originating from raphe on midline), they are homoplasious among ingroups and then cannot strongly characterize the species.

Moore (1993) mentioned two characters as synapomorphies of Hispidoberycidae, i.e., a very long and unusually stout spine on the opercle, and an extremely spinulose ornamentation to all dermal bones of the head. The opercular spine of *H. ambagiosus* is particularly long and stout among Berycida (sensu Nelson et al., 2016), but such strong opercular spines comparable with that of *H. ambagiosus* are present in other taxa of "Berycida" (e.g., holocentrids and trachichthyid *Paratrachichthys trailli*). In addition, stephanoberycids and gibberichthyids in Stephanoberyciformes also have a distinct opercular spine even though it is smaller than that of *H. ambagiosus*. Regarding an extremely spinulose ornamentation to all dermal bones of the head, the density and extent of spines of the head in *H. ambagiosus* are certainly remarkable among "Berycida". Nevertheless, such spinulose ornamentation to

dermal bones of the head is also observed in other taxa of "Berycida" (e.g., Anoplogastridae, Monocentridae, trachichthyid *Trachichthys australis*). Among Stephanoberyciformes, stephanoberycids and gibberichthyids also possess sparse spinulation on dermal bones of the head. Accordingly, these features cannot strongly characterize *H. ambagiosus*.

On the other hand, many diagnostic characters of *Hispidoberyx ambagiosus* were inferred to be primitive among Stephanoberyciformes, i.e., the presence of vomerine teeth (character 5-0), the presence of palatine teeth (character 14-0) (according to DELTRAN), the presence of dorsal-fin spines (character 46-1), the presence of anal-fin spines (character 48-1) and the presence of the trunk canal supported by scales (character 80-0). Therefore, it can be noted that *H. ambagiosus* is a species retaining many primitive characters among Stephanoberyciformes. Among Cetomimoidei, Barbourisiidae is considered to be more primitive taxon than Cetomimidae based on the presence of the pelvic fins and pleural ribs, elongated gill rakers, and tiny, embedded scales on the head and body (vs. absent, absent or modified, and absent, respectively, in Cetomimidae) (Paxton, 1989; Fujii et al., 2007). Kotlyar (1991a) mentioned that the external appearance of *H. ambagiosus* resembles that of *Barbourisia rufa*. Such a similarity between these species is considered to be caused by their retention of primitive features in each suborder of Stephanoberyciformes.

Hispidoberyx ambagiosus has an impressive bright red coloration when fresh as well as *Barbourisia rufa* (Fig. 54). Although the body coloration was not used for the analysis in this study, it can be roughly divided into the following three categories among stephanoberyciforms examined in this study: (I) reddish colors; (II) brownish colors; and (III) greyish to blackish colors (Table 4). Character evolutions of the body coloration estimated by using MacClade version 4.0 (Maddison & Maddison, 2000) with a character setting as "ordered" revealed that the reddish body color is primitive among stephanoberyciforms (Fig. 55).

Among Stephanoberyciformes, *Hispidoberyx ambagiosus* has the dorsal fin situated on the

relatively anterior part of the body when compared with the other stephanoberyciform taxa in which the dorsal fin is situated on the almost opposite side of the anal fin (Fig. 54). Although the position of the dorsal-fin origin (i.e., the position of insertion of the first dorsal-fin proximal pterygiophore) was not used for the analysis (see "Other variations" in the section on the axial skeleton and median-fin supports), the posteriorly placed dorsal fin is considered to be derived condition among entire ingroups because all outgroups have the dorsal fin positioned far anterior to the anal fin. In addition, a fossil species of Barbourisiidae, *Miobarbourisia aomori* Fujii, Uyeno & Shimaguchi, 2007 is known to have the dorsal fin positioned far anterior to the anal fin (Fujii et al., 2007). This fact suggests that the common ancestor of stephanoberyciforms also possessed the dorsal fin located anterior to the anal fin and that *H. ambagiosus* is solely retaining the primitive condition among extant stephanoberyciforms.

As a result, it was revealed that *Hispidoberyx ambagiosus* retains many primitive characters among Stephanoberyciformes, although it also has several derived characters which cannot strongly show peculiarity of the species.

Table 4. Fresh body colorations of stephanoberyciforms examined in this study.

Taxa	Categories designated in this study	Fresh body colorations and references
Hispidoberyx ambagiosus	I	bright red (Kotlyar, 1981; this study); pink (Yang et al., 1988)
Stephanoberyx monae	II	brown* (Mincarone et al., 2014)
Acanthochaenus luetkenii	III	dark charcoal to grey (Stewart, 2015)
Gibberichthys pumilus	III	black (de Sylva & Eschmeyer, 1977)
Rondeletia loricata	I, II	dark red (Okamura, 1985; Amaoka, 1995); orange-brown (Paxton, 2008); dark brown (Paxton, 2015)
Barbourisia rufa	I	bright red (Okamura, 1985); reddish-orange (Amaoka, 1995); orange-red (Paxton, 2008)
Cetostoma regani	I, III	reddish orange (Amaoka, 1983); black (Paxton, 1989)

* Not documented, but confirmed from color photograph of fresh specimen.

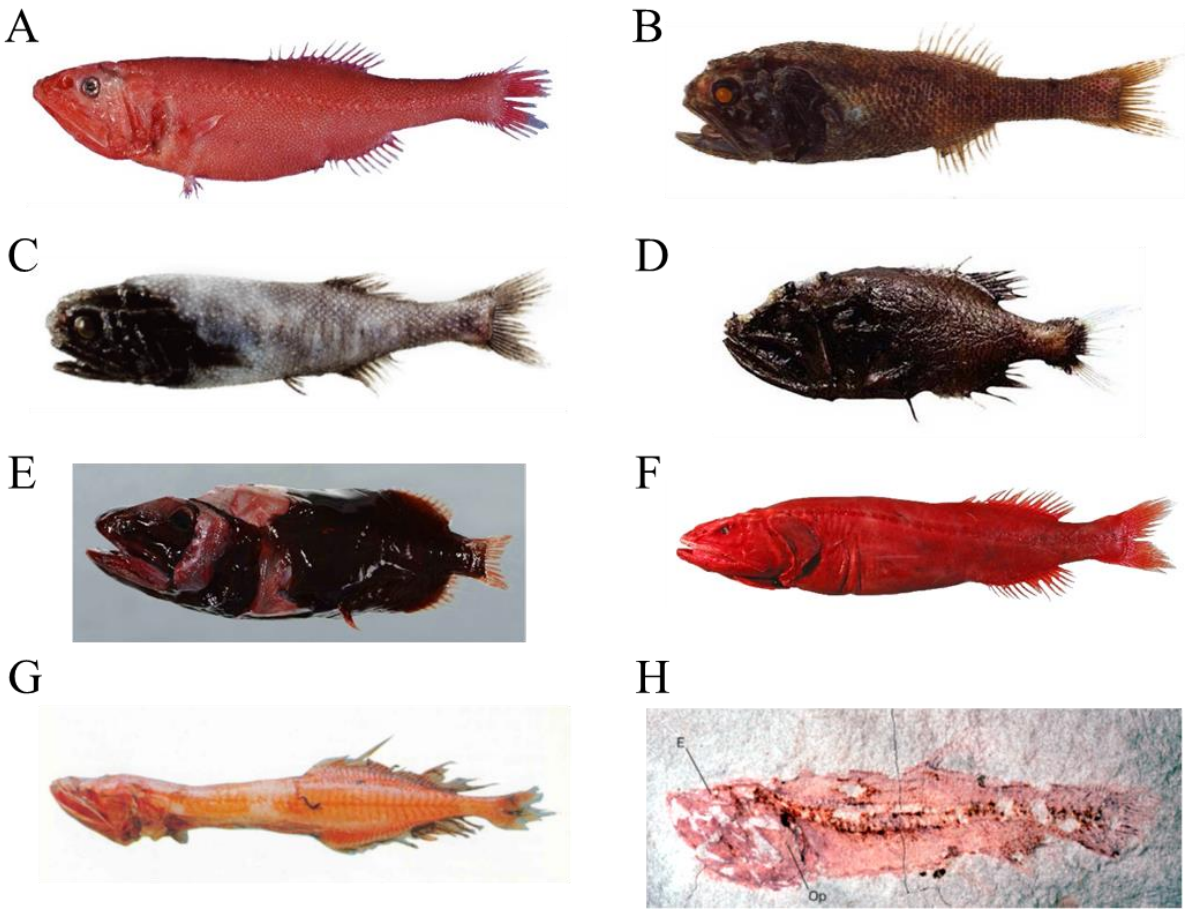

Figure 54. Fresh specimens of extant species (A–G) and fossil specimen of extinct species (H) of Stephanoberyciformes. A, *Hispidoberyx ambagiosus*, HUMZ 193967, 173.9 mm SL; B, *Stephanoberyx monae*, MNRJ 36369, 102 mm SL; C, *Acanthochaenus luetkenii*, MNRJ 36417, 97 mm SL; D, *Gibberichthys pumilus*, NSMT-P 40240, 74.0 mm SL; E, *Rondeletia loricata*, AMS I.42718-001, 105 mm SL; F, *Barbourisia rufa*, HUMZ 191050, 324.5 mm SL; G, *Cetostoma regani*, HUMZ 78240, 166 mm SL; H, *Miobarbourisia aomori*, AOPM No. 491, 74 mm SL. B and C from Mincarone et al. (2014), D from Uyeno & Sato (1983), E from Paxton (2015), and H from Fujii et al. (2007).

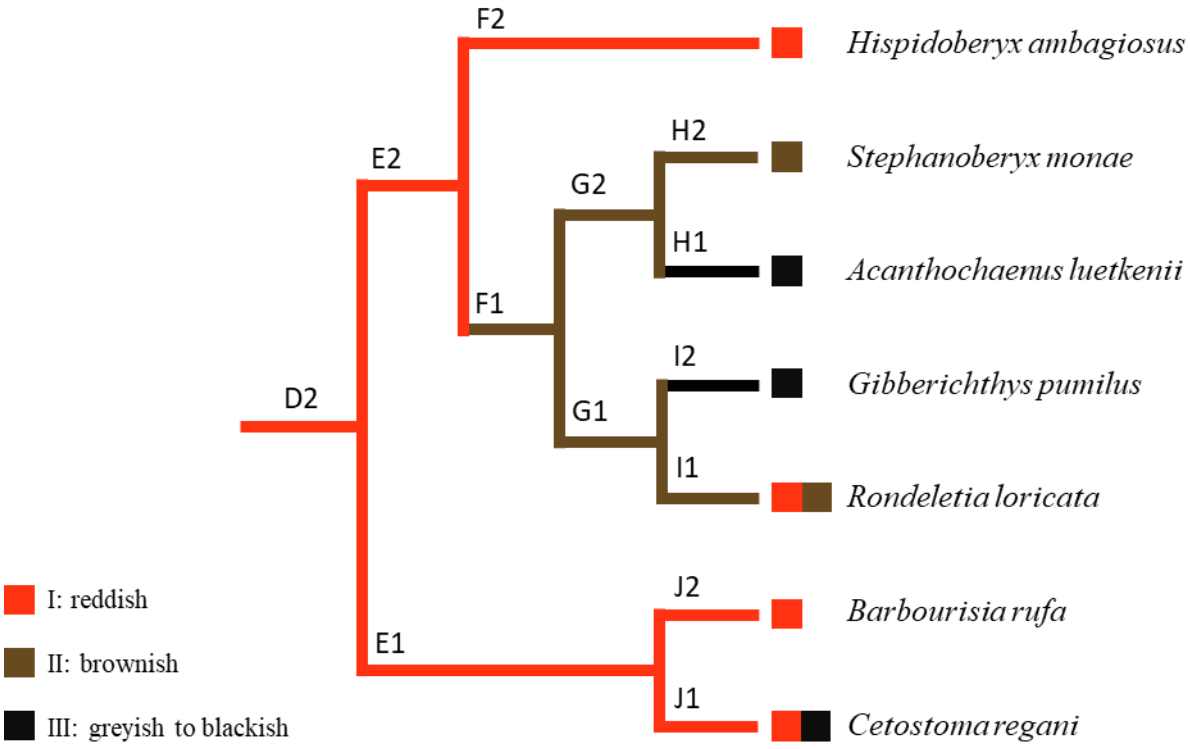

Figure 55. Character evolution of body coloration among Stephanoberyciformes.

7-2. Inhabiting depths of stephanoberyciforms

Hispidoberyx ambagiosus is a deep-sea fish collected from depths of 560–1360 m (Kotlyar, 2004a; Paxton et al., 2001; this study). Although the other stephanoberyciforms are also deep-sea taxa usually known from depths of 200 m or more, their depth ranges are very wide. For example, some specimens of *Rondeletia loricata*, *Barbourisia rufa* and *Cetostoma regani* are known from depths of ca. 100 m at shallowest (Paxton, 1989; Kotlyar, 1995, 1996a), whereas stephanoberycid *Acanthochaenus luetkenii* has been reported from depth of 5400 m at deepest (Mincarone et al., 2014). Previously reported inhabiting depths of stephanoberyciforms used in this study are shown in Table 5. For estimation of the evolutions of inhabiting depth in Stephanoberyciformes, inhabiting depths are divided into the following 11 categories in this study: (I) from 0 to 499 m depth; (II) from 500 to 999 m depth; (III) from 1000 to 1499 m depth; (IV) from 1500 to 1999 m depth; (V) from 2000 to 2499 m depth; (VI) from 2500 to 2999 m depth; (VII) from 3000 to 3499 m depth; (VIII) from 3500 to 3999 m depth; (IX) from 4000 to 4499 m depth; (X) from 4500 to 4999 m depth; and (XI) from 5000 to 5499 m depth. Then, the evolutions of inhabiting depth were estimated on the inferred cladogram of stephanoberyciforms following the zoogeographical methodology shown by Sawada (1982). As the result, the inhabiting depth of the common ancestor of stephanoberyciforms was inferred to be 1000–1499 m depth (Fig. 56). Accordingly, it is assumed that *H. ambagiosus*, known from 560–1360 m depth, retains a primitive feature among stephanoberyciforms also on the ecological aspect, distributing in the similar depth with the ancestor and having additional adaptation to shallower waters.

Table 5. Inhabiting depths of stephanoberyciforms examined in this study.

Taxa	Categories designated in this study	Inhabiting depths (m) and references
Hispidoberyx ambagiosus	II–III	560–1360 (Paxton et al., 2001; Kotlyar, 2004a; this study)
Stephanoberyx monae	II–X	945–4777 (Kotlyar, 2004b; Mincarone et al., 2014)
Acanthochaenus luetkenii	III–XI	1183–5400 (Kotlyar, 2004b; Mincarone et al., 2014)
Gibberichthys pumilus	I–IV	320–1929 (Kotlyar, 2004c; Mincarone et al., 2014)
Rondeletia loricata	I–V	100–2350 (Kotlyar, 1996a; Paxton et al., 2001)
Barbourisia rufa	I–V	120–2000 (Kotlyar, 1995; Paxton et al., 2001)
Cetostoma regani	I–V	110–2250 (Paxton, 1986, 1989)

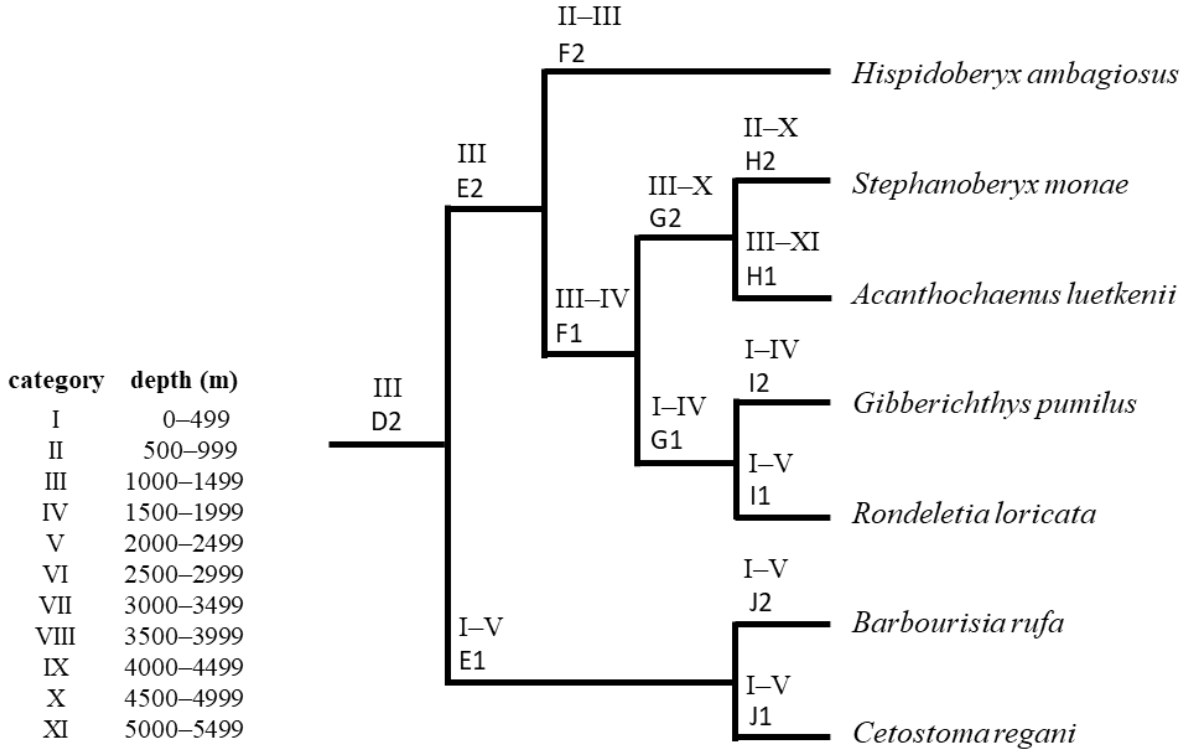

Figure 56. Character evolution of inhabiting depth among Stephanoberyciformes.

7-3. Evolution of Tominaga's organ in Stephanoberycoidei

Among Stephanoberyciformes, four families in Stephanoberycoidei, Hispidoberycidae, Stephanoberycidae (only in *Stephanoberyx monae*), Gibberichthyidae and Rondeletiidae, share a unique secretory organ called as "Tominaga's organ". However, Tominaga's organ in each family exhibits different morphological features, respectively (Paxton et al., 2001; this study) (Fig. 57). In this section, evolutions of several characters on Tominaga's organ are estimated on the inferred cladogram of stephanoberycoids by using MacClade version 4.0 (Maddison & Maddison, 2000) to reveal the process of diversification of Tominaga's organ.

Number of lobes of organ. Tominaga's organ in *Hispidoberyx ambagiosus* has no distinct lobes as well as *Stephanoberyx monae* and *Gibberichthys pumilus*, whereas the organ in *Rondeletia loricata* is divided into lateral and medial lobes (see also Paxton et al., 2001 for *G. pumilus* and *R. loricata*). As the result of the estimation, the common ancestor of stephanoberycoids was inferred to have the organ with a single lobe, while the organ with two lobes in *R. loricata* was inferred to be a derived condition among the suborder (Fig. 58A).

Position and presence or absence of external openings. In *Hispidoberyx ambagiosus*, Tominaga's organ posteriorly has a long duct which reaches the posteroventral portion of the eye and opens externally. On the other hand, Tominaga's organ in *Stephanoberyx monae* and *Rondeletia loricata* has external openings to the posterior portion of the nasal rosette, while the organ in *Gibberichthys pumilus* has no external openings (see also Paxton et al., 2001 for *R. loricata* and *G. pumilus*). As the result of estimation using a character setting as "unordered", although the absence of external openings in *G. pumilus* was inferred to be a derived condition among stephanoberycoids, the condition in the common ancestor of stephanoberycoids was not specified whether the presence of external opening to the posterior portion of the eye or the posterior portion of the nasal rosette (Fig. 58B). However, it is apparent that the common ancestor had the openings.

In *H. ambagiosus*, several small pores are observed on the posterior floor of the nasal

cavity posterior to the nasal rosette. Although blind pockets posteriorly extend from these pores, they do not reach Tominaga's organ. Such a condition in *H. ambagiosus* can be assumed to be preliminary or vestigial conditions in *S. monae* and *R. loricata*, i.e., the organ with eternal openings to the posterior portion of the nasal rosette.

Size of organ. *Hispidoberyx ambagiosus*, *Gibberichthys pumilus* and *Rondeletia loricata* have well developed Tominaga's organ (Paxton et al., 2001; this study), whereas *Stephanoberyx monae* has an apparently smaller organ than that in the former. The estimation of character evolutions revealed that the common ancestor of stephanoberycoids has a well developed organ and the smaller size of the organ in *S. monae* is a derived condition among the suborder, according to ACCTRAN and DELTRAN having different character evolutions, respectively (Fig. 58C, D). Because other stephanoberycid species, *Acanthochaenus luetkenii* and *Abyssoberyx levisquamosus* are known to lack the organ (Paxton et al., 2001) (unknown in *Malacosarcus macrostoma*), this family is considered to have a reductive trend of Tominaga's organ. Two examined stephanoberycids, *S. monae* and *A. luetkenii*, were revealed to exclusively have the other enigmatic secretory organ which is tentatively called as "prepectoral organ" in this study (unknown in *A. levisquamosus* and *M. macrostoma*). Besides, stephanoberycids are known to inhabit particularly deep waters among stephanoberyciform families (Table 5). These features of Stephanoberycidae might be related with the reductive trend of Tominaga's organ in the family.

As the result, Tominaga's organ in the common ancestor of stephanoberycoids was estimated to be characterized by a single lobe, the presence of some external openings and well developed size of the organ. Because *Hispidoberyx ambagiosus* also has these characters with the common ancestor, the species is considered to retain primitive conditions of Tominaga's organ among Stephanoberycoidei.

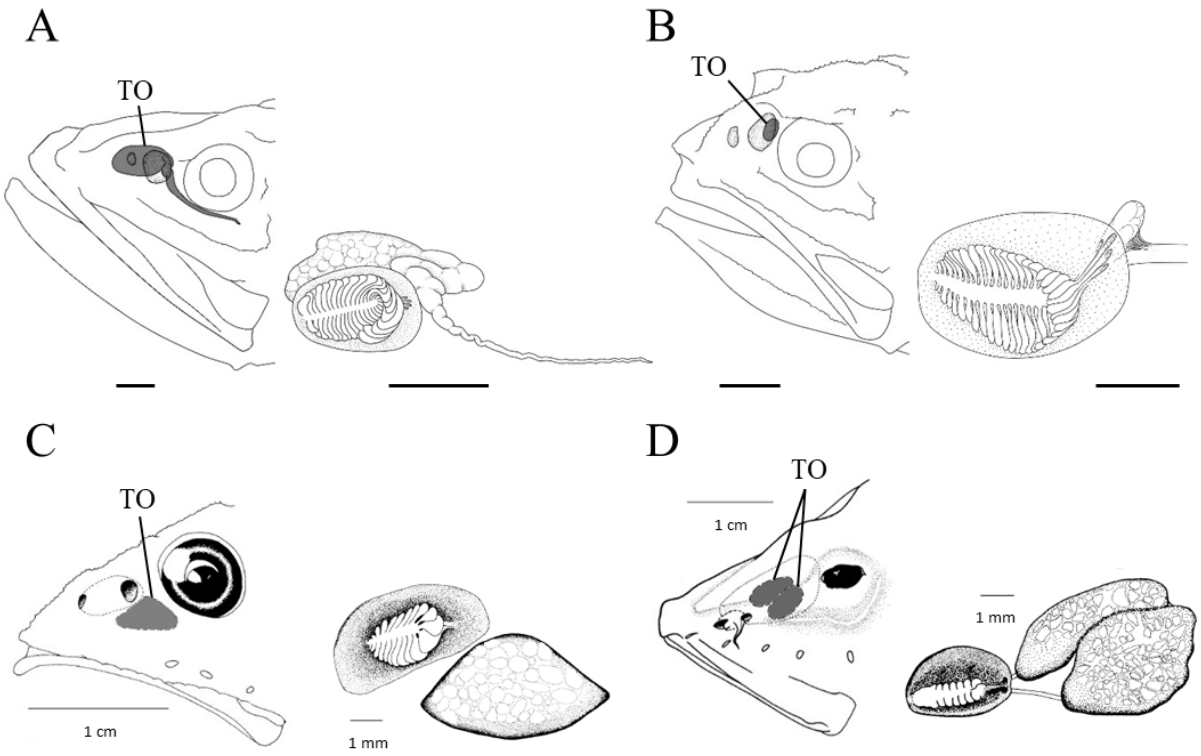

Figure 57. Position (left) and detail (right) of Tominaga's organ in (A) *Hispidoberyx ambagiosus*, (B) *Stephanoberyx monae*, (C) *Gibberichthys pumilus* and (D) *Rondeletia loricata*. TO, Tominaga's organ. C and D modified from Paxton et al. (2001). Scales in A and B indicate 5 mm.

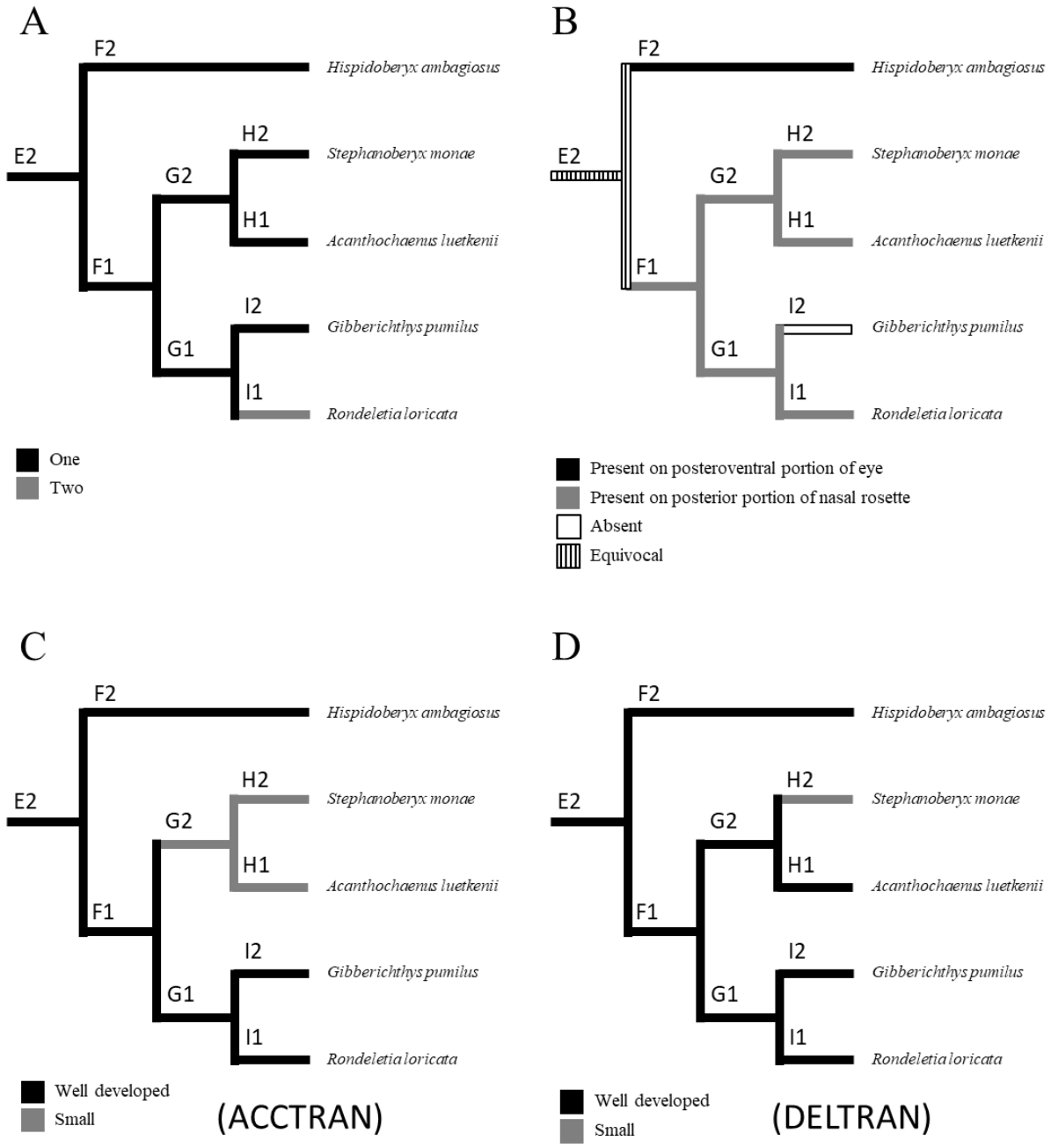

Figure 58. Character evolutions of Tominaga's organ among Stephanoberycoidei. A, number of lobes of organ; B, position and presence or absence of external openings; C and D, size of organ

7-4. Conclusion

As the result of the phylogenetic analysis in this study, *Hispidoberyx ambagiosus* was inferred to be included in Stephanoberyciformes which is strongly supported by the following five unambiguous synapomorphies including three autapomorphies (shown by asterisks): exoccipital condyles on both sides detached (character 11-1*); ethmo-maxillary and palato-premaxillary ligaments partially confluent (character 17-1); abdominal hemal arches absent (character 42-0); unnamed muscle on lateral portion of supracarinalis anterior thin and band-like (character 72-1*); and papillate lateral line system on trunk present (character 79-1*). In this order, this species was placed in Stephanoberycoidei well supported by four unambiguous synapomorphies including three autapomorphies: Y-shaped pattern of frontal ridges present (character 8-1*); lateral pelvic radials absent (character 40-1); separated tendon on posteroventral portion of section A2 inserting onto quadrate distinct (character 58-1*); and Tominaga's organ present (character 74-1*). Moreover, the analysis inferred that this species has two unambiguous apomorphies, pelvic-fin spine present (character 39-1) and hyohyoides inferioris originating from raphe on midline (character 61-2), as homoplasious characters among ingroups. Although the present study found several new morphological characters of *H. ambagiosus*, only one of them was assumed to be an autapomorphy of the species (hyohyoides inferioris originating from raphe on midline), while many peculiar characters of the species were inferred to be synapomorphies of Stephanoberyciformes or Stephanoberycoidei as mentioned above. Therefore, although *H. ambagiosus* has many derived characters, they cannot strongly show peculiarity of the species.

On the other hand, the analysis inferred that many diagnostic characters of *Hispidoberyx ambagiosus* (i.e., the presence of vomerine and palatine teeth, dorsal and anal-fin spines, and trunk canal supported by scales) are primitive among Stephanoberyciformes. In addition, two characters of the species not included in the analysis, the reddish body coloration and dorsal fin located anterior to the anal fin, were also estimated to be primitive condition among the

order. Furthermore, the inhabiting depth of the species was also inferred to retain that of the common ancestor of stephanoberyciforms with additional adaptation to shallower waters. Regarding a stephanoberycoid unique synapomorphy, Tominaga's organ, it was assumed that *H. ambagiosus* retains primitive conditions of the organ (a single lobe, the presence of external openings and well developed size of the organ) among the suborder.

Finally, it is regarded in this study that *Hispidoberyx ambagiosus* is a unique species which possesses many peculiar derived characters shared with other stephanoberyciforms and stephanoberycoids, but also retains many primitive features and has less distinctive derived characters among the suborder. Accordingly, taking into account the phylogenetic position of the species which was inferred to be branched off from the other stephanoberycoids at first, it is concluded that *H. ambagiosus* is a species which morphologically (and possibly ecologically) less evolved from the common ancestor of stephanoberycoids.

VIII. Summary

The present study was carried out to describe osteology, myology and other morphology of beryciform fish *Hispidoberyx ambagiosus* in detail, to reconstruct the phylogenetic relationships of the species and related taxa, and to reassess the phylogenetic position of the species based on the phylogenetic relationships. The results of this study are summarized below.

1. After comparative anatomy of *Hispidoberyx ambagiosus* and its related taxa, osteology, myology and some other internal and external morphology of the species were described in detail.
2. As the result of the phylogenetic analysis based on characters in 80 transformation series, three most parsimonious trees were obtained.
3. *Hispidoberyx ambagiosus* was inferred to form a monophyletic group together with Stephanoberycidae, Gibberichthyidae, Rondeletiidae, Barbourisiidae and Cetomimidae. In this clade, this species was inferred to be a sister taxon of a monophyletic group formed by the former three families.
4. The series Berycida (sensu Nelson et al., 2016) was inferred to be non-monophyletic. In addition, among three orders recognized in Berycida by Nelson et al. (2016), Beryciformes in which *Hispidoberyx ambagiosus* had been included was also inferred to be non-monophyletic.
5. New classification of *Hispidoberyx ambagiosus* and its related taxa at order to family levels was proposed based on the inferred relationships as below.

Series “Berycida” (sensu Nelson et al., 2016)

Order Stephanoberyciformes (new usage)

Suborder Stephanoberycoidei (new usage)

Family Gibberichthyidae Parr, 1933

Family Hispidoberycidae Kotlyar, 1981

Family Rondeletiidae Goode & Bean, 1895

Family Stephanoberycidae Gill, 1844

Suborder Cetomimoidei (new usage)

Family Barbourisiidae Parr, 1945

Family Cetomimidae Goode & Bean, 1895

Order Melamphaiformes (new name)

Family Melamphaidae Gill, 1893

Order Beryciformes (new usage)

Family Berycidae Lowe, 1839

Order Trachichthyiformes sensu Nelson et al., 2016

Suborder Anoplogastroidei sensu Nelson et al., 2016

Family Anoplogastridae Gill, 1893

Family Diretmidae Gill, 1893

Suborder Trachichthyoidei sensu Nelson et al., 2016

Family Anomalopidae Gill, 1889

Family Monocentridae Gill, 1859

Family Trachichthyidae Bleeker, 1856

Order Holocentriformes sensu Nelson et al., 2016

Family Holocentridae Bonaparte, 1833

6. The present study found only one autapomorphy of *Hispidoberyx ambagiosus*, while many peculiar characters of the species were inferred to be synapomorphies of Stephanoberyciformes or Stephanoberycoidei.
7. It was inferred that *Hispidoberyx ambagiosus* retains many primitive morphological

characters among Stephanoberyciformes and Stephanoberycoidei. The inhabiting depth of the species was also inferred to retain that of the common ancestor of stephanoberyciforms with additional adaptation to shallower waters.

8. It was concluded that *Hispidoberyx ambagiosus* is : 1) a unique species which possesses many peculiar derived characters shared with other stephanoberyciforms or stephanoberycoids; 2) a species which also retains many primitive features and has less distinctive derived characters among the order and suborder; and 3) a species which morphologically (and possibly ecologically) less evolved from the common ancestor of stephanoberycoids.

IX. Acknowledgments

I am especially grateful to Prof. S. Wada (Faculty of Fisheries Sciences, Hokkaido University) for his critical reading of the manuscript and valuable advice. I also sincerely thanks to Prof. H. Imamura, Assoc. Prof. T. Kawai and Assist. Prof. F. Tashiro for their guidance during this study and critical reading of the manuscript. My special thanks go to Profs. Emer. K. Amaoka, K. Nakaya and M. Yabe for their helpful advices and encouragements.

I deeply appreciate following persons for providing specimens: M. McGrouther and A. Hay (AMS); J. Maclaine (BMNH); H. Senou (KPM); G. Shinohara (NSMT); and J. Williams (USNM). My sincere thanks go to E. Vasil'eva (ZMMU) for her kind assistance during my visit to ZMMU. I am also grateful to members of JDSTA (Japan Deep Sea Trawlers Association), OFCF (Overseas Fishery Cooperation Foundation of Japan) and RIMF (Research Institute for Marine Fisheries, Indonesia), and the crew of R/V *Baruna Jaya* IV, for collecting specimens of *Hispidoberyx ambagiosus* examined in this study.

I express special thanks to my parents for their financial supports and encouragements, and all members of Laboratory of Marine Biology and Biodiversity (Systematic Ichthyology), Hokkaido University for their kind advices and assistances.

X. References

Amaoka, K. (1983) 77 *Cetostoma regani* Zugmayer. *In*: Amaoka, K., Nakaya, K., Araya, H. & Yasui, T. (Eds.), *Fishes from the north-eastern Sea of Japan and the Okhotsk Sea off Hokkaido.* Japan Fisheries Resource Conservation Association, Tokyo, pp. 124–125.

Amaoka, K. (1995) Barbourisiidae, Rondeletiidae. *In*: Okamura, O., Amaoka, K., Takeda, M., Yano, K., Okada, K. & Chikuni, S. (Eds.), *Fishes collected by the R/V Shinkai Maru around Greenland*. Japan Marine Fishery Resources Research Center, Tokyo, pp. 148–149.

Betancur-R, R., Broughton, R.E., Wiley, E.O., Carpenter, K., Lopez, J.A., Li, C., Holcroft, N.I., Arcila, D., Sanciangco, M., Cureton, J.C. II, Zhang, F., Buser, T., Campbell, M.A., Ballesteros, J.A., Roa-Varon, A., Willis, S., Borden, W.C., Rowley, T., Reneau, P.C., Hough, D.J., Lu, G., Grande, T., Arratia, G. & Ortí, G. (2013) The tree of life and a new classification of bony fishes. *PLOS Currents Tree of Life*, 2013 Apr 18, 1st Edition. Available from: http://currents.plos.org/treeoflife/index.html%3Fp=4341.html (accessed 9 December 2019)

Betancur-R, R., Wiley, E.O., Arratia, G., Acero, A., Bailly, N., Miya, M., Lecointre, G. & Ortí, G. (2017) Phylogenetic classification of bony fishes. *BMC Evolutionary Biology*, 17, 162.

Chen, W.-J., Santini, F., Carnevale, G., Chen, J.-N., Liu, S.-H., Lavoué, S. & Mayden, R.L. (2014) New insights on early evolution of spiny-rayed fishes (Teleostei: Acanthomorpha). *Frontiers in Marine Science*, 1, 1–17.

Davesne, D., Gallut, C., Barriel, V., Janvier, P., Lecointre, G. & Otero, O. (2016) The phylogenetic intrarelationships of spiny-rayed fishes (Acanthomorpha, Teleostei, Actinopterygii): fossil taxa increase the congruence of morphology with molecular data. *Frontiers in Ecology and Evolution*, 4, 129.

de Pinna, M.C.C. (1996) Teleostean monophyly. *In*: Stiassny, M.L.J., Parenti, L.R. & Johnson,

G.D. (Eds.), *Interrelationships of Fishes*. Academic Press, San Diego, pp. 147–162.

de Sylva, D.P. & Eschmeyer, W.N. (1977) Systematics and biology of the deep-sea fish family Gibberichthyidae, a senior synonym of the family Kasidoroidae. *Proceedings of the California Academy of Sciences, 4th series*, 41, 215–231.

Dornburg, A., Townsend, J.P., Brooks, W., Spriggs, E., Eytan, R.I., Moore, J.A., Wainwright, P.C., Lemmon, A., Lemmon, E.M. & Near, T.J. (2017) New insights on the sister lineage of percomorph fishes with an anchored hybrid enrichment dataset. *Molecular Phylogenetics and Evolution*, 110, 27–38.

Ebeling, A.W. & Weed, W.H. III (1973) Order Xenoberyces (Stephanoberyciformes). *In*: Cohen, D.M. (Ed.), *Memoir Sears Foundation for Marine Research, number 1. Fishes of the Western North Atlantic, part 6*. Sears Foundation for Marine Research, Yale University, New Haven, pp. 397–478.

Endo, H. (2002) Phylogeny of the order Gadiformes (Teleostei, Paracanthopterygii). *Memoirs of the Graduate School of Fisheries Science, Hokkaido University*, 49, 75–149.

Farris, J.A. (1970) Method for computing Wagner trees. *Systematic Zoology*, 19, 83–92.

Fitch, W.M. (1971) Toward defining the course of evolution: minimal change for a specific tree topology. *Systematic Zoology*, 20, 406–416.

Fricke, R. & Eschmeyer, W.N. (2019) A guide to fish collections in the Catalogue of Fishes. Online version, updated 4 December 2019. Available from: http://researcharchive.calacademy.org/research/ichthyology/catalog/collections.asp (accessed 10 December 2019)

Fujii, E., Uyeno, T. & Shimaguchi, T. (2007) *Miobarbourisia aomori* gen. et sp. nov. (order Stephanoberyciformes), Miocene whalefish from Aomori, Japan. *Bulletin of the National Museum of Nature and Science, Series C*, 33, 89–93.

Fujita, K. (1990) *The caudal skeleton of teleostean fishes*. Tokai University Press, Tokyo, xii + 897 pp. (in Japanese, with English summary)

Greenwood, P.H. & Rosen, D.E. (1971) Notes on the structure and relationships of the alepocephaloid fishes. *American Museum Novitates*, 2373, 1–41.

Greenwood, P.H., Rosen, D.E., Weitzman, S.H. & Myers, G.S. (1966) Phyletic studies of teleostean fishes, with a provisional classification of living forms. *Bulletin of the American Museum of Natural History*, 131, 339–456.

Hennig, W. (1966) *Phylogenetic systematic*. University of Illinois Press, Urbana, 263 pp.

Hughes, L.C., Ortí, G., Huang, Y., Sun, Y., Baldwin, C.C., Thompson, A.W., Arcila, D., Betancur-R, R., Li, C., Becker, L., Bellora, N., Zhao, X., Li, X., Wang, M., Fang, C., Xie, B., Zhou, Z., Huang, H., Chen, S., Venkatesh, B. & Shi, O. (2018) Comprehensive phylogeny of fishes (Actinopterygii) based on genomic and transcriptomic data. *Proceedings of the National Academy of Science of the United States of America*, 115, 6249– 6254.

Johnson, G.D. (1975) The procurrent spur, an undescribed perciform character and its phylogenetic implications. *Occasional papers of the California Academy of Sciences*, 121, 1–23.

Johnson, G.D. (1992) Monophyly of the euteleostean clades—Neoteleostei, Eurypterygii, and Ctenosquamata. *Copeia*, 8–25.

Johnson, G.D. & Patterson, C. (1993) Percomorph phylogeny: a survey of acanthomorphs and a new proposal. *Bulletin of Marine Science*, 52, 554–626.

Johnson, G.D., Paxton, J.R., Sutton, T.T., Satoh, T.P., Sado, T., Nishida, M. & Miya, M. (2009) Deep-sea mystery solved: astonishing larval transformations and extreme sexual dimorphism unite three fish families. *Biology Letters*, 5, 235–239.

Kido, K. (1988) Phylogeny of the family Liparididae, with the taxonomy of the species found around Japan. *Memoirs of the Faculty of Fisheries, Hokkaido University*, 35, 125–256.

Kotlyar, A.N. (1981) A new family, genus and species of Beryciformes, Hispidoberycidae fam. n., *Hispidoberyx ambagiosus* gen. et sp. n. (Beryciformes). *Voprosy Ikhtiologii*, 21,

411–416. (In Russian. English translation in Journal of Ichthyology, 21, 9–13.)

Kotlyar, A.N. (1987) Classification and distribution of fishes of the family Anoplogastridae (Beryciformes). *Journal of Ichthyology*, 27, 133–153.

Kotlyar, A.N. (1991a) Osteology of *Hispidoberyx ambagiosus* (Hispidoberycidae) and its position within the order Beryciformes. *Journal of Ichthyology*, 31, 99–108.

Kotlyar, A.N. (1991b) Osteology of the suborder Stephanoberycoidei. Communication 1. The Stephanoberycidae and Gibberichthyidae. *Journal of Ichthyology*, 31, 18–32.

Kotlyar, A.N. (1995) Osteology and distribution of *Barbourisia rufa* (Barbourisiidae). *Journal of Ichthyology*, 35, 140–150.

Kotlyar, A.N. (1996a) Osteological intraspecific structure, and distribution of *Rondeletia loricata* (Rondeletiidae). *Journal of Ichthyology*, 36, 207–221.

Kotlyar, A.N. (1996b) *Beryciform Fishes of the World Ocean*. VNIRO Publishing, Moscow, 368 pp. (in Russian, with English summary)

Kotlyar, A.N. (2004a) Family Hispidoberycidae Kotlyar 1981 – hispidoberycids. *California Academy of Sciences Annotated Checklists of Fishes*, 26, 1–2.

Kotlyar, A.N. (2004b) Family Stephanoberycidae Gill 1884 – pricklefishes. *California Academy of Sciences Annotated Checklists of Fishes*, 27, 1–3.

Kotlyar, A.N. (2004c) Family Gibberichthyidae Parr 1933 – gibberfishes. *California Academy of Sciences Annotated Checklists of Fishes*, 28, 1–3.

Maddison, W.P. & Maddison, D.R. (2000) *MacClade: analysis of phylogeny and character evolution. version 4*. Sinauer Associates, Sunderland.

Maddison, W.P. & Maddison, D.R. (2018) *Mesquite: a modular system for evolutionary analysis. version 3.51.* Available from: http://www.mesquiteproject.org (accessed 9 December 2019).

Merrett, N.R. & Moore, J.A. (2005) A new genus and species of deep demersal fish (Teleostei: Stephanoberycidae) from the tropical eastern North Atlantic. *Journal of Fish*

Biology, 67, 1699–1710.

Mincarone, M.M., Di Dario, F. & Costa, P.A.S. (2014) Deep-sea bigscales, pricklefishes, gibberfishes and whalefishes (Teleostei: Stephanoberycoidei) off Brazil: new records, range extensions for the south-western Atlantic Ocean and remarks on the taxonomy of *Poromitra*. *Journal of Fish Biology*, 85, 1546–1570.

Miya, M., Kawaguchi, A. & Nishida, M. (2001) Mitogenomic exploration of higher teleostean phylogenies: a case study for moderate-scale evolutionary genomics with 38 newly determined complete mitochondrial DNA sequences. *Molecular Biology and Evolution*, 18, 1993–2009.

Miya, M., Satoh, T.P. & Nishida, M. (2005) The phylogenetic position of toadfishes (order Batrachoidiformes) in the higher ray-finned fish as inferred from partitioned Bayesian analysis of 102 whole mitochondrial genome sequences. *Biological Journal of the Linnean Society*, 85, 289–306.

Miya, M., Takeshima, H., Endo, H., Ishiguro, N.B., Inoue, J.G., Mukai, T., Satoh, T.P., Yamaguchi, M., Kawaguchi, A., Mabuchi, K., Shirai, S.M. & Nishida, M. (2003) Major patterns of higher teleostean phylogenies: a new perspective based on 100 complete mitochondrial DNA sequences. *Molecular Biology and Evolution*, 26, 121–138.

Moore, J.A. (1993) Phylogeny of the Trachichthyiformes (Teleostei: Percomorpha). *Bulletin of Marine Science*, 52, 114–36.

Near, T.J., Dornburg, A., Eytan, R.I., Keck, B.P., Smith, W.L., Kuhn, K.L., Moore, J.A., Price, S.A., Burbrink, F.T., Friedman, M. & Wainwright, P.C. (2013) Phylogeny and tempo of diversification in the superradiation of spiny-rayed fishes. *Proceedings of the National Academy of Science of the United States of America*, 110, 12738–12743.

Near, T.J., Eytan, R.I., Dornburg, A., Kuhn, K.L., Moore, J.A., Davis, M.P., Wainwright, P.C., Friedman, M. & Smith, W.L. (2012) Resolution of ray-finned fish phylogeny and timing of diversification. *Proceedings of the National Academy of Science of the United States of*

America, 109, 13698–13703.

Nelson, G. (1973) Classification as an expression of phylogenetic relationship. *Systematic Zoology*, 22, 344–359.

Nelson, J.S. (1976) *Fishes of the world*. Wiley-interscience, New York, 416 pp.

Nelson, J.S. (1984) *Fishes of the world, 2nd ed*. John Wiley & Sons, New York, xv + 523 pp.

Nelson, J.S. (2006) *Fishes of the world, 4th ed*. John Wiley & Sons, xix + 601 pp.

Nelson, J.S., Grande, T.C. & Wilson, M.V.H. (2016) *Fishes of the world, 5th ed*. John Wiley & Sons, Hoboken, xli + 707 pp.

Okamura, O. (1985) 220 *Barbourisia rufa* Parr, 221 *Rondeletia loricata* Abe and Hotta. *In*: Okamura, O. (Ed.), *Fishes of the Okinawa Trough and the adjacent waters II*. Japan Fisheries Resource Conservation Association, Tokyo, pp. 440–443.

Overseas Fishery Cooperation Foundation, Japan & Agency for Marine and Fisheries Research, Ministry of Marine Affairs and Fisheries, Indonesia (2006) *The Japan-Indonesia Deep Sea Fishery Resources Joint Exploration Project (Final Report)*. Overseas Fishery Cooperation Foundation of Japan, Tokyo, VIII + 154 + 58 pp.

Patterson, C. & Johnson, G.D. (1995) The intermuscular bones and ligaments of teleostean fishes. *Smithsonian Contribution to Zoology*, 559, 1–85.

Paxton, J.R. (1974) Morphology and distribution patterns of the whalefishes of the family Rondeletiidae. *Journal of the Marine Biological Association of India*, 15, 175–188.

Paxton, J.R. (1986) Cetomimidae. *In*: Whitehead, P.J.P., Bauchot, M.-L., Hureau, J.-C., Nielsen, J. G. & Tortonese, E. (Eds.), *Fishes of the North-eastern Atlantic and the Mediterranean. Volume II*. UNESCO, Paris, pp. 524–525.

Paxton, J.R. (1989) Synopsis of the whalefishes (family Cetomimidae) with descriptions of four new genera. *Records of the Australian Museum*, 41, 135–206.

Paxton, J.R. (2008) Family Rondeletiidae, Family Barbourisiidae. *In*: Gomon, M.F., Bray, D.J. & Kuiter R.H. (Eds.), *Fishes of Australia's southern coast*. New Holland Publishers,

Sydney, pp. 413–414.

Paxton, J.R. (2015) 133 Family Rondeletiidae. *In*: Roberts, C.D., Stewart, A.L. & Struthers, C.D. (Eds.), *The fishes of New Zeeland*. Te Papa Press, Wellington, pp. 994–995.

Paxton, J.R., Johnson, G.D. & Trnski,T. (2001) Larvae and juveniles of the deepsea "Whalefishes" *Barbourisia* and *Rondeletia* (Stephanoberyciformes: Barbourisiidae, Rondeletiidae), with comments on family relationships. *Records of the Australian Museum*, 53, 407–425.

Rojo, A.L. (1991) *Dictionary of evolutionary fish osteology*. CRC Press, Boca Raton, 273 pp.

Rosen, D.E. (1973) Interrelationships of higher euteleostean fishes. *In*: Greenwood, P.H., Miles R.S. & Patterson, C. (Eds.), *Interrelationships of Fishes*. Academic Press, New York, pp. 397–513.

Sasaki, K., Tanaka, Y. & Takata, Y. (2006) Cranial morphology of *Ateleopus japonicus* (Ateleopodidae: Ateleopodiformes), with a discussion on metamorphic mouth migration and lampridiform affinities. *Ichthyological Research*, 53, 254–263.

Sawada, Y. (1982) Phylogeny and zoogeography of the superfamily Cobitoidea (Cyprinoidei, Cypriniformes). *Memoirs of the Faculty Fisheries, Hokkaido University*, 28, 65–223.

Springer, V.G. & Johnson, G.D. (2004) Study of the dorsal gill-arch musculature of teleostome fishes, with special reference to the Actinopterygii. *Bulletin of the Biological Society of Washington*, 11, i–vi + 1–260, pls. 1–205.

Stewart, A.L. (2015) 132 Family Stephanoberycidae. *In*: Roberts, C.D., Stewart, A.L. & Struthers, C.D. (Eds.), *The fishes of New Zeeland*. Te Papa Press, Wellington, pp. 992–993.

Stiassny, M.L.J. (1986) The limits and relationships of the acanthomorph teleosts. *Journal of Zoology*, 1, 411–460.

Stiassny, M.L.J. (1996) Basal ctenosquamate relationships and the interrelationships of the myctophiform (scopelomorph) fishes. *In*: Stiassny, M.L.J., Parenti, L.R. & Johnson, G.D.

(Eds.), *Interrelationships of Fishes*. Academic Press, San Diego, pp. 405–426.

Stiassny, M.L.J. & Moore, J.A. (1992) A review of the pelvic girdle of atherinomorph fishes. *Zoological Journal of Linnean Society*, 104, 209–42.

Swofford, D.L. (2002) *PAUP*: phylogenetic analysis using parsimony, version 4*. Sinauer Associates, Sunderland, Massachusetts.

Swofford, D.L. & Maddison, W.P. (1987) Reconstructing ancestral character states under Wagner parsimony. *Mathematical Biosciences*, 87, 199–229.

Tominaga, Y. (1970) On the glandular organs before the eyes of the red-coated whalefish, *Rondeletia loricata*. *Zoological Magazine*, 79, 368. (In Japanese)

Uyeno, T. & Sato, Y. (1983) Gibberichthyidae. *In*: Uyeno, T., Matsuura, K. & Fujii, E. (Eds.), *Fishes trawled off Suriname and French Guiana*. Japan Marine Fishery Resource Research Center, Tokyo, p. 279.

Vilasri, V. (2013) Comparative anatomy and phylogenetic systematics of the family Uranoscopidae (Actinopterygii: Perciformes). *Memoirs of the Faculty of Fisheries Science, Hokkaido University*, 55, 1–106.

Watrous, L.E. & Wheeler, Q.D. (1981) The out-group comparison method of character analysis. *Systematic Zoology*, 30, 1–11.

Webb, J.F. (1989) Gross morphology and evolution of the mechanoreceptive lateral-line system in teleost fishes. *Brain, Behavior and Evolution*, 33, 34–53.

Wiley, E.O. (1981) *Phylogenetics: the theory and practice of phylogenetic systematics.* Wiley-interscience, New York, 439 pp.

Wiley, E.O. & Johnson, G.D. (2010) A teleost classification based on monophyletic groups. *In*: Nelson, J.S., Schultze, H.-P. & Wilson, M.V.H. (Eds.), *Origin and Phylogenetic Interrelationships of Teleosts*. Verlag Dr. Friedrich Pfeil, München, pp. 123–182.

Winterbottom, R. (1974) A descriptive synonymy of the striated muscles of the Teleostei. *Proceedings of the Academy of Natural Sciences of Philadelphia*, 125, 225–317.

Yabe, M. (1985) Comparative osteology and myology of the superfamily Cottoidea (Pisces: Scorpaeniformes), and its phylogenetic classification. *Memoirs of the Faculty of Fisheries, Hokkaido University*, 32, 1–130.

Yang, Y.-R., Zeng, B.-G. & Paxton, J.R. (1988) Additional specimens of the deepsea fish *Hispidoberyx ambagiousus* [sic] (Hispidoberycidae, Berciformes [sic]) from the South China Sea, with comments on the family relationships. *Uo*, 38, 3–8.

Zehren, S.J. (1979) The comparative osteology and phylogeny of the Beryciformes (Pisces: Teleostei). *Evolutionary Monographs*, 1, 1–389.